

Applications of the 4 mm Dynamic Shear Rheometer Geometry for the Forensic  
Evaluation of Bituminous Materials

By

Kristen E. Derewecki

A thesis submitted to the

Graduate School-New Brunswick

Rutgers, The State University of New Jersey

in partial fulfillment of the requirements

for the degree of

Master of Science

Graduate Program in Civil Engineering

written under the direction of

Dr. Ali Maher

And approved by

---

---

---

New Brunswick, New Jersey

October 2013

## **ABSTRACT OF THE THESIS**

Applications of the 4 mm Dynamic Shear Rheometer Geometry for the Forensic

Evaluation of Bituminous Materials

by Kristen E. Derewecki

Thesis Director:

Dr. Ali Maher

The current asphalt binder performance grading system requires the use of multiple pieces of testing equipment to determine high, intermediate and low temperature properties. To properly grade an asphalt binder, numerous hours of labor must be expended to run through all of the required aging and testing. Additionally when creating master curves to compare stiffness and phase angle with respect to frequency, multiple pieces of equipment are required. This not only creates inefficiencies with respect to time and money, but also brings an approximation into the data as opposed to a direct reading. In order to forensically evaluate asphalt binders, the asphalt must be extracted and recovered from roadway cores. During the extraction/ recovery process the amount of binder required results in coring a considerable amount of the road in question as well as running through an expensive and time consuming chemically intensive process to extract the bituminous material. This paper investigates the potential of the 4 mm Dynamic Shear Rheometer geometry and its potential applications in evaluating binder properties for all failure mechanisms without the need for additional equipment and reducing the amount of asphalt required.

## **Acknowledgements**

The author would like to take the time to thank Dr. Thomas Bennert, Dr. Ali Maher, and the faculty/staff of the CAIT department for supporting their graduate studies. In addition, thank you to Chris Ericson, Ed Wass Sr., Maher Saad and Donatas Zvirblis for their help with this research.

## Table of Contents

Abstract .....	ii
Acknowledgements .....	iii
Table of Tables .....	vii
Table of Figures .....	viii
Chapter 1: Background .....	1
INTRODUCTION .....	1
BASICS OF ASPHALT .....	1
Origin .....	1
Distillation.....	1
Uses.....	4
Roadway Applications .....	4
Testing Processes .....	4
Analysis and Research Need.....	5
Chapter 2: Empirical Binder Testing .....	7
INTRODUCTION .....	7
TEST METHODS.....	8
Penetration Testing .....	8
Viscosity .....	9
Flashpoint.....	12

Thin Film and Rolling Thin Film Oven .....	13
Ductility .....	15
Chapter 3: Superpave Binder Evaluation.....	16
INTRODUCTION .....	16
RHEOLOGY.....	17
Background .....	17
Workability .....	19
Rutting Resistance .....	21
Fatigue Cracking Resistance.....	23
Thermal Cracking Resistance .....	25
Chapter 4: Master Curves .....	28
INTRODUCTION .....	28
BACKGROUND .....	28
Master Curve Components .....	28
Shift Factors .....	32
Black Space Diagrams .....	35
Problems with Traditional Master Curves .....	36
Chapter 5: Work Plan.....	39
DETAILED WORK PLAN .....	39
Subtask 5a .....	39

Subtask 5b .....	42
Subtask 5c .....	43
EQUIPMENT .....	44
Chapter 6: Results .....	48
INTRODUCTION .....	48
METHODOLOGY .....	48
Continuous Grading .....	49
Frequency Sweeps .....	50
Master Curves .....	56
Error .....	56
CONCLUSIONS.....	69
Chapter 7: Final Conclusions.....	70
References.....	75
Appendix A: 4 mm Master Curve Sequence User Manual.....	77
Appendix B: RHEA User Manual .....	94
Appendix C: Continuous Grading Data for Binders Used.....	61

## **Table of Tables**

Table 1 List of Empirical Binder Tests and Methods .....	7
Table 2 Binder Continuous and Performance Grades.....	49
Table 3 Testing Parameters.....	51

## Table of Figures

Figure 1 Asphalt Distillation Process .....	3
Figure 2 Asphalt Penetrometer .....	8
Figure 3 Capillary Tube Viscometer.....	11
Figure 4 Kinematic Viscometer .....	11
Figure 5 Cleveland Open Cup Flash Point Tester .....	12
Figure 6 Thin Film Oven .....	13
Figure 7 Rolling Thin Film Oven .....	14
Figure 8 Ductility Tester .....	15
Figure 9 Couette Rotational Viscometer Schematic .....	20
Figure 10 Brookfield Rotational Viscometer.....	20
Figure 11 Dynamic Shear Rheometer.....	23
Figure 12 Pressure Aging Vessel & Degassing Oven .....	24
Figure 13 Bending Beam Rheometer.....	26
Figure 14 Molded Asphalt Beams .....	27
Figure 15 Viscous Material Categories.....	29
Figure 16 Correlation of $G^*$ , $G'$ & $G''$ .....	30
Figure 17 Typical Rheological Spectra for AC-5 & AC-40 Asphalt Binders .....	31
Figure 18 Typical Frequency Sweep .....	32
Figure 19 Modified Trimming Tool .....	44
Figure 20 Traditional and Modified Trimming Tool.....	44
Figure 21 Cooling Chamber with Drain .....	45
Figure 22 Copper Tubing with Nipple Attachments.....	45



Figure 23 Cooling Chamber During Test .....	46
Figure 24 Paralle Plates Unloaded (4mm) .....	46
Figure 25 Parallel Plates for Size Comparison (4mm Top, 8mm Bottom).....	47
Figure 26 Sample Being Loaded on 4 mm Plates .....	47
Figure 27 Trimmed Sample on 4 mm Plates .....	47
Figure 28 PG 64-22 #2 Frequency Sweep (4mm) .....	52
Figure 29 RE Pierson #2 Frequency Sweep (4mm).....	53
Figure 30 PG 76-22 #1 Frequency Sweep (8mm) .....	55
Figure 31 PG 64-22 Master Curves (4mm) .....	56
Figure 32 PG 76-22 Master Curves (4mm) .....	57
Figure 33 RE Pierson Master Curves (4mm).....	58
Figure 34 RI DOT 64-28 Master Curves (4mm) .....	58
Figure 35 RI DOT 64-28 Master Curves (4mm & 8mm).....	59
Figure 36 PG 64-22 Master Curves (4mm & 8mm) .....	60
Figure 37 PG 76-22 Master Curves (4mm & 8mm) .....	61
Figure 38 RE Pierson Master Curves (4mm & 8mm) .....	61
Figure 39 RI DOT 64-28 30°C Isotherms .....	62
Figure 40 PG 64-22 30°C Isotherms.....	63
Figure 41 RE Pierson 30°C Isotherms .....	64
Figure 42 PG 76-22 30°C Isotherms.....	65
Figure 43 RI DOT 64-28 Black Space Diagram.....	66
Figure 44 PG 64-22 Black Space Diagram.....	67
Figure 45 RE Pierson Black Space Diagram .....	67

Figure 46 PG 76-22 Black Space Diagram.....	68
---	----

## **Chapter 1: Background**

### **INTRODUCTION**

Asphalt binder comprises about 15% by volume of a hot-mix asphalt (HMA) design. In spite of this small percentage, asphalt binders play a key role in the physical characterization of the mix and are the major cost element. As such, an entire spectrum of testing has been developed and improved upon through the years to properly understand the physical characteristics and failure mechanisms of this component (1, 2).

### **BASICS OF ASPHALT**

#### **Origin**

The American Society for Testing and Materials (ASTM) defines asphalt as a dark brown to black cementitious material, predominantly consisting of bitumens, which can be found in nature or as a by-product of petroleum processing (2). Natural asphalts can be found in locations such as Trinidad Lake (TLA), and are a result of the evaporation of volatile portions of natural asphalt deposits, leaving behind asphalt fractions. Currently, natural asphalts are only used as add-in to blended petroleum derived asphalt, but in the early 1900s, they were the primary source. They have fallen out of favor due to the substantial portion of mineral matter present as well as the laborious process associated with the mining of the material (2). The majority of the asphalt binders used in the United States are derived from the crude oil distillation process. Residuum from the distillation process becomes asphalt binder, with greater gravity and lower sulfur content being desirable qualities (3). As such the older the crude source, the better its application as asphalt binder.

## **Distillation and Production**

In general petroleum refiners produce asphalt binder, as a by-product of the refining process. Second party formulators, who purchase blend stock from refiners and produce and market their own binders, also produce asphalt binder (1, 3). Prior to the introduction of Superpave specifications, the regulations governing asphalt were fairly lenient and as such asphalt binders were simply a way to make a profit off of a product formerly seen as waste. With the introduction of new specifications, asphalt was not seen as a value-added product, and as such refineries either opted to remove themselves from the market entirely or work to produce quality binder products (1, 3).

As mentioned above, asphalt binders come from two sources, as a naturally occurring product, as in TLA and a by-product of the crude oil refining process. The latter is responsible for the majority of the asphalt produced and used in this country and as such will be the area of focus. In order to understand the process of asphalt distillation, a general overview of the crude oil refining process is necessary.

Crude petroleum is pumped into a heat exchanger or tube heater, where heat is applied rapidly for the initial distillation. In the atmospheric distillation tower, volatile components, which are generally lighter, vaporize and are pulled into a separate section to be further refined into other components. These lighter fractions include light, medium and heavy distillates that can be refined into gasoline, kerosene and diesel, in addition to other petroleum products (3). Following the atmospheric distillation process, the residue remaining makes up the heavy fraction of the crude petroleum. The 'topped crude' yielded from the vacuum distillation may yield a straight run asphalt, however if the high boiling fractions are not volatile enough, they cannot be removed with

distillation alone. In this case the addition of a solvent to extract the asphalt may become necessary (3). Due to the varying production practices, different grades of asphalt can be produced. In the past, in order to attain a stiffer asphalt binder, the practice was to blow hot air on the product. Air blown asphalts have gone out of favor in recent years to be replaced by other modification techniques, namely those including the addition of polymer, rubbers or waxes (2,3). Based on the nature of the additive, the binder can be modified in order to make it more rutting resistant, more workable or more durable. The grades of binder can be evaluated using a matrix of tests.

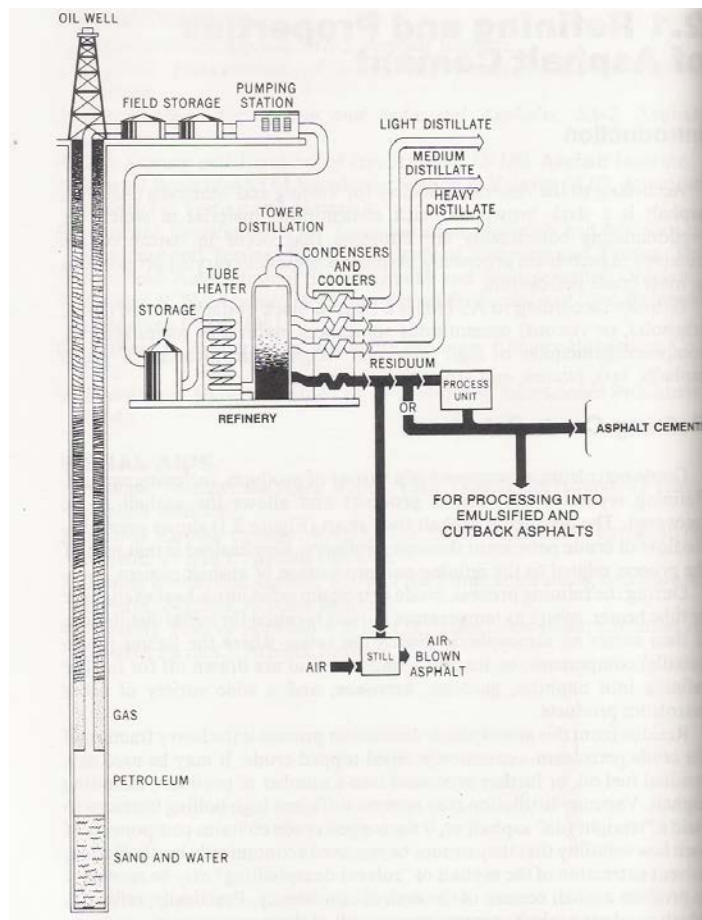


**Figure 1 Asphalt Distillation Process (3)**

## **Uses**

Annually, nearly 100 million metric tons of asphalt is used, with approximately one quarter of that being used by the United States (2). The vast majority of this is used for paving applications, but a significant portion is also used by roofing industry. It has also been used in the past as a waterproofing agent. In recent years, there has been a paradigm switch in the paving and roadway construction industry and concrete pavements have been replaced by HMA due to the fact that they are easier to replace, repair and construct as well as being cheaper (2).

## **Roadway Applications**

HMA is a flexible pavement that consists of one or more compacted layers, generally made of 80% mineral aggregate, 15% asphalt and 5% air voids, by volume. The asphalt binder serves as the 'glue' that holds the mixture together. It is generally inexpensive, less than \$0.10 per pound and is a waterproof, visco-elastic adhesive. Although volumetrically asphalt is a small player in the role of HMA, it has a large influence on performance and overall cost (3).

HMA is favored due to the fact that it is a flexible pavement, as opposed to concrete which is rigid, meaning that the roadway flexes as it is loaded and failure mechanisms are not catastrophic. Asphalt concrete roadways are quicker to construct and can be done in phases, without having to worry about cold-joints as with rigid concrete pavements. Additionally, when replacing HMA the pavement can be milled one day and paved at a later date. This kind of schedule flexibility does not exist with other pavement types, and that along with the lower cost has resulted in its favorability (1, 6).

## **Testing Processes**

As the need and use of asphalt continues to increase, it is becoming increasingly important to understand the material and its various properties. The key physical properties of interest to engineers, technicians, construction workers and others who work with asphalt binder are viscosity, purity and safety(2). However understanding the failure mechanisms and conditions under which failure occurs is also considerably important.

In the past, binder grades were based on penetration and/ or viscosity tests. This led to grading scales that were empirical and not applicable to a binders full spectrum of performances and working temperatures (1, 3, 5). In an effort to more accurately evaluate asphalt binders, the Superpave grading system was created. This system correlates climatic conditions with a binders grade, enabling the correct binder to be chosen based on the region where it will be used. Additionally, the advent of Superpave enabled producers to better understand the effects of certain modifiers, which can improve the performance of a binder under certain conditions (1, 2, 8). With older forms of testing, such as penetration and viscosity, the effects of modifiers either went unnoticed due to the testing temperatures or were unable to be run all together, due to a high viscosity level. Superpave testing enables the producer to better understand the way in which binder properties relate to mixture performance. As the modifiers used in asphalt production increase, it becomes increasingly necessary to understand the way in which they are altering the asphalt binders and their performance.

## **Analysis and Research Needs**

The results of Superpave testing can be correlated directly with a performance grade, giving an idea of the different failure mechanisms. Another option for analyzing binders

is by developing a master curve of frequency sweeps shifted to a reference temperature. This enables one to see the correlation with stiffness or phase angle over a range of reduced frequencies and from this a full range of the properties from the glassy modulus to the viscous range of the binder can be demonstrated (5). However, due to the limitations of equipment, this sweep needs to be done using different pieces of equipment and in some cases requires an approximation instead of a direct reading. As a result, alternative geometries and methods are being explored to make the process more efficient and accurate.



## Chapter 2: Empirical Binder Testing

### INTRODUCTION

In general, the characteristics of importance of asphalt cements are consistency, purity and safety. The ramifications of these properties extend beyond getting the optimum product for the application, but to the safety of those working with the material. Until the introduction of Superpave specifications, the properties of asphalt binders were generally tested using empirical tests. Although considered suitable at the time, these empirical tests made way for more scientific and performance based tests.

Prior to the integration of Superpave testing methods, labs used the following tests and methods:

Test	Test Method (ASTM)
Absolute Viscosity at 60°C	D2171
Kinematic Viscosity at 135°C	D445
Penetration	D946
Flashpoint (Cleveland Open Cup)	D92
Thin Film Oven Test	D1754
Rolling Thin Film Oven Test	D2872
Ductility	D113
Solubility in Trichlorethylene	D2042
Water	D95

**Table 1 List of Empirical Binder Tests and Methods**

These tests yield a combination of empirical and scientific results, all of which aid in determining the consistency, purity or safety relative to the asphalt binders (3).

## TEST METHODS

### Penetration Testing

Prior to the advent of Superpave and performance grading, asphalt binder grades relied upon the results of the penetration test. The results yielded a value upon which one could compare the consistency of the asphalt against other binders. This test measures the depth that a needle, with a weight applied, goes into a sample of asphalt at a certain temperature. The weight is applied for a set length of time and the depth that the needle penetrated into the asphalt sample is recorded in 0.1mm (2, 3).



**Figure 2 Asphalt Penetrometer**

These penetration depths translated into the standard grades, which were 40-50, 60-70, 85-100, 120-150 and 200-300. These penetration grades are indicative of the consistency

of the asphalt at room temperature, since the test runs at 25°C (3). The lower the grade, the firmer the asphalt is at room temperature. Based on these grades, asphalts could be selected for different applications. However, since this test is empirical in nature, it runs into certain limitations. The first of which being that it has no scientific units upon which it can be compared with the results of other tests. Additionally, the consistency at room temperature is of little consequence when the asphalt generally is heated to temperatures around 135°C for pumping, mixing and compaction and generally sees a full spectrum of temperatures during its service life. Finally, this test has additional limitations when evaluating the properties of polymer-modified binders. At lower temperatures, asphalt binders act primarily as an elastic material, becoming viscous once they reach a certain temperature (5, 8). When a binder is polymer or otherwise modified, this alteration in properties is seen at temperatures other than 25°C and would not be noticed by the penetration test. Despite the fact that some countries still use the penetration grading system, it has fallen out of favor with the majority of labs and has been replaced by more scientific based tests.

### **Viscosity**

Viscosity measurements relate directly to the ‘consistency’ component of binder.

Viscosity describes a fluid’s resistance to flow. Asphalt binders are visco-elastic materials. As such, at high temperatures they act as viscous liquids, but in lower temperature they perform as an elastic solid (2, 4, 5). The viscous properties of binders are important because they indicate the temperature at which producers and users should store, pump, mix and compact asphalts.

Viscosity relates the shear stress to the shear strain. The Newtonian definition of viscosity is described by the following equation (5):

$$\eta = \tau / \dot{\gamma}$$

where

$$\eta = \text{viscosity}$$

$$\tau = \text{shear or resisting stress between layers}$$

$$\dot{\gamma} = \text{shear strain rate}$$

Viscosity depends on the microstructure within a material, namely the number and type of attractive bonds and the particle or molecular interaction. It can be reduced when temperature are increased and likewise can be increased when there are suspended solids or high levels of flocculation (5).

Viscosity can be evaluated using a variety of testing equipment, but historically capillary viscometers with pressure driven flow were used. Capillary viscometers can evaluate absolute and kinematic viscosities. When used to evaluate absolute viscosity, a U-shaped tube with timing marks is filled with asphalt and placed in a 60°C water bath. A vacuum is applied and pulls the asphalt through the tube. The amount of time the asphalt takes to pass the timing marks is multiplied by a calibration factor and yields the viscosity in Pascal-seconds (Pa·s) (3).



**Figure 3 Capillary Tube Viscometer**

Contrary to absolute viscosity, kinematic viscosity measured by capillary tube does not employ an outside force, such as a vacuum or pump to measure the resistance. Instead it utilizes gravity. In this test, a cross arm tube with timing marks is filled with asphalt and heated in an oil bath set at 135°C. The amount of time the asphalt takes to pass the timing marks is multiplied by a calibration factor and yields the viscosity in centistokes or  $\text{mm}^2/\text{s}$  (3).



**Figure 4 Kinematic Viscometer**

Both capillary measurements have restrictions which have caused them to be phased out of most conventional asphalt testing. Since the tubes are so narrow, asphalts that have any kind of particulate matter or unincorporated solids do not flow properly.

Additionally binders which have been modified with certain polymers may not be able to flow at these temperatures or under these conditions and as such alternative viscometers have replaced capillary tubes.

### **Flash Point**

One of the primary concerns in handling asphalt is the safety of those working with the materials. The flash point test, using the Cleveland open cup apparatus, determines the temperature at which a specific bitumen sample will flash. This is the point at which the volatiles released by heating asphalt spontaneously flash in the presence of an open flame (2,3). The next step, where volatiles spontaneously combust in the presence of a flame, is the fire point. Specifications rarely call for fire point to be tested and the flash point occurs at a temperature much lower than that of fire point.

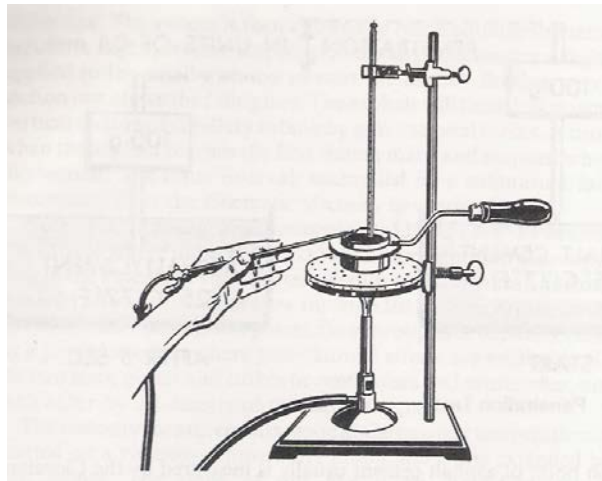


**Figure 5 Cleveland Open Cup Flash Point Tester (3)**

The flash point test utilizes the apparatus above, called the Cleveland Open Cup Flash Tester. The operator heats and a certain quantity of asphalt and pours it into a brass cup. An electric element heats the material using the heating rate set forth by the specifications. The operator passes a small flame over the cup at certain intervals until an instantaneous flash occurs (3).

### **Thin Film and Rolling Thin Film Oven Tests**

The thin film oven (TFO) test simulates the hardening conditions that occur in a hot mix plant facility. Additionally, tests such as penetration, mass loss and/or viscosity tests are run on the thin film oven aged material in order to determine its resiliency. This particular aging method involves a small volume of asphalt binder placed in a flat-bottomed pan, to have a layer thickness of 3 mm. The operator weighs the pan prior to placing it into a ventilated oven on a rotating shelf. Following a certain period of aging, the operator removes the sample and reweighs it. This change in mass is represented as a percentage of the original weight. This material can be stored in order to run additional tests on the residue (3).

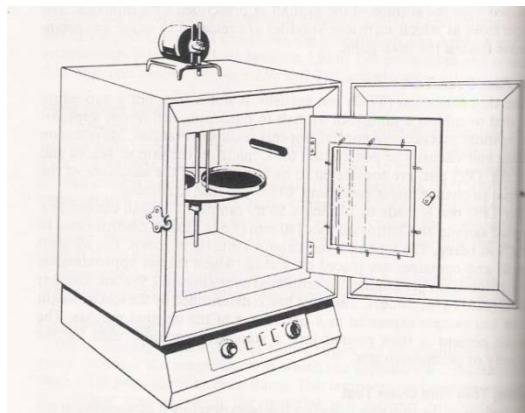


**Figure 6 Thin Film Oven (3)**

A second test representative of HMA aging uses the rolling thin film over (RTFO). Similar to the TFO, this process hardens a film of asphalt for later testing, however the method employed is different. Instead of having a pan, in which a small volume of asphalt is poured, a larger bottle is used with a greater amount of asphalt. These bottles are placed into a rack, where they rotate in a ventilated oven with an air jet. The combination of the rotation and the air jet blasts, which removes vapors, better mimic the HMA aging because each time the bottle rotates, a new thin film is exposed to the jet blast (2,3). As compared to the TFO, the RTFO material is being aged consistently throughout instead of just on the top layer. Additionally, with this test a greater amount of aged residue is produced and in a much shorter time than with the TFO. This material is used to determine mass loss as well as run additional tests, particularly Superpave tests.

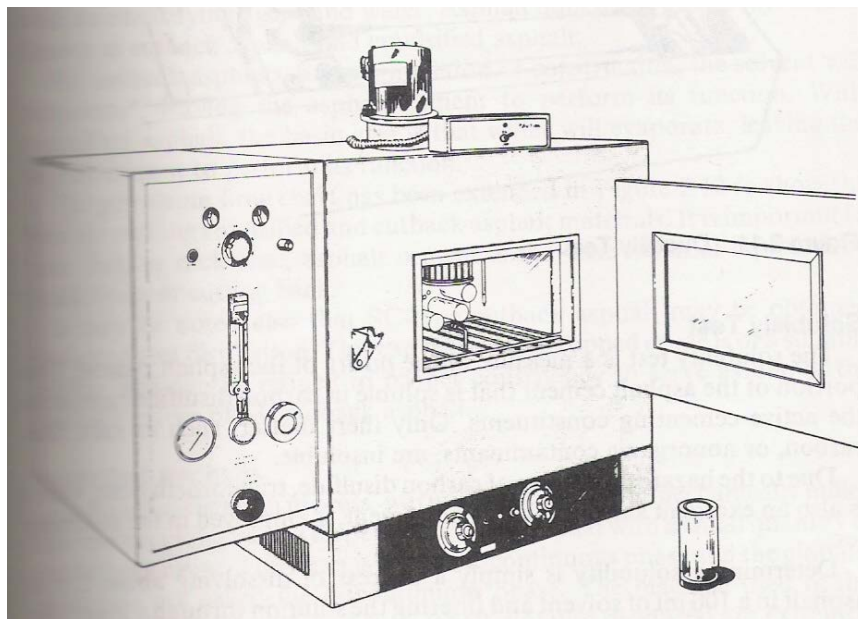


**Figure 7 Rolling Thin Film Oven (3)**



## Ductility

Ductility is the ability of a material to deform under a tensile force. Asphalt with poor ductility will have inadequate adhesive properties and as such not be effective in binding with aggregates. The ductility test takes a sample of asphalt at 25°C, in a water bath, and pulls it apart at a rate of 5 cm/min. This test is used to set a minimum ductility that a binder should have, which has been set at greater than 100 cm (3). Anything less than this is deemed to be insufficient. However, this test does not yield any engineering properties and is a purely empirical test.

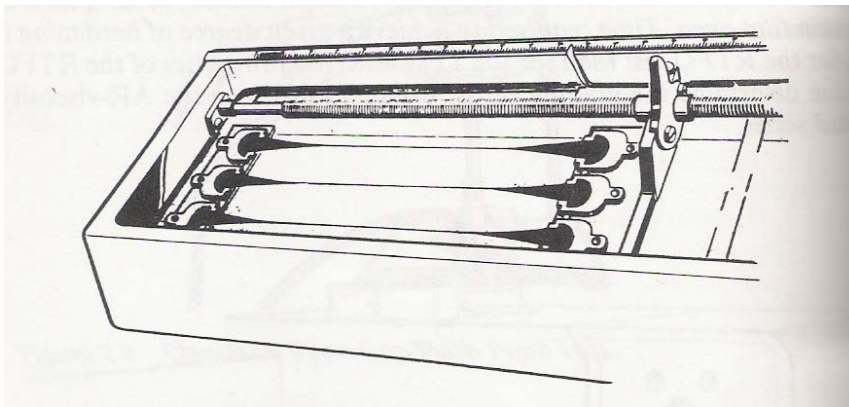


**Figure 8 Ductility Tester (3)**

## **Chapter 3: Superpave Binder Evaluation**

### **INTRODUCTION**

Conventional binder testing takes into account the capillary viscosity measurements as well as the results from some empirical tests. This methodology, while being used widely throughout the asphalt industry, was inherently flawed. This system of grading does not enable a technician or producer to properly compare the results from one sample to that of another.

Tests, such as penetration and ductility, make up the basis for the conventional binder grading system. Most binders in the past followed the 'Pen' naming convention. This meant that based on the results of the penetration test, the producer would grade the binder accordingly (2,3). Ductility testing was used to determine whether or not the binder would act as a good or poor adhesive (5). However, these tests have no engineering units or properties associated with them. As such, each measurement and test is independent of one another and the results cannot be aggregated. Despite this, attempts have been made to correlate these tests with those founded on engineering units, but none of these have actually been based on fact, only correlation factors (4,5,8). In addition to these empirical tests, viscosity measures are also used to determine the properties of asphalt binders. These results, however, are only applicable when the binder acts like a viscous fluid, not when it is acting as a viscoelastic solid (5).

Due to the inadequacies of the conventional binder grading system the Strategic Highway Research Program (SHRP) worked to devise a new system of grading based on

performance and engineering principles rather than empirical factors and viscosity. The main goal of the program was “to identify the physical properties of asphalt cement binders that are related to pavement performance and methods to reliably measure those properties” (5). In order to do so researchers took into effect the key asphalt pavement failures, which include rutting, fatigue cracking and thermal cracking. These properties were evaluated using rheological properties as opposed to prior conventions (5).

## **RHEOLOGY**

### **Background**

Rheology, like viscosity, is a material's resistance to deformation. However, unlike viscosity, which evaluates a material at one specific temperature and shear rate, rheology evaluates the time-temperature response (2). In this way, rheology can be used to understand materials that exhibit plastic, elastic and viscous properties based on the test temperature. Asphalt's properties vary greatly depending on the temperature at which they are evaluated. Near mixing and compaction temperatures, it acts as a Newtonian – viscous fluid. At low temperatures asphalt is an elastic material with relatively low creep deformation rates, below this it becomes a brittle elastic solid with very low creep and flow. Below the glass transition temperature ( $T_g$ ), the asphalt is best characterized as a glassy solid (4,5).

Rheological properties are centered on the complex modulus and phase angle of the material as a function of frequency and temperature. The complex modulus,  $G^*$ , is the total resistance to deformation under a load. Phase angle,  $\delta$ , is the distribution of

response between in-phase and out of phase component (4,5). In-phase is indicative of the elastic component, where energy is stored, and out of phase represents the viscous component, where energy is lost. When the variation of  $G^*$  and  $\delta$  is observed as a function of frequency at a constant temperature it creates the master curve (5).

Once SHRP outlined the major failure mechanisms and the shift to rheology over empirical testing, it was necessary to determine when each failure mechanism was most prevalent and how to test for them in the laboratory setting. The properties and performance of asphalt binders can be broken into four temperature ranges that signify different stages in pavement life as well as failure mechanisms (1,5,8). At temperature above 100°C, most binders are Newtonian fluids and act completely viscous. This stage impacts the mixing and compaction stages of the asphalt, since it is the only time that the asphalt will be heated to this temperature. As such, it is not indicative of a failure mechanism, but the binder consistency must be controlled in order to ensure that the final product will perform properly (2,5). Binders at temperatures ranging from 45°C to 100°C are representative of binders at the highest pavement service temperatures. This temperature range is most susceptible to failure by rutting. In this temperature range, viscosity is not an accurate measurement because it assumes viscous behavior, which may or may not be the case, instead measurements of  $G^*$  and  $\delta$  are favorable since they are representative of the resistance to deformation and elasticity or recovery (2,5). At temperature from 0°C to 45°C pavements generally fail due to fatigue damage due to repeated cyclic loading. Similar to rutting, the relationship between  $G^*$  and  $\delta$  is the key factor in determining the resistance to failure. Both are functions of the frequency of loading, which must be simulated to model the rate of loading of pavement under traffic

in order to get useful results (2,5). For temperatures below 0°C down to -50°C, pavements are in the thermal cracking zone. As a result of cooling, the pavement incurs shrinkage due to thermal stresses. In order to evaluate this failure, the stiffness and relaxation rate of the material must be measured, which are related to  $G^*$  and  $\delta$  respectively (2,5). Understanding the way in which materials fail and the temperatures at which they do so allowed for new more effective and useful testing methods to be developed.

### **Workability**

The ability of an asphalt to be effectively stored, pumped, mixed and compacted may be the single most important characteristic. As such the properties of an asphalt binder in the viscous stage must be evaluated. With the advent of Superpave, the type of viscometer used switched from the traditional capillary tube to the rotational viscometer. The rotational viscometer, can be used to test asphalt viscosity at high temperatures and is generally run at 135°C. The relationship between the shear stress and shear strain rate remains the same as in the aforementioned section assuming that the material is behaving as a Newtonian fluid. Rotational viscometers can be characterized as ‘Couette’ or ‘Searle’ depending on whether the cup or bob is rotating. With asphalt applications, the ‘Couette’ variety is employed and the bob, a cylindrical spindle rotates at a constant rotational speed of 20 RPM while emerged in a cup containing a set volume of asphalt (1,2,5,8). The test measures the torque needed to rotate the spindle and this is converted to viscosity in centipoises (cP) or a millipascal second (mPa·s).

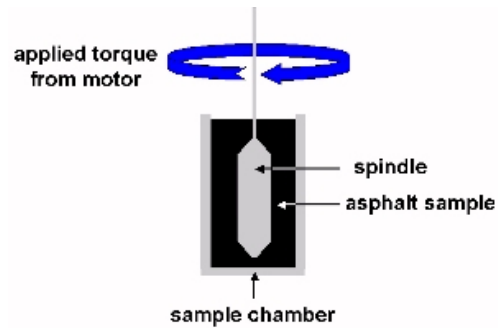


**Figure 9 Couette Rotational Viscometer Schematic**

This test method has generally replaced other viscosity measurements due to the fact that it is applicable with a broad range of asphalts, including those that are polymer modified or contain particulate matter, which generally cannot be tested by capillary tube viscometers. In Superpave, since viscosity does not correlate to a failure mechanism, a maximum value has been set, and any viscosity reading greater than that limit are not workable enough at conventional temperatures.



**Figure 10 Brookfield Rotational Viscometer**

## Rutting Resistance

Rutting is an accumulation of pavement deformations caused by the repeated loading of traffic. As a failure mechanism, it occurs in the wheel path and is most prevalent in warm climates and with soft binders. It is a stress- controlled cyclic phenomenon, when observed in the surface layers of the pavement. Each cycle does work to deform the layer, however some is recovered by elastic rebound and the remainder is lost in permanent deformation and heat (2,5). The work associated can be defined as follows

$$W_c = \pi \cdot \sigma_0 \cdot \varepsilon \cdot \sin\delta$$

Where

$\sigma_0$  = stress

$\varepsilon$  = strain

$\delta$  = phase angle

Given that equation,

$$\varepsilon = \sigma_0 / G^*$$

Where

$G^*$  = complex shear modulus

And it can be further manipulated to show that work dissipated per loading cycle is

inversely proportional to  $G^*/\sin\delta$

$$W_c = \pi \cdot \sigma_0^2 \cdot [G^*/\sin\delta]^{-1}$$

In this equation,  $G^*$  represents the total resistance to deformation and  $\sin\delta$  is the relative non-elasticity, as well as the ratio of the loss modulus,  $G''$ , to the complex modulus,  $G^*$ , the permanent component of deformation. Based on this relationship, rutting resistance can be improved by increasing the value of  $G^*$  or decreasing the overall non-elasticity

(2,5,8).  $G^*$  and  $\delta$  are functions of temperature and frequency of loading and as  $G^*$  increases and  $\delta$  decreases a pavement exhibits greater resistance to rutting. As such, the specifications set the test parameters as the 7-day maximum temperature and a frequency of 10 radians/ second, which is representative of a stress wave from a vehicle traveling 50 to 60 mph (5). In the testing paradigm, samples are tested at a uniform frequency, but the binder the testing temperatures will vary. These measurements allow for the engineering properties such as the visco-elastic nature of the material, climactic conditions and loading conditions to be taken into account. This was not possible for conventional binder testing methods, and pavement distress can be better understood as a result.

A Dyanmic Shear Rheometer tests original and RTFO aged binders' resistance to rutting. As previously mentioned, the testing parameters involve a frequency of 10 radians/ second and a temperature based on the 7-day peak of a roadway. The results of the test yield the stiffness, which is found by dividing  $G^*$  by  $\sin\delta$ . Due to oxidative aging,  $G^*$  increases and  $\sin\delta$  decreases, indicating that once a material is aged it demonstrates a greater resistance to rutting, making the early characteristics more critical than that of the aged (2,5). For this reason, the failure parameters are different for virgin and aged material. Virgin tested material fails at the temperature where the  $G^*/\sin\delta$  value is less than 1 KPa, and RTFO aged material fails when it is less than 2.2 Kpa. The samples are tested in 6°C increments, which correlate with the common grade temperatures of asphalts produced. Samples are tested using 25 mm geometries and a working gap of 1 mm. The sequence run for original and RTFO material is identical with the exception of the failure parameters.



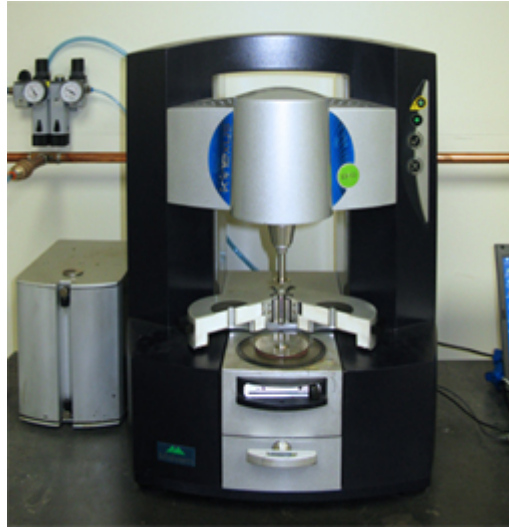


**Figure 11 Dynamic Shear Rheometer**

### **Fatigue Cracking Resistance**

Failure due to fatigue cracking is not as prevalent or visible as that of rutting, but the SHRP committee felt that it was worth testing and better understanding. Depending on whether the pavement is thick or thin, fatigue cracking is controlled by stress or strain. In the case of thin pavement layers, it is strain controlled and becomes a prominent failure mechanism. As a result, deformations occur from a lack of support from subsurface layers (1,5,8). This can occur due to poor design or construction as well as saturation of base layers in rainy seasons.

The work dissipated per loading cycle is represented by the following equation

$$W_c = \pi \cdot \sigma \cdot \epsilon_0 \cdot \sin \delta$$

Where under strain controlled conditions

$$\sigma = \varepsilon_0 \bullet G^*$$

And thus

$$W_c = \pi \bullet \sigma \bullet \varepsilon_0^2 \bullet [G^* \bullet \sin \delta]$$

The work in this situation is dissipated via cracking, crack propagation, heat or plastic flow. Dissipation is limited by limiting the value of  $G^* \bullet \sin \delta$ . A lower  $G^*$  value indicates a softer material more apt to deform without developing large stresses and cracks. When  $\delta$  is smaller, the binder tends to be more elastic and recover without dissipating energy.

The material tested for fatigue cracking failure is aged by the Pressure Aging Vessel (PAV) in order to simulate the worst case scenario for oxidative aging. The PAV simulates the aging that an asphalt might experience in a 5 to 10 year period by aging a binder sample for 20 hours at 350psi and at 100°C (2).



**Figure 12 Pressure Aging Vessel & Degassing Oven**

The critical parameter is the value of  $G^*$ , which is increased significantly after being PAV aged. This test is also run on the DSR, but instead of using the 25mm geometries and a 1mm working gap an 8mm sample is tested at a 2mm gap (2). This is due to the increased stiffness of the material and the limitations of the torque induced by the DSR. Additionally, the testing temperature is the intermediate temperature as determined from the 7-day maximum and single day lowest design temperatures of the asphalt (2,5). Intermediate temperatures were selected since most fatigue cracking failures occur when the material is stiff, but not due to extreme thermal conditions. Similar to the Original and RTFO tests, a 10 radians/ second loading cycle is used to simulate traffic conditions.

### **Thermal Cracking Resistance**

The fourth failure mechanism examined by the SHRP committee was thermal cracking. As a result of environmental cooling, stresses develop within the asphalt due to thermal shrinkage (1,5,8). In colder regions this serves as the predominant failure mechanism.

When asphalt is cooled, the shrinkage of the asphaltic layer is restricted, resulting in tensile stresses from the friction underlying layers that are either warmer or have a smaller coefficient of thermal contraction. If these stresses exceed the tensile stress of the material and if they are not relaxed by the flow of the asphaltic layer, cracking may occur (5). Stresses depend upon the stiffness and relaxation. Stiffness can be defined as the resistance to deformation within the asphalt. In the past thermal cracking was solely correlated with stiffness, but this does not take into account asphalt's viscoelastic properties and ability to relax. Even under cold temperatures, asphalt is still able to relax

stresses by dissipating energy (5). When an asphalt flows under stress and has less of an elastic response, it is better able to relax the stresses endured under the conditions that cause thermal cracking.

In order to evaluate an asphalt's resistance to thermal cracking, the Bending Beam Rheometer (BBR) was developed. This instrument takes into account both the stiffness and relaxation rates by evaluating the creep response. In order to make the test viable in the production laboratory setting, the traditional 7200-second loading time was reduced and correlated to a much shorter 240-second period. Due to the shorter testing period, the temperature needed to be increased 10°C for the test to remain accurate. Based on the testing specifications, maximum stiffness and minimum relaxation rate values are set forth to be 300 MPa and 0.3 respectively.



**Figure 13 Bending Beam Rheometer**

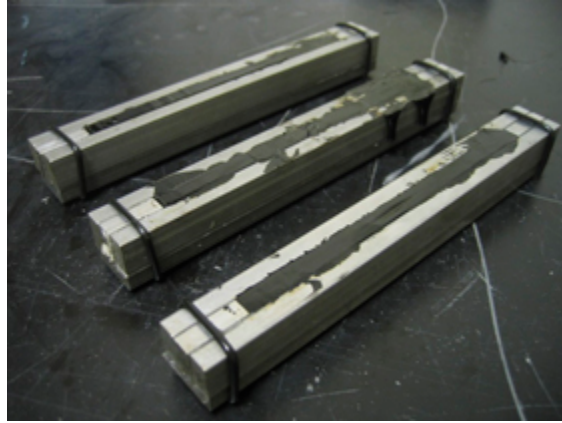


**Figure 14 Molded Asphalt Beams**

## **Chapter 4: Master Curves**

### **INTRODUCTION**

Asphalt binders behave differently in cold, warm and hot temperatures and as such need to be evaluated by different means. With the exception of certain polymer modified asphalts, most asphalts fall under the thermo-rheologically simple material (TSM) category. “TSMs are a special class of viscoelastic materials whose temperature dependence of mechanical properties is particularly responsive to analytical description. This group of materials allows for a simple and realistic viscoelastic elastic equation for which response under constant temperatures can be used to predict response under transient temperatures”(9).

### **BACKGROUND**

#### **Master Curve Components**

Generally speaking, at extremely low temperatures, asphalt acts as a glassy solid. Binders transition to an elastic solid at slightly warmer temperatures, followed by a transition to viscoelastic material at intermediate temperatures and a viscous liquid at high temperatures. The temperature ranges listed are general, but cover the majority of asphalt binders. In the viscous range, binders may act as a Newtonian, Dilatant or Pseudoplastic fluid. The majority act linearly, as a Newtonian fluid, meaning that as shear stress increases, as does shear rate and vice versa. Asphalt binder that contain certain polymers act as shear thickening or dilatant fluids. As such, when shear strain is increased, as is the viscosity. On the contrary, warm asphalts, that have not entered the

linear range of a Newtonian fluid, may act as a pseudoplastic or shear thinning fluid. In this range, the viscosity decreases with an increased shear rate.

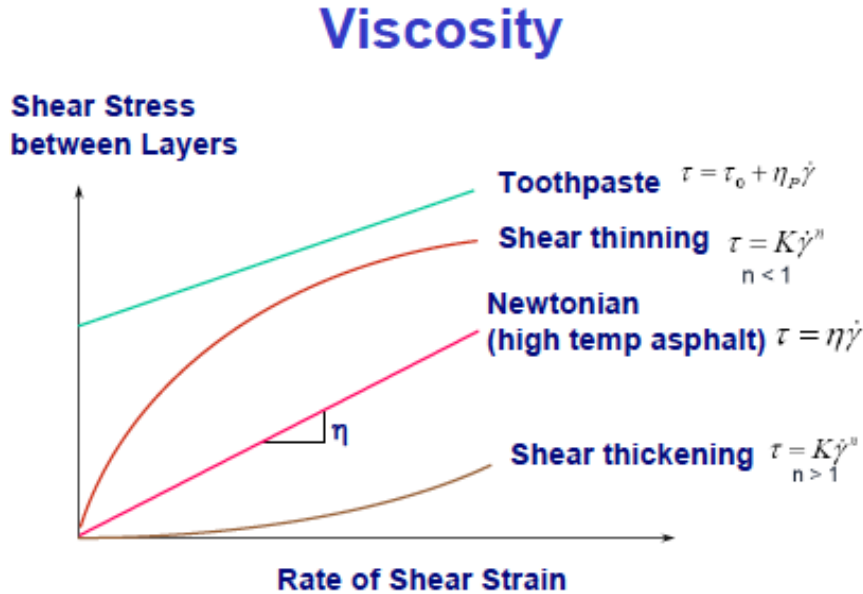


**Figure 15 Viscous Material Categories (11)**

In the case of a Newtonian fluid and a TSM, there is a similarity between the effects of time and temperature on characteristics such as modulus, compliance, etc. As such, properties measured at different temperatures for shorter time, or frequencies, can be shifted to obtain properties along larger time, or frequency, scales at a single temperature. The shift factor is a function of temperature and the time, or frequency becomes reduced after time- temperature superposition.

As stated before, the DSR results yield  $G^*$  and  $\delta$ , which are the complex modulus and phase angle respectively. In the case of Superpave, these have been used to grade asphalt binders by using the aforementioned criteria and a pass/ fail system. The complex shear modulus is defined as

$$G^* = \tau_{\max} / \gamma_{\max}$$

Where

$$\tau_{\max} = \text{Max stress}$$

$$\gamma_{\max} = \text{Max shear strain}$$

The complex shear modulus allows for the gap between the elastic and viscous phases to be spanned. In the elastic realm, the graphs of stress and strain are in phase,  $\delta = 0^\circ$ . In the viscous phase, the strain is out of phase with the stress,  $\delta = 90^\circ$ . The complex modulus can be seen as a vector sum of the storage and viscous modulus, as seen below

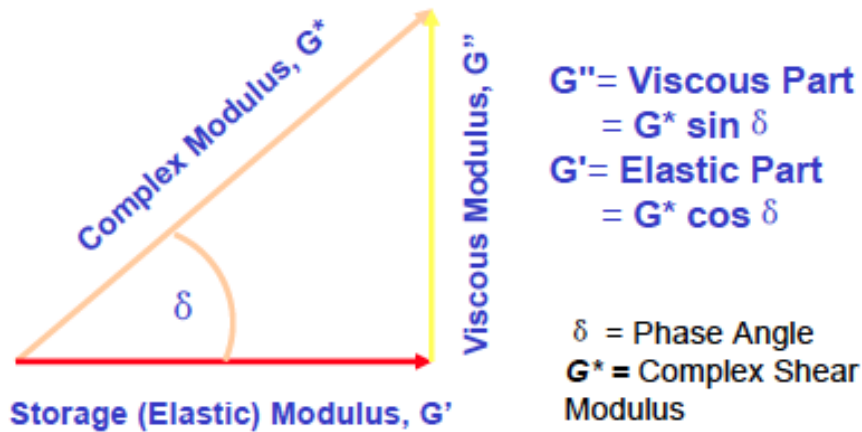


**Figure 16 Correlation of  $G^*$ ,  $G'$  &  $G''$  (11)**

The elastic and viscous components of the complex modulus are also known as the storage ( $G'$ ) and loss ( $G''$ ) moduli, both of which serve their purposes in the evaluation of other binder properties.



The creation of an asphalt binder master curve is reliant on four factors, the complex modulus, the frequency, the temperature and the shift factor. A master curve can be defined as the variation of  $G^*$  or  $\delta$  as a function of frequency at a constant temperature. An isochronal curve is the variation of  $G^*$  or  $\delta$  as a function of temperature at a given frequency or loading rate (12).

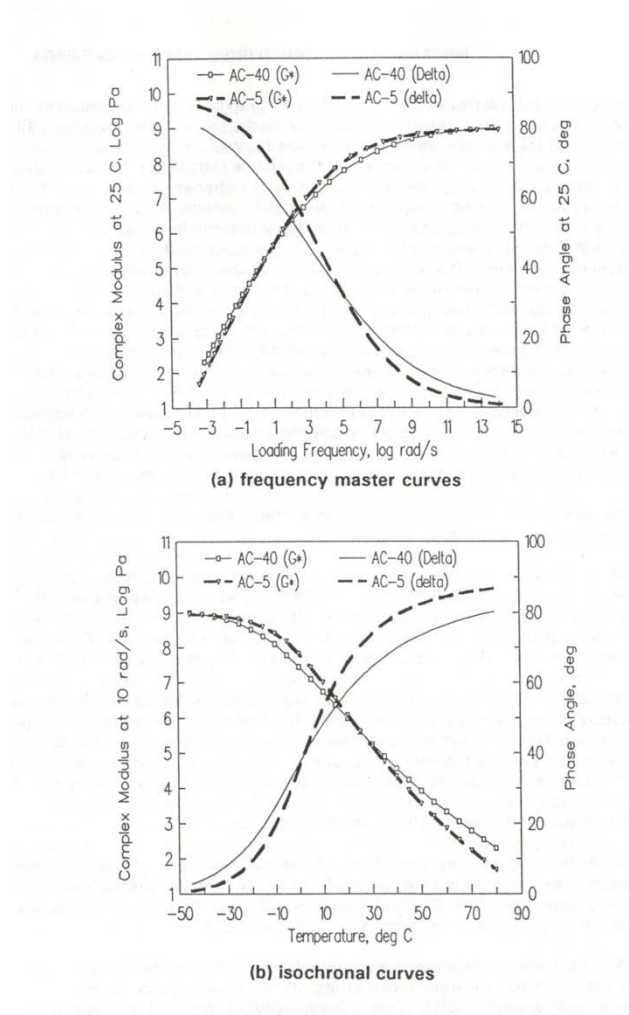


**Figure 17 Typical rheological spectra for AC-5 and AC- 40 asphalt binders (3)**

The figures above represent a sample that has already been shifted. In the case of the master curve, a sample is run through a frequency sweep in order to extract the raw data required. The sample is run at a selected range of frequencies for each desired temperature and the  $G^*$  or  $\delta$  values are extracted. These can then be plotted as a discrete temperature frequency sweep and then the data can be shifted to become a continuous master curve.

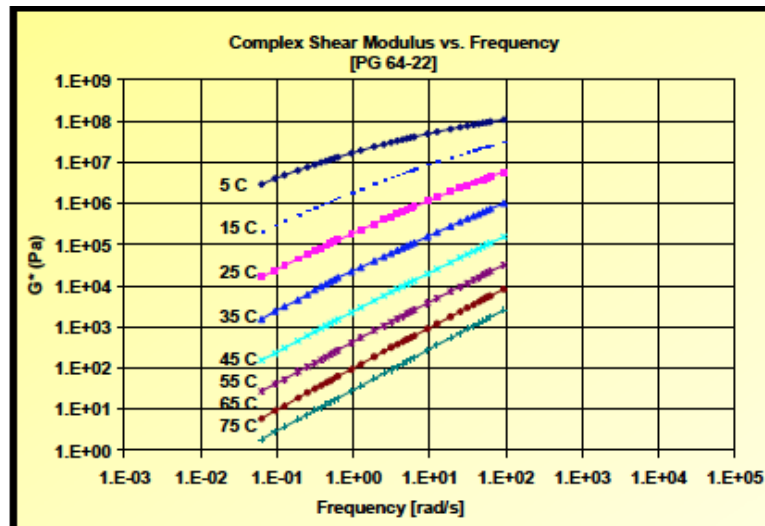


**Figure 18 Typical Frequency Sweep (11)**

### Shift Factors

Different shift factors exist which allow the discrete data to be converted into a master curve. When shifting asphaltic materials, four shift factors have been most commonly used, they include the Arrhenius Model, Williams-Landel-Ferry Model (WLF), the Sigmoid Model and the Christensen- Andersen - Marasteanu Model (CAM). In each case, an arbitrary reference temperature,  $T_{ref}$ , is selected and at this temperature the shift factor

is equal to 1. For fluids obeying the Arrhenius laws of reaction rates, the following shift factor is applicable:

$$\text{Log } a_t = E / 2.03R (1/T - 1/T_{\text{ref}})$$

Where

$a_t$  = shift factor

$E$  = activation energy (J/ mol)

$R$  = ideal gas constant (J/ mol. K)

$T$  = experimental temperature (K)

$T_{\text{ref}}$  = reference temperature (K)

The second model commonly used for shifting master curves is the WLF shift factor in which:

$$\text{Log } a_t = - C_1(T - T_{\text{ref}}) / C_2(T + T_{\text{ref}})$$

Where

$a_t$  = shift factor

$C_1, C_2$  = empirical constants or pre-determined variables

$T$  = experimental temperature (K)

$T_{\text{ref}}$  = reference temperature (K)

WLF yields good results about the glassy transition temperature of a sample based on free volume concepts, however below this temperature, the sample is undergoing physical hardening and free volume is changing with time, so Arrhenius yields better results(12).

The sigmoid model is primarily used when creating master curves of asphalt mixtures and as such will not be discussed here. The CAM model is primarily applicable to fit master curves to BBR creep stiffness data (12).

Shifting frequency sweep into a master curve allows for interpolation and extrapolation of the data. By utilizing any of the above shift factors, or by manually shifting the data a user may create a master curve. However, this can become extremely tedious and laborious especially with large data sets. As such software has been developed to manipulate extracted data and create master curves as well as other useful plots. The software utilized for this set of experiment was RHEA produced by Abatech Inc. The analysis is done using the shifting procedures defined by Gordon and Shaw (1994). In this method, the initial shift is done using WLF parameters. The data is then refined by using pairwise shifts and straight lines representing each data set, and then using pairwise shifts with polynomials representing the data being shifted. The order of the polynomial is an empirical function of the number of data points and the decades of time / frequency covered by the isotherm pair. This gives shift factors for each successive pair, which are summed from zero at the lowest temperature to obtain a distribution of shifts with temperature above the lowest. The shift at  $T_{ref}$  is interpolated and subtracted from every temperature's shift factor, causing  $T_{ref}$  to become the origin of the shift factors (13).

The RHEA software not only yields a master curve graph, which allows for interpretation of data between and beyond data points for  $G^*$  and  $\delta$  for a reference temperature, but it also gives a multitude of other plots that provide additional information as well as validate or invalidate the results of your master curve. In order for a master curve of pairwise shifts to be created in the first place, the data points in each isotherm cannot have extreme error. This is not always possible due to errors with the DSR, material or other outside source, but with RHEA outlying points may be removed to create the master curve. Other plots developed from the raw data include Transient Modulus Stiffness Master Curve Graph, Transient Compliance Master Curve Graph, Storage and Loss Modulus Master Curve Graph,  $G^*$  versus  $\delta$  - Black space, Arrhenius shift factors and WLF shift factors (13).

### **Black Space Diagrams**

Black Space or Black Diagrams are particularly useful in determining or detecting testing errors. As mentioned above, RHEA allows for any outlying points to be removed in order for the master curve to be created. However these points may not actually be outliers, but may be a result of testing errors such as gouging the material, improper testing temperatures, incorrect torque, or a compliance issue. Since asphalt binders do not exhibit sudden changes in their behavior with respect to time or temperature, any discontinuities may be a result of testing error. The Black Diagram is a plot of phase angle ( $\delta$ ) versus  $\log |G^*|$ , which does not require the data to be shifted. A smooth Black Diagram should result if the material is linear, thermorheologically simple and if there are not testing errors. On the contrary if any of the aforementioned conditions are not met, the diagram will be a series of disjointed lines. At high temperatures, the graph should

reach a horizontal asymptote as it enters or comes near the realm of behaving as a Newtonian Fluid. At low temperatures where the phase angle is approaching zero, the plot should come close to intercepting the  $|G^*|$  axis at the glassy modulus (14).

### **Problems with Traditional Master Curves**

A traditional master curve is done using the 8 mm or 25 mm plates with unaged, RTFO aged or PAV aged material. Recently, master curves have been used on extracted asphalts as a tool for forensic analysis. However, due to limitations of both the equipment and material, this must be done in two or three separate tests. Traditional parallel plates have testing problems at both high and low temperatures. At high temperatures, asphalt materials have the potential to flow out from between the plates and give inaccurate readings. At low temperatures, the DSR is limited by the torque it is able to produce. Since the binder is incredibly stiff at these temperatures, the machine is not able to obtain to proper frequencies and in some cases may break the sample due to the force. Additionally, at low temperatures the samples may not bond to the plates and as a result will produce inaccurate readings and results (15). To fix this problem, the low end of the master curve is commonly created using BBR results. This stiffness data can be converted into  $G^*$  by dividing it by 3 and the time can be converted to radians/second, or frequency, by taking the inverse. Although this makes for a very good approximation, there are other more accurate ways in which the low temperature end of the master curve spectrum can be demonstrated using only the DSR.

By using a series of three geometries, a user can collect data from the low, intermediate and high temperature ranges. At the intermediate temperature range, parallel plates are

utilized, as in a traditional master curve. For low temperatures where the stiffness is high, a torsion bar fixture can be used in the DSR. This allows for the same oscillating movement that the parallel plates exhibits on the sample. In this way  $G^*$  and phase angle are measured directly as opposed to approximating it as with the BBR data. For high temperatures, a cup and bob apparatus is used. This enables the operator to get data at the range where the binder transitions to a Newtonian fluid. In the viscous ranges on parallel plates the material tends to flow out, however with the cup and bob this is not the case. Although the use of these three geometries yields more accurate measures of  $G^*$  and phase angle there are issues that arise. The torsion bar sample is very difficult to mold and load, as such it has not caught on as broadly as the use of the BBR approximation. Additionally as with the BBR approximation, a large quantity of asphalt is needed for both the torsion bar and cup and bob apparatus. The amount of time required for the molding and testing of the torsion bar and BBR samples is also a factor that affects the efficiency of the testing process both time wise and monetarily (15).

In order to create a master curve utilizing one sample and one testing machine the DSR plates, cooling system and sample need to be modified. By altering these three factors, a sequence can be created and used that will evaluate a binder from the glassy modulus to the transition to a Newtonian fluid. Instead of using 8 mm or 25 mm plates 4 mm plates were machined and utilized. Due to the smaller area of the geometries, a higher torque can be exacted on the sample without having to increase the torque in the machine, which would be a costly upgrade, or require a whole new machine altogether. By upgrading the cooling system, the DSR can reach the temperatures required to reach the glassy modulus, or at least the temperatures at which the BBR tests samples. Altering the

cooling system from cycling room temperature water to cool the peltier plates to cycling colder water or coolant can allow the temperature to drop enough to test the sample.

Finally, the sample needs to be molded and trimmed properly due to the amount of error that can come about from gouging the sample or leaving excess material. Once all of these issues are addressed and the compliance is corrected for the sample a complete master curve can be completed using very little material at a much lower time and money cost.



## **Chapter 5: Work Plan**

### **DETAILED WORKPLAN**

A thorough Literature Review on relevant published journal articles, technical reports, and conference presentations regarding binder testing, binder master curves and the 4 mm DSR geometries has been conducted. Based on the Literature Review and proceedings at technical conferences, the following workplan was developed.

#### **Subtask 5a – Determine limitations of equipment and run preliminary trim trials**

The researcher shall run preliminary tests to determine the limitations of the equipment. This shall be done in order to determine the sample type to be tested in the apparatus.

The test to be completed runs a temperature and frequency sweep in order to develop a master curve of the asphalt binder. In order to do so, the temperatures range from the point at which glassy transition occurs until the material exhibits viscous properties. The latter has already been determined to be around 60 - 70°C from previous tests. Glassy transition on the contrary occurs at very low temperatures, as cold as -40°C. As such, it was necessary to determine the limitations of the DSR in the realm of cooling. This was done by loading a sample and having the machine hold the temperature for a period of 20 minutes. This period is representative of the amount of time required to bring the sample to temperature as well as run the test. The DSR without modifications was only capable of maintaining temperatures of about 0°C. The DSR cools and heats by using peltier plates and a heat exchanger, the latter fails to maintain cold temperatures because the cooling fluid heats up to a temperature where it can no longer cool the peltier plates. As such, alternative solutions were examined, the first of which included buying a new heat

exchanger designed to work at very cold temperatures. However, this was not economically viable. Instead, a cooling system was built as an add-on to the existing heat exchanger. This system acts as an extra cooling chamber in order to keep the heat exchanger fluid cool enough to allow the temperature to drop and stabilize. Following trials to determine the threshold of the cooling apparatus, the coldest maintainable temperature was  $-20^{\circ}\text{C}$ . Although this was not as low as reached in other researcher's tests, it was the upper limits of the equipment's threshold in the working budget.

At the onset of testing, molds and a trimming device had to be specified. Due to unavailability of a 4 mm DSR mold, the 8 mm mold was utilized and excess material was to be trimmed accordingly. Initially, the same trimming tool as used with traditional DSR samples was tested. This was unfit because the dimensions were too large to work with the alternate geometries and smaller sample size. As such an alternative trimming tool was developed. This tool was modified from existing mini stainless steel lab spatulas. Because of the dimensional constraints, the minimum spatula thickness, as outline in the DSR specifications, was ignored, and a smaller tapered spatula with a width of  $\frac{1}{4}$ " was selected. This was seen as acceptable because the maximum working gap to be utilized was to be 2 mm, and the trimming tool was 6.35 mm, giving enough excess surface area for the purpose. However, since no square spatulas were available in this size needed, modifications were necessary. As with all trimming tools, it was necessary to bend the tool approximately  $45^{\circ}$  in order to enable the operator to properly trim the sample. However this specific tool was tapered, so the edges were ground flat so that the trimming contact area was straight and able to contact the sample properly.

In order to enable to operator to get precise results, it was necessary to run a series of trim trials. The nature of DSR operation requires some practice in trimming the samples, and due to the smaller surface area of the sample in conjunction with the use of stiff material, the possibility for error is great. As such, in order to reduce error, trimming was practiced until the results garnered from multiple tests had similarities in line with the precision and bias of other DSR tests, which was under 7% error. The sample to be used was a fairly stiff polymer modified binder, a PG 82-22, which would be representative of the stiffness encountered by most RTFO or PAV aged binders, which could be used in the future. Due to the nature of the smaller geometry and the stiff material, the possibility of incorrectly trimming the sample by gouging out material or leaving excess material is increased. Because of the smaller surface area of the geometries, any trimming errors will be greatly represented in the results and should be avoided as much as possible. Trim trials were conducted by trimming the sample at multiple heights in order to give to reduce error. A working gap of 2 mm was decided upon and as such the material was loaded and an initial trim gap of 2.5 mm was selected. This allows for a 'rough trim' to be performed prior to the final trim. The material is loaded at 45°C, the same temperature used for 8 mm PAV DSR testing. Following the initial trim, the material allowed to reach temperature for approximately 5 minutes before the final trim. The final trim occurs at 2.1 mm, and the working gap is 2.0 mm, which allows for the characteristic 'bulge' at 5% of the working gap, as outlined in DSR specifications. The material is ready to run once trimming is completed.

Following trim trials, the torque at low temperatures was evaluated. Prior to this, a correction and compliance factor was applied in order to account for any changes in gap

height occurring due to thermal expansion or contraction of the material or plates. This ensures that a gap of 2 mm was continuous throughout the duration of the test. The torque evaluation involved completing a frequency sweep at low temperatures and examining the sample to see if there was physical evidence of a break as well as the harmonic distortion values, which are indicative of poor results. High harmonic distortion values, greater than 10%, mean that an error of some sort occurred during the test and generally invalidate the results for that run. From these results, the researcher could determine the working temperatures, strain rates and frequencies to be used for the 4 mm master curve portion of the study.

#### **Subtask 5b –Determine the materials to be tested and their properties**

The researcher shall determine the asphalt binders to be tested as well as performance grade them. The binders selected should have varying properties. As such, three binders were chosen for this experiment. They include binders of with different high and low temperature grades. This will allow the researcher to determine the effectiveness of the test for different binder grades. The grades selected include a PG 76-22, a PG 64-28, a PG 64-22 and an extracted binder equivalent to an 82-22. Each of these binders has strengths and weaknesses in different failure mechanisms. The PG 64-28 is designed to endure colder temperatures and not crack as readily in cold pavement temperatures. This binder would be used in the Northeast as well as other areas that have fatigue cracking problems due to winter conditions. The 76-22 and the extracted binder are not expected to fare as well in the colder climates when evaluated for fatigue cracking. However, they are both designed to prevent failure by rutting, or with the high temperature susceptibility in mind. Additionally, the extracted binder represents an inherently stiffer material that

has limited quantities. This is of particular interest because the 4 mm master curve can characterize the low, intermediate and high temperature properties of a binder with much less material, saving time and money. The selected binders will be performance graded, as per the ASTM specifications, as well as run through traditional and 4 mm master curve sequences.

#### **Subtask 5c –Evaluate results and make recommendations**

Following the completion of the testing portion of the study, the results are to be compiled and evaluated to determine whether or not the 4 mm testing sequence and cooling apparatus yield results similar to those produced by others. By creating master curves using the 4 mm data and that of the traditional master curve including the low temperature BBR conversion. By doing a full master curve ranging from low, thermal cracking range temperatures up to high, rutting resistance temperatures, the researcher is able to see how the new method of creating master curves compares with the traditional methodology. The data will be plugged into RHEA, which is the conventional analysis tool for Mechanistic Empirical Pavement Design Guide (MEPDG). Following this, it will be analyzed and the researcher will determine if it is necessary to apply a correction factor based on the different binder types or if the data correlates directly. If it does not correlate to all binder types, the researcher will recommend additional testing with various binders to determine whether or not this is a viable test method for the testing needs of the laboratory. If the data does correlate directly, it will be recommended that additional testing, such as round robin studies, be conducted in order to ensure that the results yielded by the laboratory are comparable with those of other laboratories. In this way it will be possible to create a viable ASTM specification in the future.

## EQUIPMENT

In order to complete the research required to set up and execute the 4 mm sequence, equipment needed to be modified or built. The first piece of equipment was the trimming tool. As mentioned above, the tool used and specified for most other DSR applications is too large. A small laboratory spatula had to be modified to allow the operator to properly trim the sample. This was done by taking the spatula, bending the tip to a 45° angle as well as sanding all of the rounded edges to become squared off. Pictured below is the modified trimming tool as well as the traditional tool for size reference.



**Figure 19 Modified Trimming Tool**



**Figure 20 Traditional and Modified Trimming Tools**

In addition, a cooling device needed to be built to account for the fact that the heat exchanger could not reach nor maintain the temperatures required for the test. The options presented included purchasing a heat exchanger specific to the DSR used in the lab, which would cost \$12,000 or build one out of common materials for under \$200. The latter option was chosen due to budgetary constraints. The cooling chamber was built out of an Igloo 40 – quart cooler with a drain installed.



**Figure 21 Cooling Chamber with Drain**

Next, copper was coiled in order to create the most surface area to be cooled. Each of the ends of the copper coil was fitted with nipples, which along with hose clamps allow for the polyurethane tubing of the DSR for to connected.



**Figure 22 Copper Tubing with Nipple Attachments**

This copper coil can then be placed inside the cooler. The shape is ideal because it is wide enough to allow for ice molded from a 6 –inch diameter cylinder to be placed inside of it. The cooler can then be filled with additional water and ice to continue to cool the fluid in the DSR as the test is run.



**Figure 23 Cooling Chamber During the Test**

The final and most important component of the test are the 4 mm parallel plates. These were machined specifically for this test. Below they are pictured alone, with the 8 mm plate for size reference and loaded with a sample.

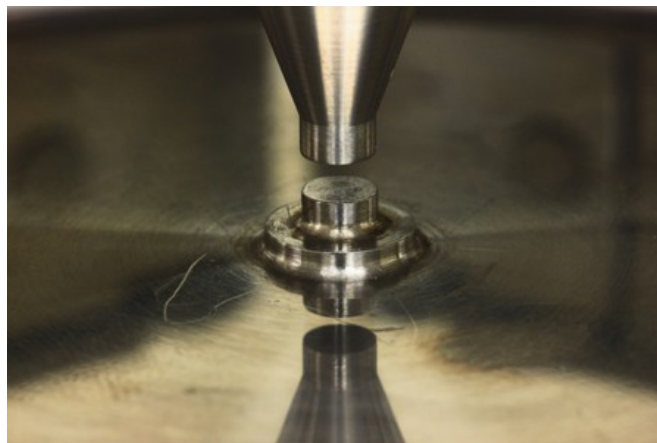


**Figure 24 Parallel Plates Unloaded (4mm)**





**Figure 25 Parallel Plates for Size Comparison (4 mm Top, 8 mm Bottom)**

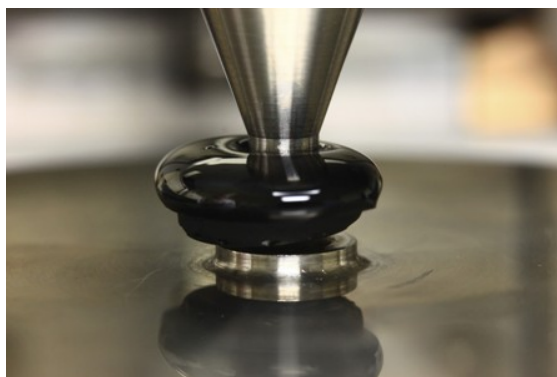


**Figure 26 Sample Being Loaded on 4 mm Plates**

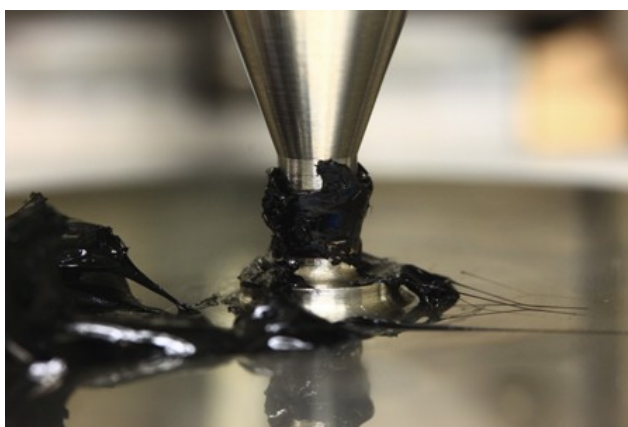


**Figure 27 Trimmed Sample on 4 mm Plates**

## **Chapter 6: Results**

### **INTRODUCTION**

The master curve data from any sample allows one to analyze the full spectrum of behaviors from glassy modulus to Newtonian flow. In the case of this experiment, glass transition temperatures could not be achieved due to equipment limitations. As such, the results consist of a comparison of the traditional and 4 mm master curve at temperatures ranging from below the temperature of the BBR tests up to intermediate/ high range temperatures.

### **METHODOLOGY**

To analyze the data from the 4 mm sequence, it is necessary to break it into four distinct categories. The first series of data required is the continuous grading information. Prior to any testing either with traditional master curves or 4 mm master curves, the materials being tested had to be evaluated. From these evaluations, the general characteristics and performance grades are determined, as well as the BBR data, which is necessary for the traditional master curve. The second necessary piece of information is the frequency sweep. These are the raw data points that have not been shifted. The next set of data is the master curves that have been shifted. These can be overlain with one another to see variations, error and precision of the different materials and tests. Finally, the black space diagrams can be used in conjunction with harmonic distortion and individual isotherm data to determine the error present and whether or not the test results can be viewed as accurate.

Each material was run multiple times as a 4 mm frequency sweep and an 8 mm frequency sweep with BBR data to supplement. Below are the RHEA and Excel graphical representations for selected materials.

### **Continuous Grading**

The binders selected were chosen based on the fact that they ran the gamut for binders utilized in the northeast region. Generally speaking, most binders in the region are a minimum of a PG 64-XX on the high temperature end, meaning that if the pavement temperatures exceed 64°C (~148°F) for seven consecutive days, the material may rut. Based on the climactic conditions, temperatures in excess of 64°C are generally not attained in the northeast region, however many major roadways are as PG 76-XX or higher for durability and longevity, and as a result they rarely fail due to rutting. On the contrary, in the northeast, asphalt pavements have issues with thermal cracking. The majority of binders in use are PG XX-22, meaning that at a one-day low temperature of -22°C (~-8 °F) the pavement may undergo thermal cracking, leading to eventual failure. Some binders used in particularly cold regions may be a PG XX-28, which have greater resistance to thermal cracking.

Below are the binders used in this test and their continuous and performance grades.

<b>Material</b>	<b>Continuous Grade</b>			<b>Performance Grade</b>
	<b>High</b>	<b>Low</b>	<b>Intermediate</b>	
PG 64-22	65.6	-27.1	18.1	64-22
PG 76-22	84.9	-25.7	24.4	82-22
PG 64-28	66.8	-28.3	20.6	64-28
RE Pierson (extraction)	86.5	-18.4	30.5	82-16

**Table 2 Binder Continuous and Performance Grades**

Based on the above grades, an accurate spectrum of the binders used in the northeast was obtained. Particularly with the low temperature grades, there was a good variation, ranging from -28 °C up to -16 °C. In the case of the RE Pierson binder, the original grade was not known since it was a forensic material. The material was cored from a roadway and then extracted using the extraction and recovery procedure. In order to complete a full performance grade on any material. At least a pint of binder (~500 grams) is required. Generally, this is not an issue because binders are supplied in gallon or 5-gallon cans and can be broken down for any testing that needs to occur. In the case of an extracted material, cores are broken down and the asphalt is extracted using trichloroethylene. Each extraction requires a 3000 gram HMA sample, 2 liters of trichloroethylene and typically yields 150 grams of extracted asphalt binder. As such, at least four extractions are required to perform a full performance grade. However, most extracted materials are viewed as at least RTFO age, and to complete the remainder of the performance grading at least 250 grams of material is required, meaning two extractions must be performed. As such, completing a full performance grade on a material can tend to be very costly and time consuming, and if less material is required for testing, time and money are saved.

### **Frequency Sweeps**

For each of the tests, a set of testing frequencies, temperatures and samples per decade were outlined, with a common temperature for a baseline comparison near the reference temperature. These values are delineated in the table below.

Test	Temperatures	Frequencies	Samples per Decade	BBR Data Used?	Reference Temperature
4 mm	-20 °C, -10°C, 0°C, 15°C, 30°C, 45°C	0.1 rad/s to 100 rad/s (0.1- 50 rad/s for 45°C)	5	No	25°C
8 mm	10°C, 20°C, 30°C, 40°C, 50°C, 60°C	0.0628 rad/s to 157 rad/s	3	Yes	25°C

**Table 3 Testing Parameters**

For the 4 mm sweeps, the following temperatures were tested: -20°C, -10 °C, 0 °C, 15 °C, 30 °C and 45 °C. The low end of the spectrum was selected because that was the limitation of the cooling equipment. As the temperatures increased, it was not necessary to have many intermediary temperatures because an adequate master curve was formed with the 15 °C increments. The frequency sweep itself was run from 0.1 to 100 rad/s taking five samples per decade.

The data extracted from the frequency sweep and used in creating the complex modulus isotherms are  $G^*$  and frequency, however phase angle, temperature and harmonic distortion also play key roles. When evaluating raw data, certain errors and discrepancies can be noted without creating a visual representation. In the event that phase angle is not trending correctly in response to temperature increases, the test can be viewed as invalid and the machinery and sample should be inspected. Additionally if temperature is not maintained properly throughout the test, the results become invalidated. The tolerance for a DSR sample run is 0.1°C and anything outside of this range may also invalidate a test. Finally as the test is run, harmonic distortion values are generated. These allow the

operator to see if the sample is being tested correctly and if the test should be aborted.

Any values above 10% distortion are not desirable. If these come as sporadic errors, they may be removed, however if all the values are harmonically distorted the test or that isotherms data may need to be discarded.

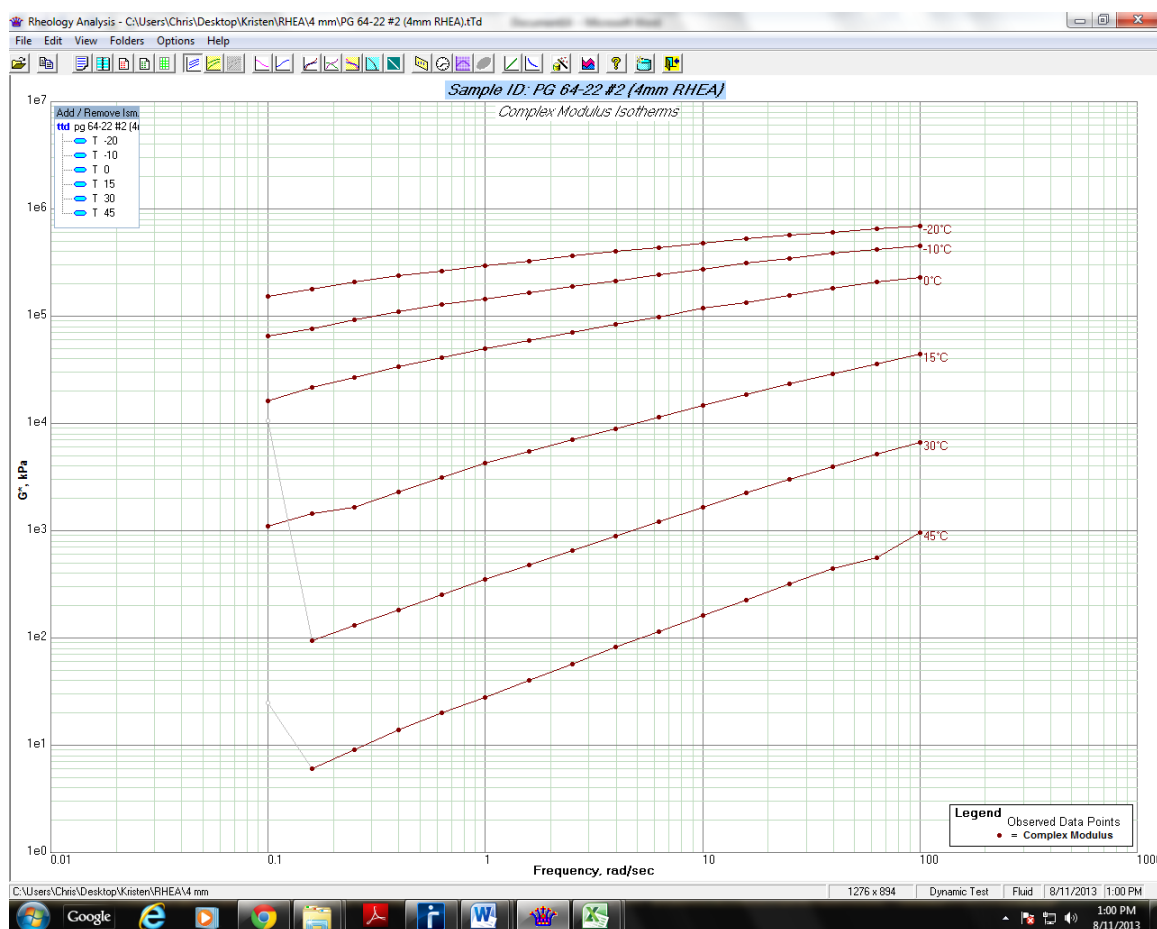


**Figure 28 PG 64-22 #2 Frequency Sweep (4mm)**

Pictured above is a screen shot of the frequency sweep of one of the PG 64-22 samples run on the 4 mm plates displayed in RHEA. The data can be manipulated in Excel as well, however when shifting the isotherms into a master curve RHEA is the interface of choice. This raw data can be manipulated and edited in order to create a shifted master

curve. When performing frequency sweeps, there are often points which have error associated with them. This can be due to outside issues such as vibrations or they can be a result of machine, human or material error. As such, the RHEA software allows for the operator to remove points that are outliers so that a smooth curve can be generated. The screen shot below is an example of a sample ran that has been edited and had outlying points removed.

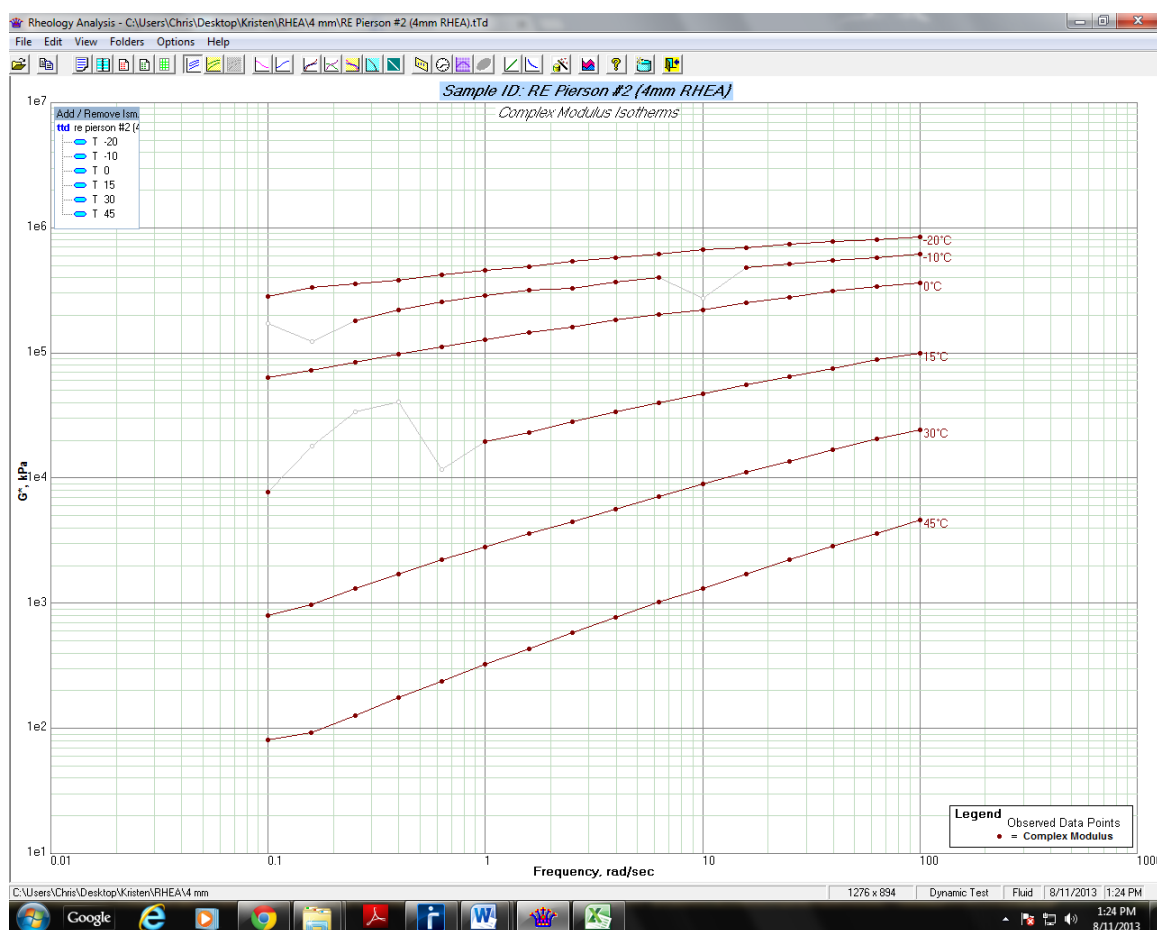


**Figure 29 RE Pierson #2 Frequency Sweep (4mm)**

In some cases, multiple points may have to be removed and if this is the case, the results may need to be discarded or viewed with discretion when creating master curves.

Unlike the 4 mm frequency sweep, the 8 mm plates are not capable of running at temperatures below 0 °C. Although the machine is capable of reaching zero, the sample cracked when attempting to test at this temperature. As such, the 8 mm frequency sweep was run at 10 °C, 20 °C, 30 °C, 40 °C, 50 °C and 60 °C and 11 frequencies from 0.0628 to 157 rad/sec. Since the area of the plate is greater, the applied torque of the DSR is less than that of the 4 mm plates. For this reason, the samples run below 0 °C broke when they were tested at these temperatures and the results had to be discarded. In the same respect, with the 8 mm a higher temperature can be achieved without the torque spinning the sample too much and having inertial effects take over, as was the case with the 4 mm sweeps at higher temperatures. Since low test temperatures were not feasible with the 8 mm plates, an approximation using BBR data had to be employed. By converting the stiffness and time to  $G^*$  and frequency additional isotherms can be generated for the BBR data. This approximated data can then be input into RHEA. Below is a sample of the 8 mm frequency sweep with BBR data.



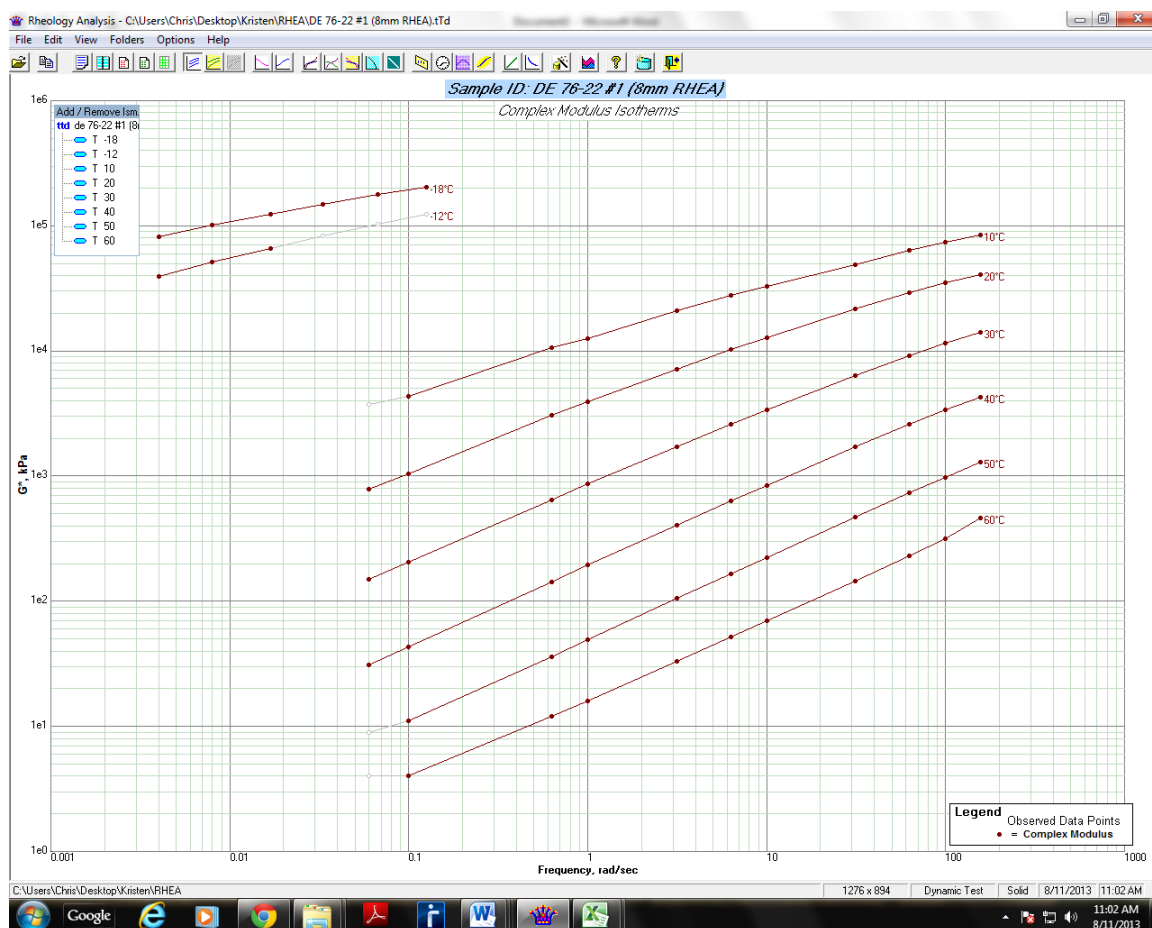


**Figure 30 PG 76-22 #1 Frequency Sweep (8mm)**

Unlike the 4 mm sweeps, which produce smooth data collections of similar length and spacing, the BBR approximation stands out and demonstrates a much larger gap in the data which must later be shifted. This can produce additional error. In the case of the above sample, multiple points of the higher BBR data approximation had to be deleted in order to allow the master curve to be created because otherwise the data does not flow from the BBR points to the DSR points. This problem is alleviated with the use of the 4 mm geometries because there is not large temperature gap between

## Master Curves

RHEA utilizes the WLF shift factors in order to take frequency sweeps and shift them into master curves. These smoothed points can be extracted from RHEA and put into Excel to create plots which can be better analyzed and aggregated than those in RHEA.

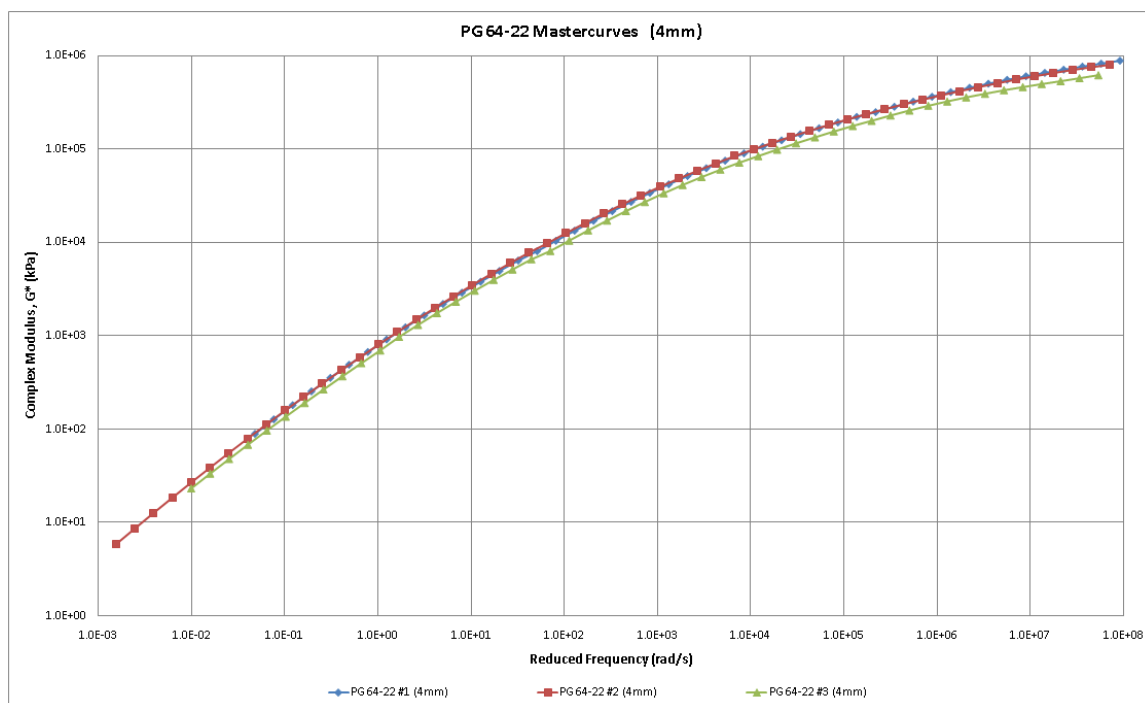


**Figure 31 PG 64-22 Master Curves (4mm)**

The excel chart above is three samples of PG 64-22 run with the 4 mm plates shifted into a master curve. From this chart the results of the 4 mm master curve show that on a log-log plot the three samples from the same operator are similar and indicate that they are from the same material. In this case, PG 64-22 #2 (4mm) extends beyond the end points of the others for the low  $G^*$  values because fewer points in that raw data needed to be hidden to create the master curve. The other three binders run on the 4 mm plates also

displayed similar results, allowing the researcher to conclude that the test was producing precise results within itself.

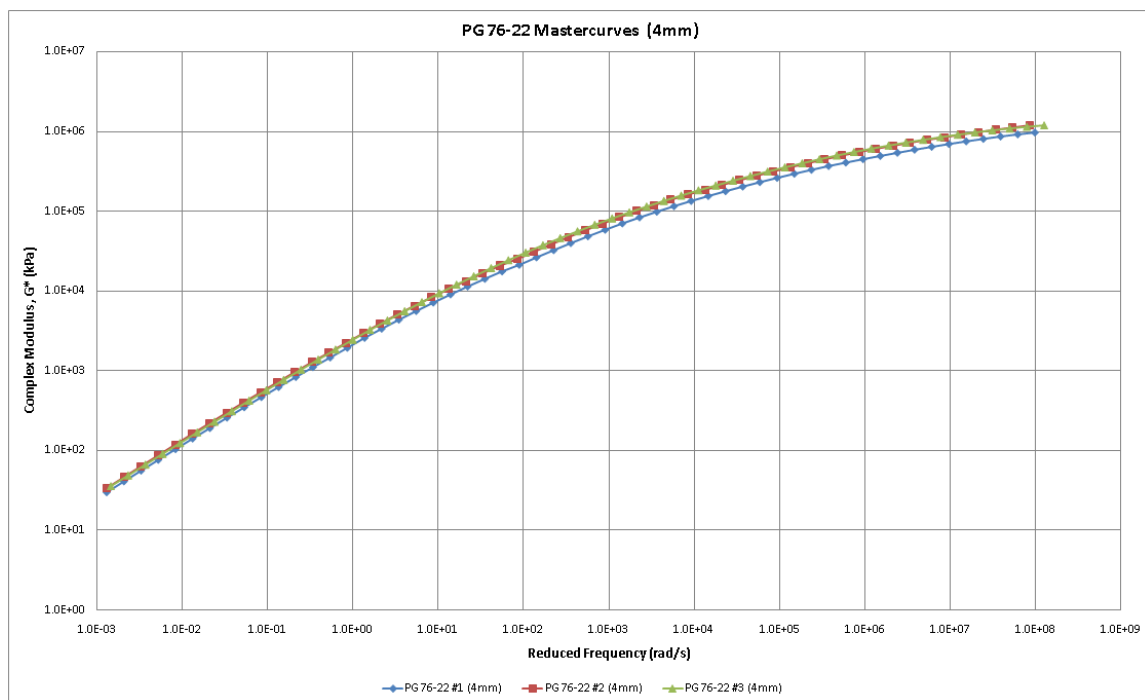


**Figure 32 PG 76-22 Master Curves (4mm)**

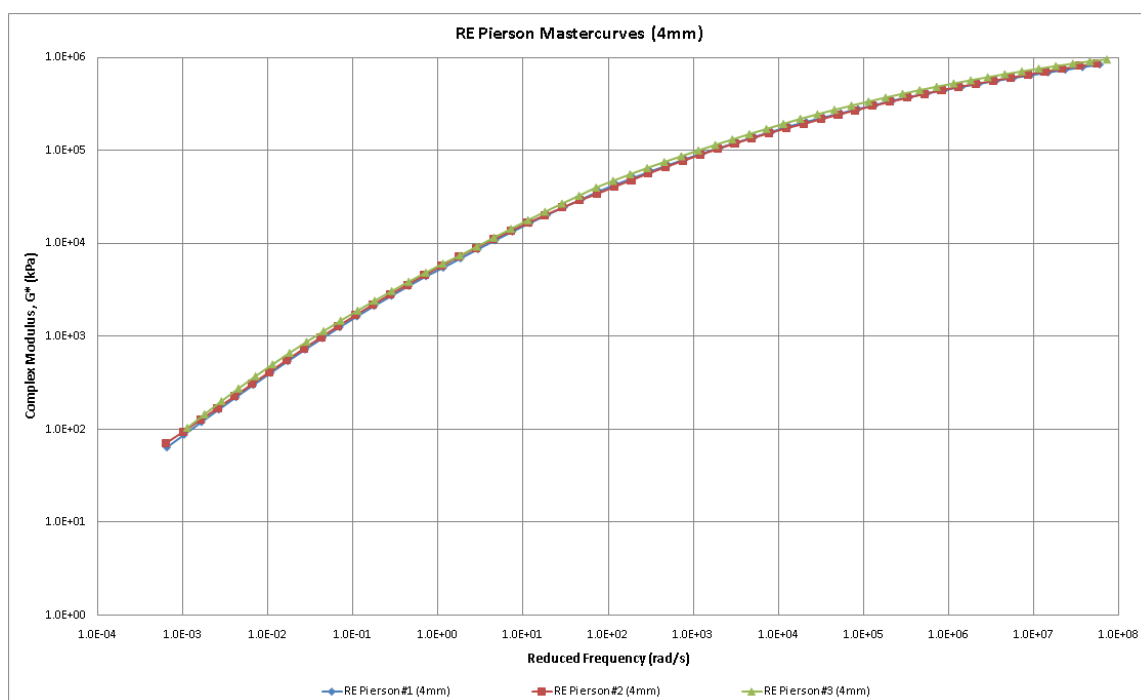


**Figure 33 RE Pierson Master Curves (4mm)**

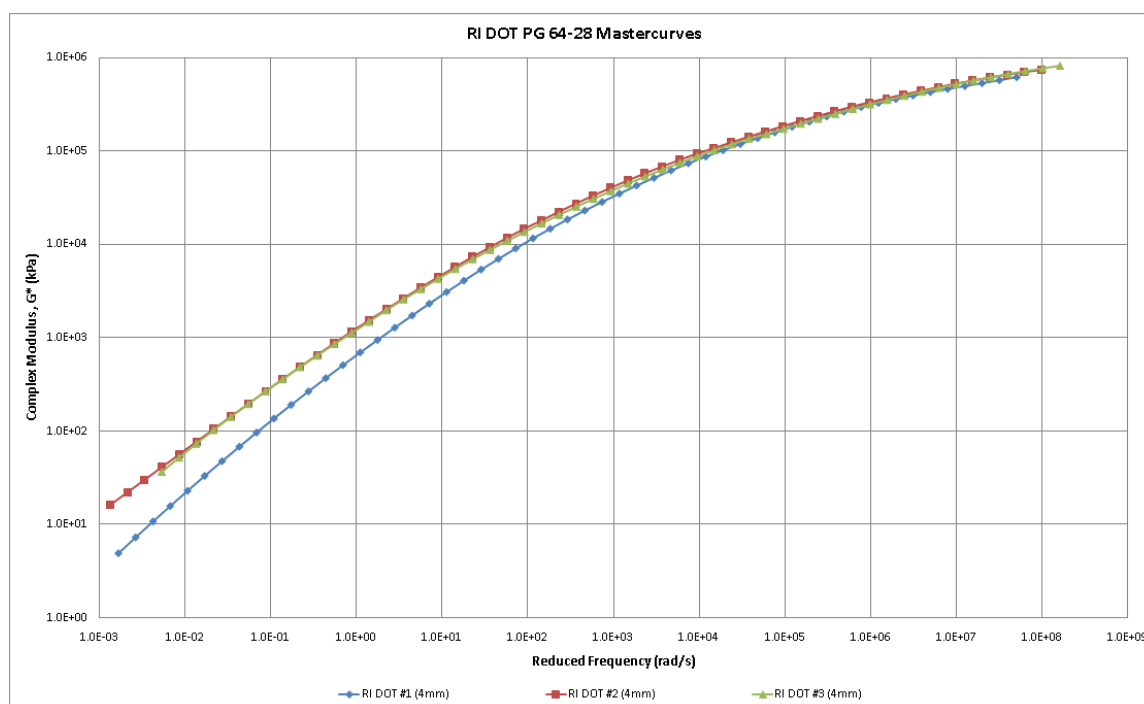


**Figure 34 RI DOT 64-28 Master Curves (4mm)**

The RI DOT 64-28 results pictured above represents the only data with an outlier. RI DOT 64-28 #1 (4mm) for the mid to lower values of  $G^*$  does not fit with the other two samples, however this must be overlain with the entire spectrum including the 8 mm traditional master curve to see which is actually the outlier. Pictured below are the compiled results. The show that RI DOT 64-28 #1 (4mm) is in fact the outlier since the 8 mm results align with the results of the 4 mm tests. However, it can be seen that for the low values of  $G^*$ , the traditional master curve extends further and gives more information. This was due to the fact that the 4 mm test was only run to 45°C, where as the traditional was run to 60°C. On the contrary, the 4 mm results give more insight into high stiffness than the approximated BBR data from the 8 mm results. This is due to the higher applied torque and lower temperatures. This is ideal because the low temperature cracking properties are they key failure method that need to be investigated.

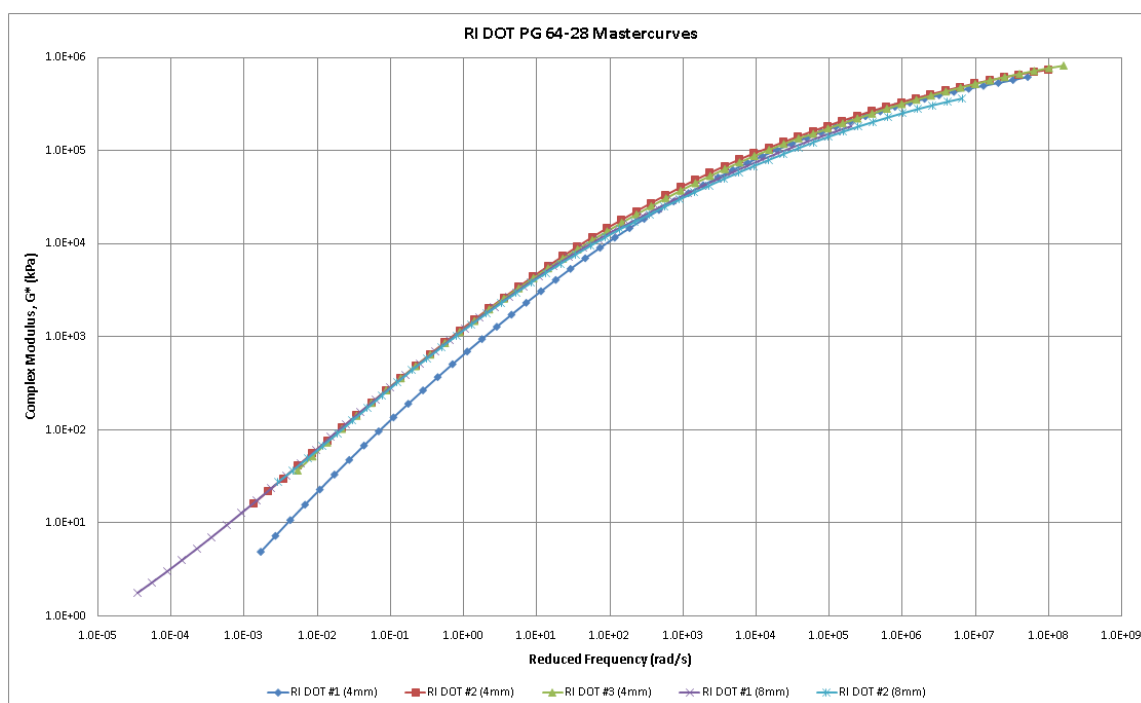


**Figure 35 RI DOT 64-28 Master Curves (4mm & 8mm)**

The same trend follows with the other combined 4 mm and 8 mm graphs, where low stiffness values are better interpreted by the 8 mm traditional master curve and high stiffness are best evaluated by the 4 mm master curve. The increase in applied torque in conjunction with the lower temperatures allows for the DSR to get readings in the high stiffness range that was not possible with the traditional set up or with the BBR data approximation.

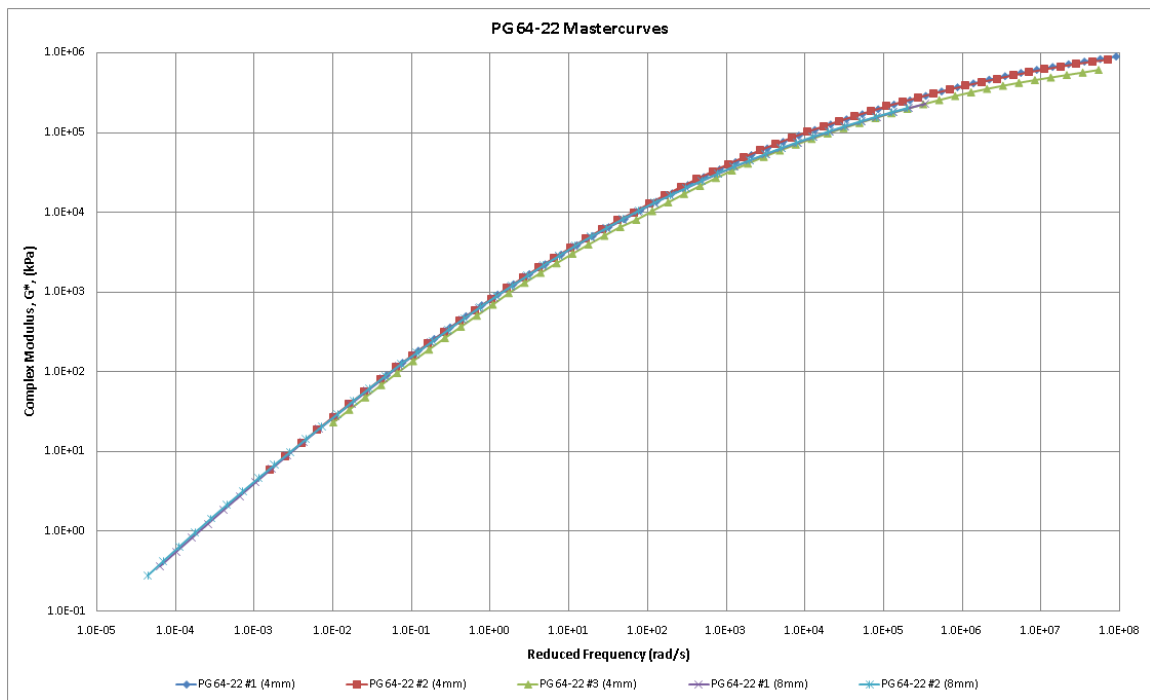


**Figure 36 PG 64-22 Master Curves (4mm & 8mm)**

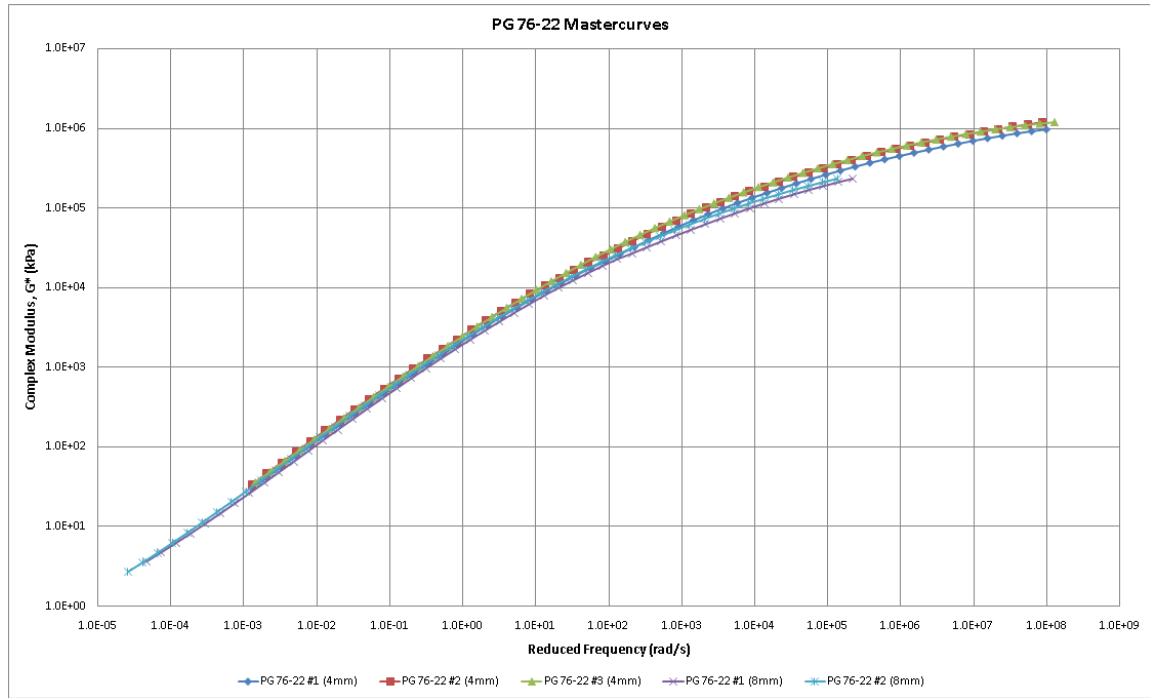


**Figure 37 PG 76-22 Master Curves (4mm & 8mm)**

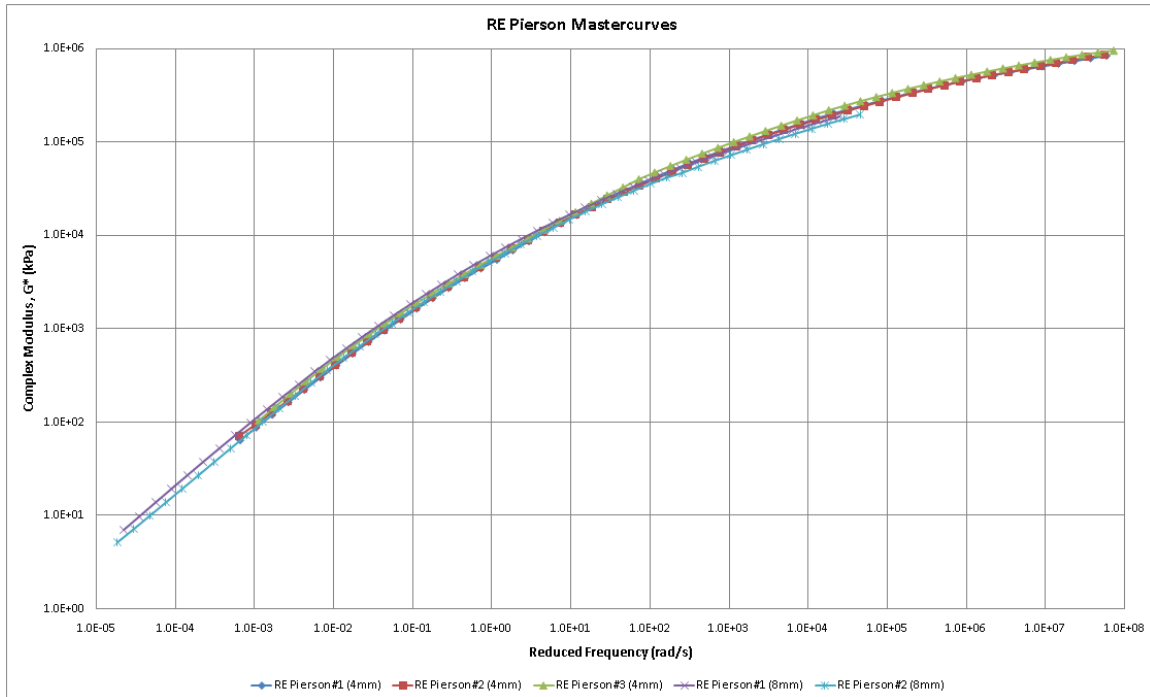


**Figure 38 RE Pierson Master Curves (4mm & 8mm)**

## Error

Upon looking at the master curves for the four different materials tested, the shifted results show that with some exceptions the 4 mm data correlates with the traditional and previously accepted data. However, this needs to be further verified by inspecting isotherm data and black space diagrams.

Each of the 4 and 8 mm tests were run at 30°C in a similar range of frequencies, and as such can be compared against one another to check for additional errors or discrepancies between the data, as well as check for outlying points.

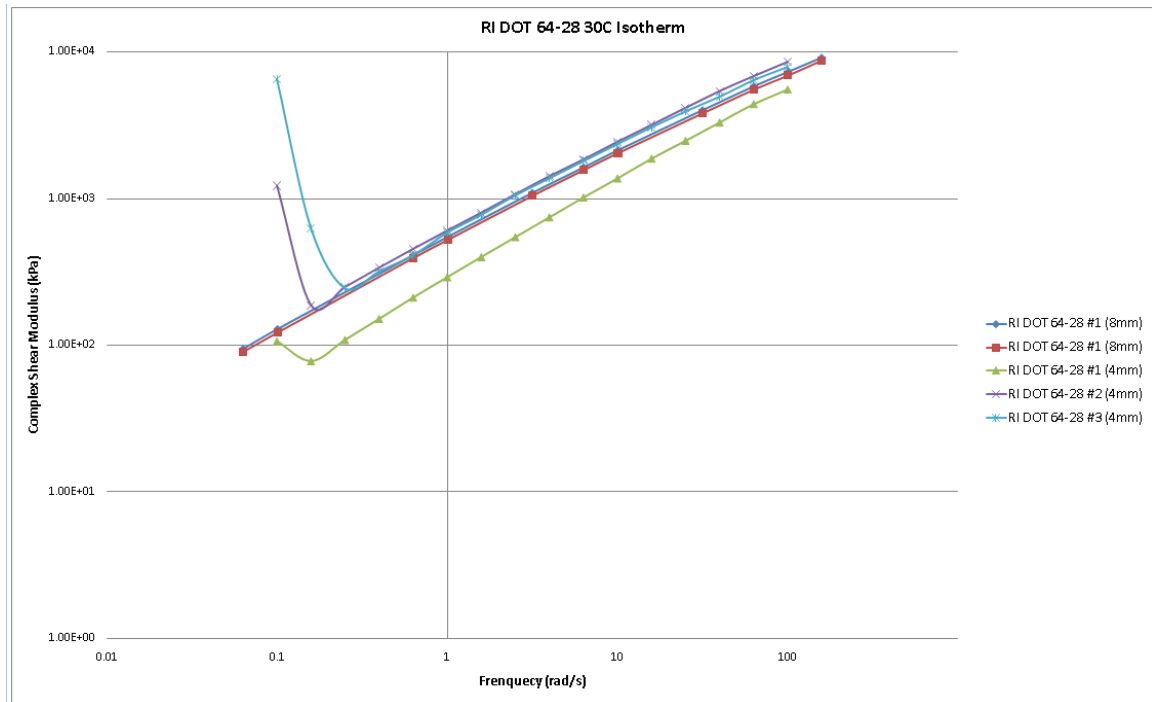


**Figure 39 RI DOT 64-28 30°C Isotherm**

In the RI DOT 64-28 isotherm, it is confirmed that sample #1 of the 4 mm test was an outlier. Additionally, it is noted that all of the low frequency data for the 4 mm test experienced errors and created outlying points. This is not shown in the master curve



plots because these data points needed to be removed in order to allow the RHEA software to create the shifted plot. This trend of outlying plots at low frequencies is present in all of the 4 mm data, with these values also having high harmonic distortion numbers.

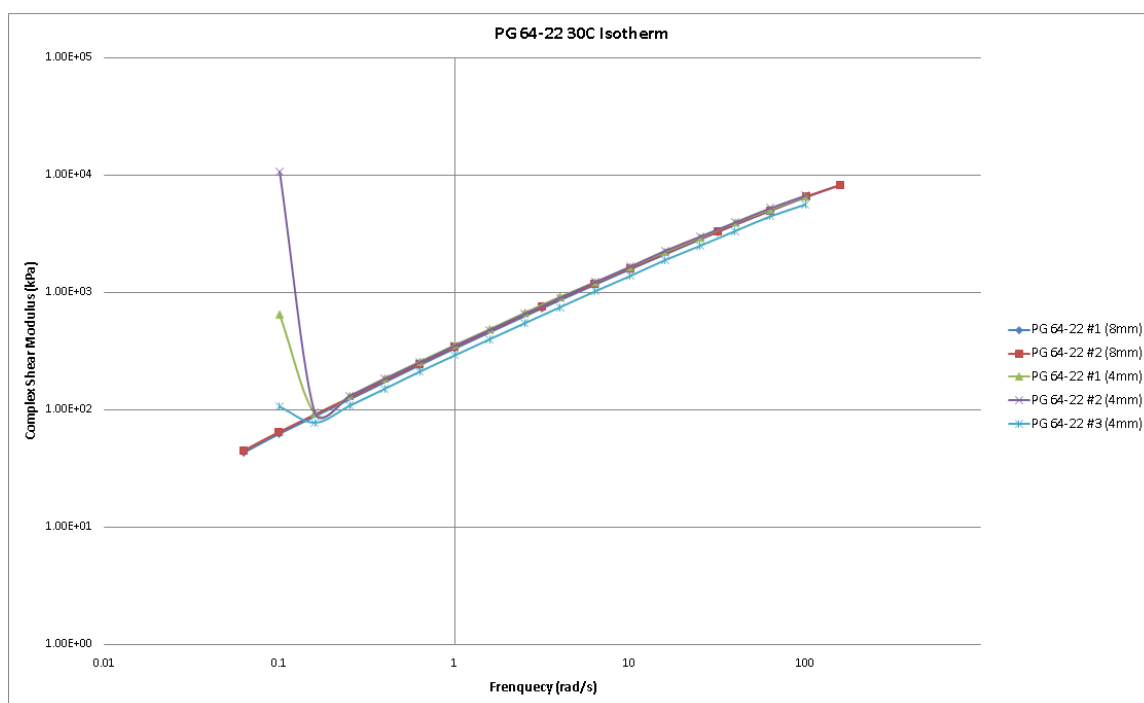


**Figure 40 PG 64-22 30°C Isotherm**

The PG 64-22 and RE Pierson results yielded similar results to the RI DOT material, however there was a greater level of precision with the results. The outlying points in the low frequencies are present in both, leading the researcher to believe that at low frequencies, the 4 mm sequence has issues attaining the readings without high levels of harmonic distortion and error and in the future the sequence may be altered to leave these points out and reduce the overall error.

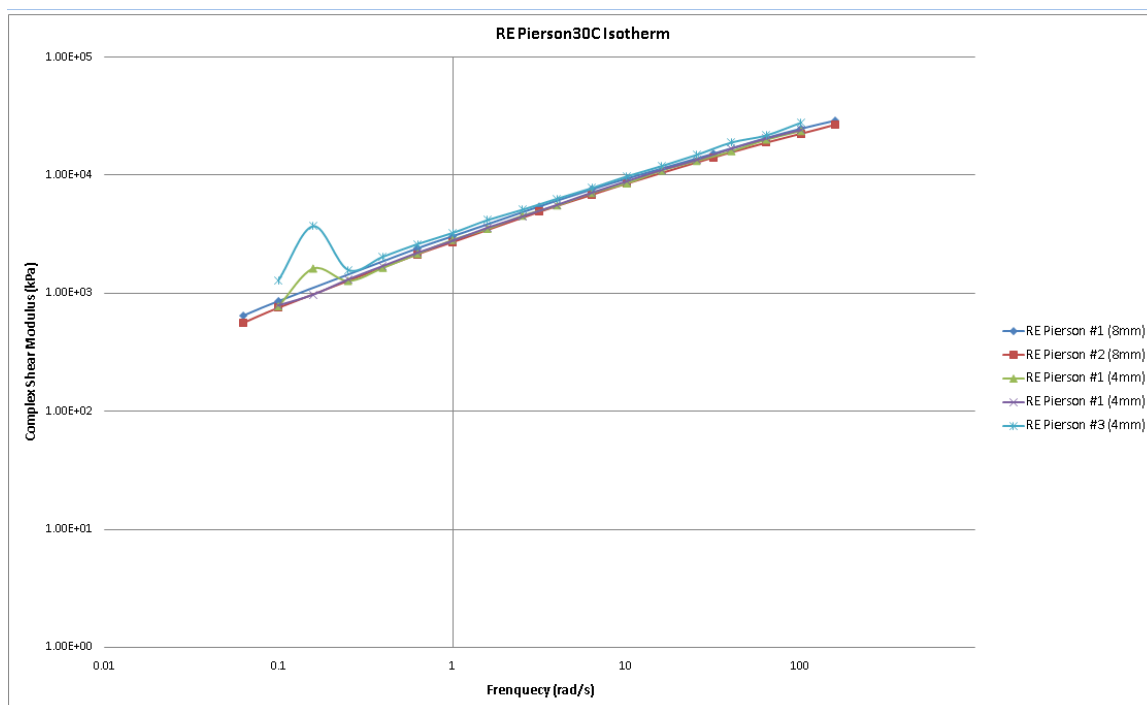


**Figure 41 RE Pierson 30°C Isotherm**

The only data set for the 30°C isotherm that was not as closely clustered as the others was the PG 76-22 data. These results show a schism in which two of the 4 mm samples are overlain with one another, one of the 4 mm and one of the 8 mm samples are overlapping and the other 8 mm is below the rest. This can also be seen in Figure 37 as the section in which the data sets begin to diverge. With the exception of the outlying RI DOT 64-28 #1 (4mm) data set, this is the only plot that exhibits this behavior. This may be due in part to the material beginning to switch from a viscoelastic behavior to a more viscous behavior due to both the temperature and applied torque. It should also be noted that with the stiffer materials, the outlying points at the low frequencies were not as pronounced as the softer materials.

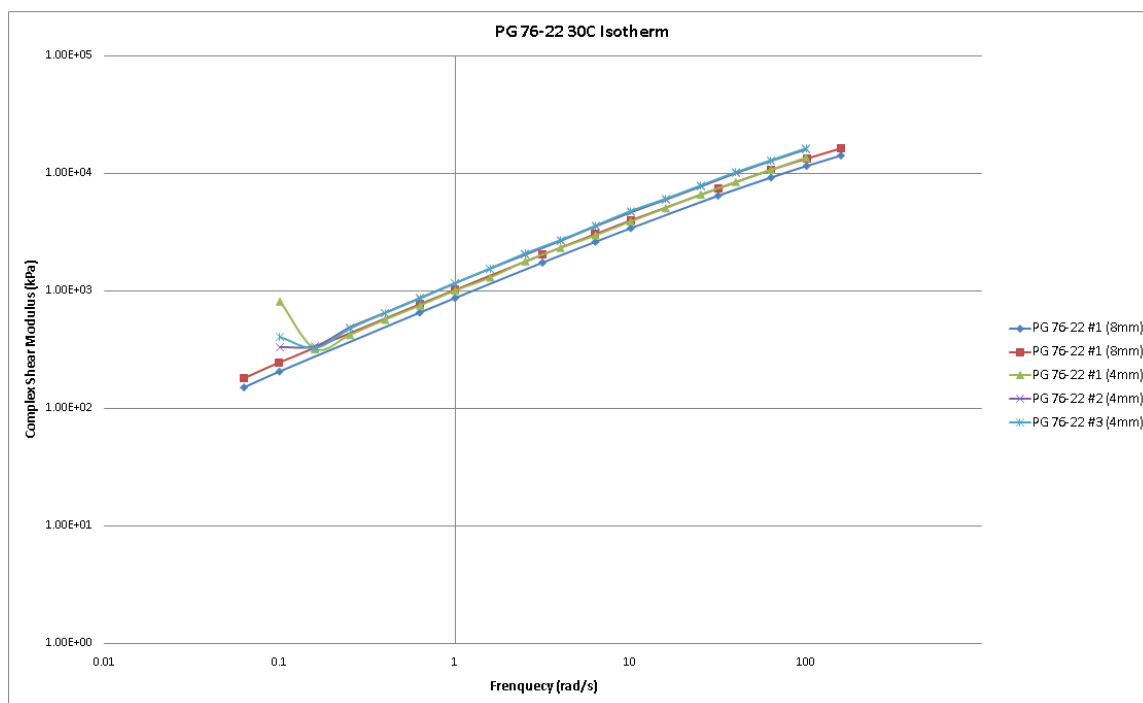


**Figure 42 PG 76-22 30°C Isotherm**

The direct comparison of isotherm data allows for the operator to look for points or data sets that may not be noticeable in the master set of shifted points. This is due to the fact that the master curve data in addition to having points removed is also smoothed. As such it is necessary to look at black space diagrams to see if the data has other errors that need to be addressed or may cause the results to be thrown out. As previously mentioned, a black space diagram plots the absolute value of  $G^*$  versus the phase angle. This plot does not need to be shifted since as  $G^*$  tends towards infinity, phase angle tends towards zero and as  $G^*$  is decreased, the material is going into phase and tends towards  $90^\circ$ . If a material has few errors and is thermoerheologically simple, the plot should be relatively smooth. In the case of the 4 mm plots for black space, certain outlying points had to be removed prior to creating the diagrams. These points were due to noise in the machine, small malfunctions or interference in the lab itself. The DSR is sensitive

enough that it can pick up readings of someone dropping something on the lab table or bumping the corner. As such any points that had harmonic distortion values above 8% were removed as were any points that had phase angles in the negative range or greater than  $90^\circ$ . This was done in an effort to eliminate any stark outliers, however some points still remained in the diagram.

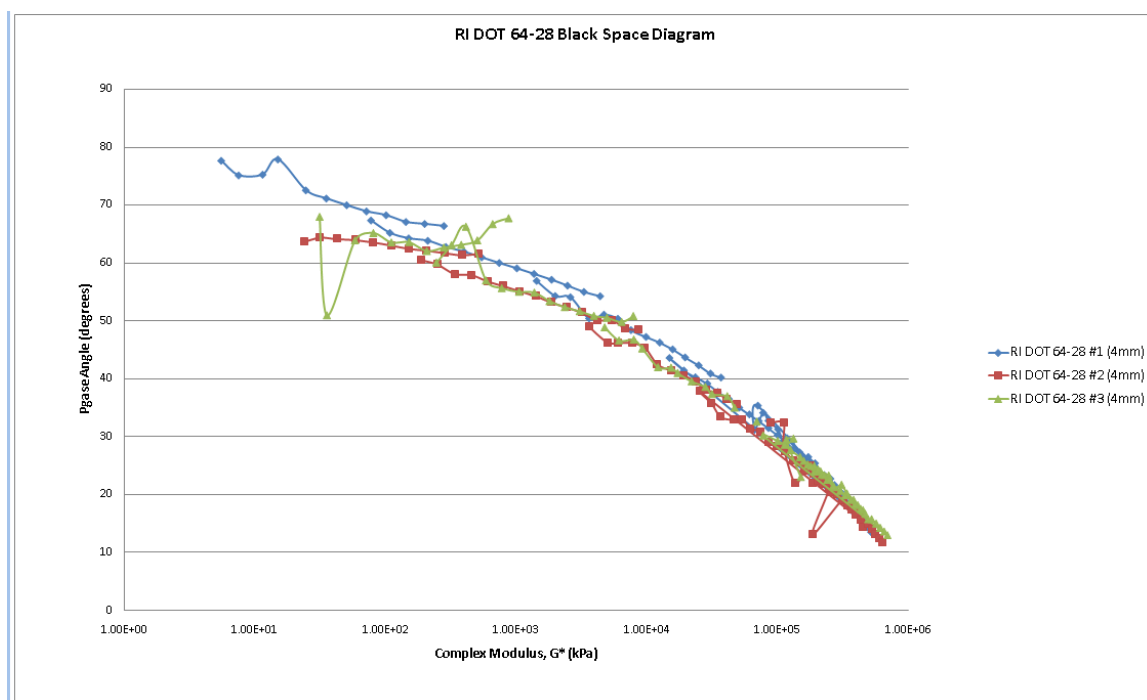


**Figure 43 RI DOT 64-28 Black Space Diagram**

From Figure 43, the outlying nature of RI DOT 64-28 #1 (4mm) is shown by the fact that it shares very few common points with the other two samples. Additionally, the gaps in between the data points show areas which had points removed due to harmonic distortion or inappropriate phase angle values. However, aside from a few points, the other two samples follow a relatively smooth curve overlapping one another. This indicates that there was relatively small error and the binder was a TSM.

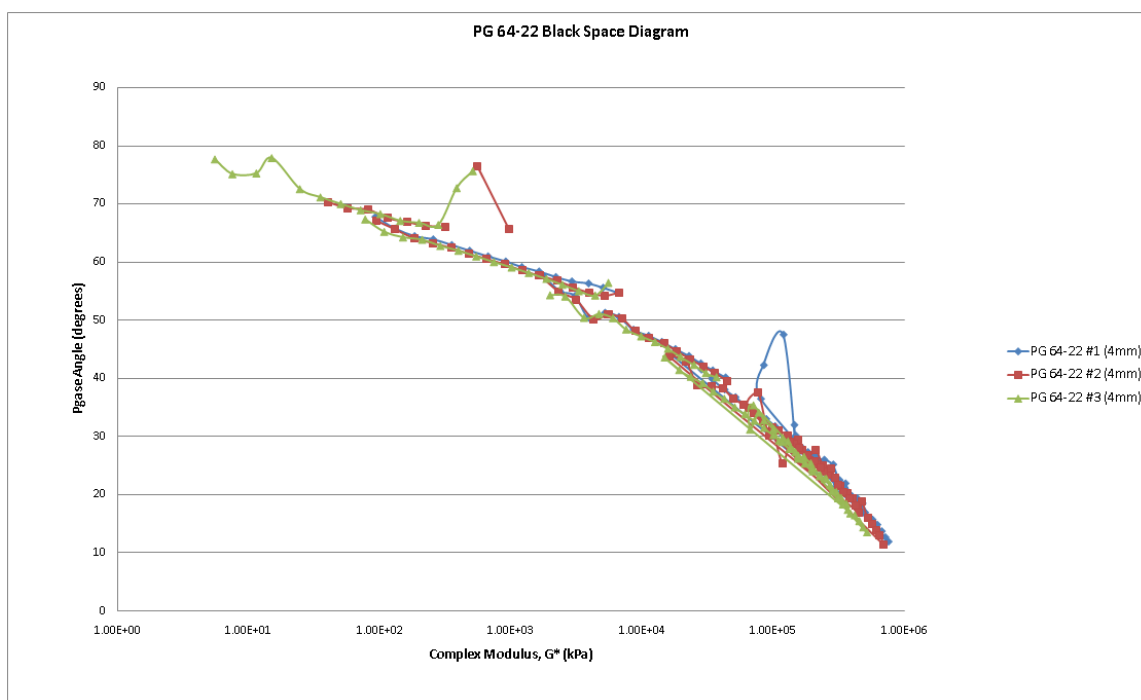


**Figure 44 PG 64-22 Black Space Diagram**

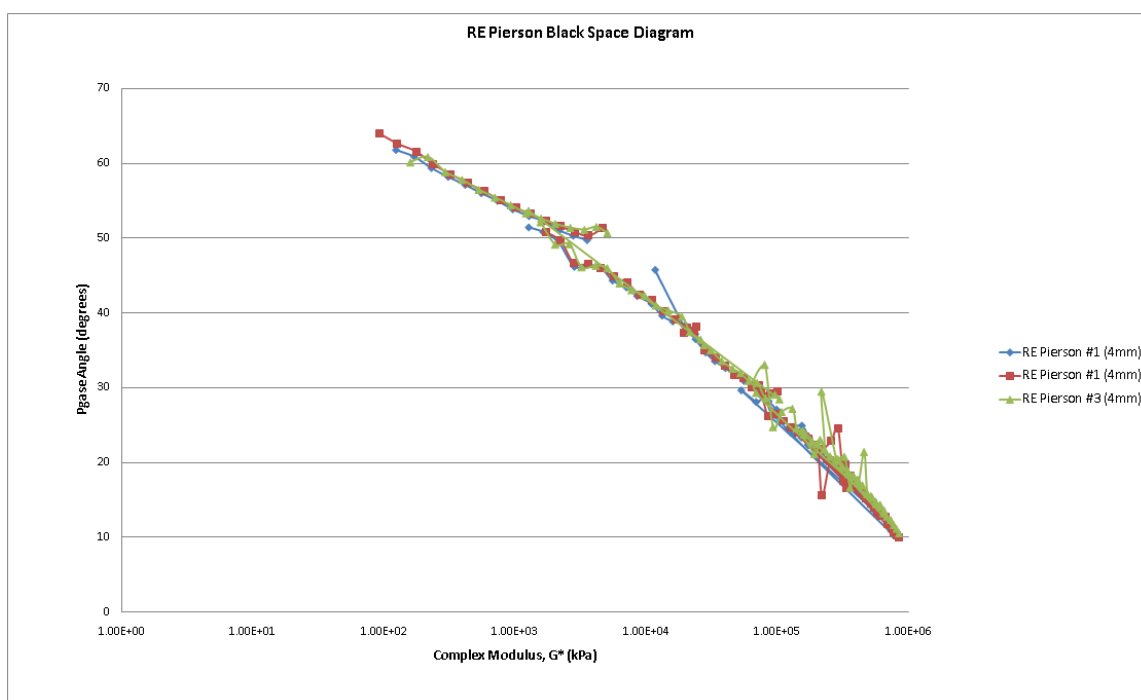


**Figure 45 RE Pierson Black Space Diagram**

Both Figures 44 and 45 depict relatively smooth black space diagrams. This is of particular interest to the researcher due to the fact that the RE Pierson was not only an extracted binder, but it was also the stiffest. At the onset of these set of experiments, it was presumed that this material would yield the worst results, however this is not proving to be the case. With the exception of the points from RE Pierson #1 (4mm) that were removed due to erratic readings in the -20°C, the results are very promising for using this technology to test other forensically extracted materials. Figure 46, like Figure 43 depicts additional outlying points. Despite these points the amount of error present is not enough to throw out the results because the points still form a relatively smoother and continuous plot tending in the correct directions for both  $G^*$  and phase angle.

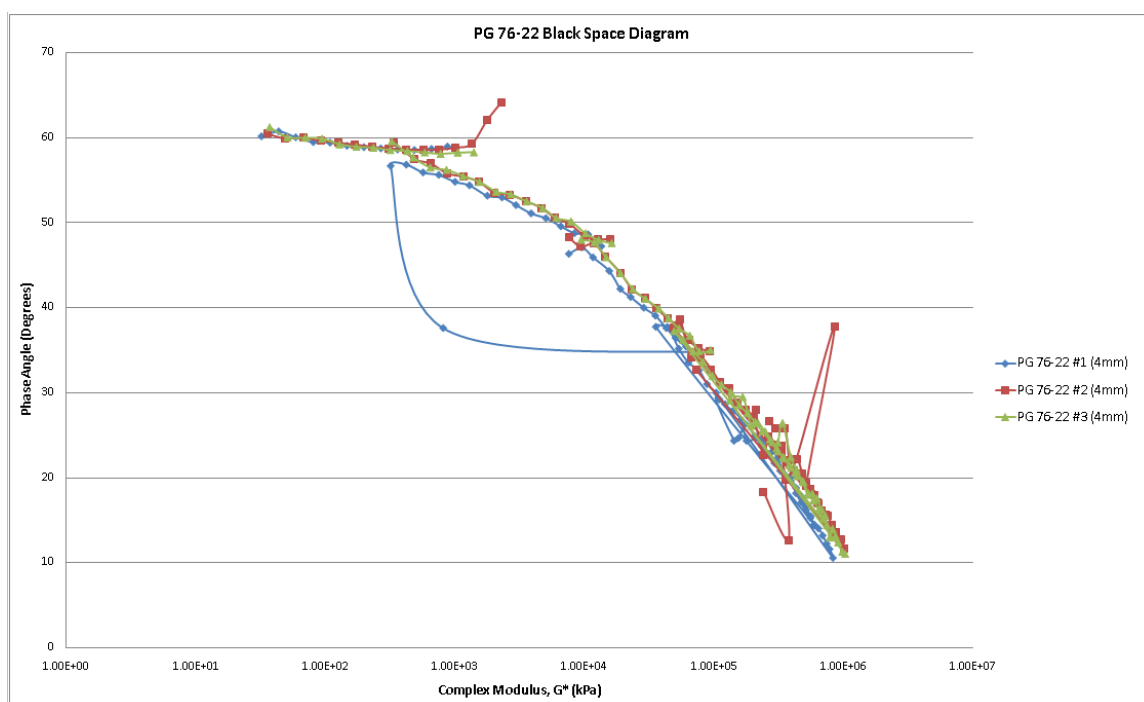


**Figure 46 PG 76-22 Black Space Diagram**

## CONCLUSIONS

From the results above, it can be deduced that the 4 mm master curve sequence yields results comparable to those of the 8 mm, or traditional master curve. Additionally, the results from the low end of the temperature spectrum proved to be valid and comparable to the BBR approximations currently used. The errors present tend to occur at the low testing frequencies where the machines sensitivity is increased, as well as at high temperatures. The former may be resolved by increasing the low end of the frequency threshold to decrease the sensitivity and decrease outliers. The latter can be eliminated by running the 4 mm plates for the low and intermediate test temperatures and then switching to a larger plate for the higher temperatures. By doing this, the operator will reduce the amount of torque creating inertial effects on a sample that has more opportunity to flow due to a higher temperature and larger gap height. This will also reduce the amount of material required as compared to a traditional master curve. By addressing these issues, master curve testing may be completed in the future using only the DSR, saving time and money on material, equipment and labor costs.

## Chapter 8: Final Conclusions

Evaluation of asphalt binders has evolved over time to become more accurate, useful and efficient. Understanding the physical binder characteristics enables producers, users and researchers to compare and evaluate binders to select the proper material for each project. Prior to Superpave, asphalt binders were tested at room temperature for penetration and ductility, and for the majority of binders this does not even begin to scratch the surface of the full spectrum of physical characteristics. Viscosity measurements only allowed researchers to see how the binder behaved in the viscous region and oftentimes viscosity measurements could not be taken on certain binders due to their high viscosity. With the advent and increasing popularity of polymer modified and otherwise enhanced binders it became necessary to alter and improve the methods of testing.

Unlike empirical testing, all Superpave testing can be correlated since it is based around rheology and not individual physical characteristics that may or may not be related. Additionally, by creating Superpave testing, there is a flow established that gives the properties of the binder and failure mechanisms throughout the stages of its service life instead of a variety of disjointed tests. The viscosity is still measured, however it is done using a couette and spindle, which allows for even very stiff polymer modified materials to be evaluated. This test also correlates to the mixing and compaction temperatures, which serves a very important function for those producing and using the binder in hot or warm mix asphalt mixtures. Virgin and RTFO aged binders are evaluated on the DSR with the 25 mm plates at high pavement temperatures to determine the complex shear modulus and phase angle to see the point at which rutting failure occurs. RTFO aged material can be correlated to the conditions right after the asphalt has been placed and



compacted into the early parts of the service life. Material that has been aged in the PAV is representative of the way the binder performs at the end of its service life, which is when fatigue cracking and thermal cracking may occur. Fatigue cracking involves complex shear modulus and phase angle, similar to rutting resistance, but it occurs at intermediate temperatures and is the least common mode of failure. This testing is also done on the DSR, but with the 8 mm plates, since the stiffness is greater, so additional torque is required. Thermal cracking resistance is done by evaluating asphalt beams subjected to a downward force from a piston in the BBR. The transducer in the rheometer measures not only the stiffness of the thermally conditioned asphalt beam, but also the relaxation rate. These two in conjunction with one another are used to determine the temperature at which the binder will fail due to thermal cracking. The above mentioned Superpave tests allow for a researcher to evaluate a binder through all the stages of its service life and see the points at which failure may occur. This lets those designing roadways select the appropriate binder for each climate and traffic level. However, running a complete Superpave performance grade requires a Brookfield Viscometer, Dynamic Shear Rheometer, Rolling Thin Film Oven, Pressure Aging Vessel, Degassing Oven and Bending Beam Rheometer. All of these pieces of equipment are necessary for the full spectrum of testing and may come with a price tag in excess of \$250,000. Additionally, to grade a binder, it may take up to 3 days with all the aging and conditioning that has to take place. Particularly with the BBR, the operator must make the beams, allow them to sit for an hour before trimming them, then condition them at the test temperature for another hour. If multiple temperatures are being tested, this process could take at minimum four to six hours. Finally, a full performance grade requires at

least a pint of binder. This is not a problem for most materials, however for extracted materials this can become an issue. The beams for the BBR each use around 15 grams of material including trim waste, and for an extraction recovery, this could be upwards of half of an extraction since at least four beams are required. As such it is necessary to consider other means to evaluate the thermal cracking resistance which use less material, saving time and money.

Master curves are created to give researchers the full spectrum of the behavior of a physical property with respect to temperature and frequency, or time. With a traditional master curve, using 25mm or 8mm plates, the properties, in particular phase angle and complex shear modulus, in the intermediate and high temperatures can be directly evaluated on the DSR in their specific isotherms. Low temperature data must be approximated from BBR data and then converted into frequency and complex shear modulus. This data can then be converted into a RHEA input, where the isotherms are smoothed into a master curve. This has advantages for researchers over performance grading because it gives one set of data for the entire range of temperatures and can span all phases, from near glassy modulus to viscoelastic to the viscous range. However with a traditional master curve, the low temperatures need to be approximated from BBR data. This results in some inaccuracies from the conversion as well as greatly increasing the amount of material required from around a gram to in excess of 45 grams.

The 4 mm master curve data can be overlain with a traditional master curve and yields the same results. In fact, with the 4 mm master curve, the results give even more insight into the stiff thermal cracking region than converting BBR data can. However with higher temperatures, there is a greater chance of error or the material flowing out from

the plates. As such, it may be advisable to run low to intermediate temperature testing with the 4 mm plates and then switch to the 8 mm or 25 mm plates for higher temperatures to get more of the stiffness spectrum than can be attained with the 4 mm plates. Additionally the 4 mm test uses only 25 mg of binder. With such a small amount of binder, complete roadway cores would not be required for extractions. Instead smaller samples could be taken from multiple locations and then extracted to give a more representative sample as well as not damage the integrity of the roadway as much as a traditional core does. In addition to saving time and money with respect to extracting binder for forensic studies, this could also eventually lead to phasing out the BBR. This would save labs money and time by eliminating an expensive piece of equipment that has a test which takes the longest amount of time between sample prep, conditioning and testing. Finally, the 4 mm sequence has applications outside of just asphalt binder. Other bituminous materials, such as crack seal and emulsions have limitations with traditional test methods. Crack seal is very stiff and cannot always be tested by traditional means. Both crack seals and emulsions should not be heated to the temperatures that most asphalt binders are heated to, making them unable to be poured into beam molds for the BBR. However they are prime candidates for the 4 mm master curve sequence since they only need to be heated enough to flow into the mold or directly onto the plate and then can be tested in the thermal cracking zone, which is their main failure mechanism due to the high stiffness. For future testing with the 4 mm plates, additional studies into the different materials should be considered. As well as studies using different sampling technique for extraction recoveries, to determine if the results are similar from one large core versus many smaller samples.

By creating a master curve using 4 mm parallel plates the operator is able to take advantage of multiple time and money saving factors, as well as getting a more accurate representation of the true qualities of the binder in the low temperature end of the stiffness spectrum. This is especially desirable because of the amount of material and variety of equipment required to evaluate the thermal cracking materials. With the application of the 4 mm DSR testing methods, the machine can be used to fully characterize a binder or other bituminous material, using less than 5 grams of material in total. As such, it is important to continue to evaluate the uses of this test methodology with alternative bituminous materials as well as with traditional asphalt binders.

## References

- 1) Anderson, Dave, Jack Youtcheff, and Mike Zupanick. "Asphalt Binders." *A2D01: Committee on Characteristics of Bituminous Materials*. Proc. of Transportation Research Board, Washington, D.C. Web. 03 Dec. 2012.  
<<http://onlinepubs.trb.org/onlinepubs/millennium/000006.pdf>>.
- 2) *The Asphalt Binder Handbook*. [Lexington, Ky.]: Asphalt Institute, 2011. Print.
- 3) *The Asphalt Handbook*. College Park, Md., USA: Asphalt Institute, 1988. Print.
- 4) Briscoe, Oliver E. *Asphalt Rheology: Relationship to Mixture : A Symposium Sponsored by ASTM Committee D-4 on Road and Paving Materials, Nashville, TN, 11 Dec. 1985*. Philadelphia, PA: ASTM, 1987. Print.
- 5) Hardin, John C. *Physical Properties of Asphalt Cement Binders*. Philadelphia, PA, U.S.A.: ASTM, 1995. Print.
- 6) Huber, Gerald A., and Dale S. Decker. *Engineering Properties of Asphalt Mixtures and the Relationship to Their Performance*. Philadelphia, PA: ASTM, 1995. Print.
- 7) Tutumluer, E., Yacoub M. Najjar, and Eyad Masad. *Recent Advances in Materials Characterization and Modeling of Pavement Systems*. Reston, VA: American Society of Civil Engineers, 2004. 65-101. Print.
- 8) West, Randy C., Donald E. Watson, Pamela A. Turner, and John R. Casola. "NCHRP Report 648 Mixing and Compaction Temperatures of Asphalt Binders in Hot-Mix Asphalt." *Transportation Research Record* (2010). Print.
- 9) Haddad, Y. M. *Viscoelasticity of Engineering Materials*. London: Chapman & Hall, 1995. N. pag. Print.
- 10) Jahromi, Saeed G., and Ali Khodaii. "Simple Methodology to Create Master

- Curves for Stiffness of Asphalt Mixtures." Proc. of 8 Th International Congress on Civil Engineering, Shiraz University, Shiraz, Iran. N.p., n.d. Web. 04 Mar. 2013.
- 11) Wang, Hao. "Lecture 2 Binder Rheology." Feb. 2012. Lecture.
- 12) Andersen, David A., and Mihai Marasteanu. "Continuous Models for Characterizing Linear Viscoelastic Behavior of Asphalt Binders." Lecture. 2010 ISAP Workshop on Asphalt Binders and Mastics. *Http://uwmarc.wisc.edu/*. Web. 30 May 2013.
- 13) Abatech, Inc., comp. *RHEA TM*. 2011. Rheology Analysis Software Users Manual. Blooming Glen, PA.
- 14) Marasteanu, Mihai, and David Anderson. "Techniques for Determining Errors in Asphalt Binder Rheological Data." *Transportation Research Record* 1766.1 (2001): 32-39. Print.
- 15) Polacco, Giovanni, Otakar J. Vacin, Dario Biondi, Jiri Stastna, and Ludovit Zanzotto. "Dynamic Master Curves of Polymer Modified Asphalt From Three Different Geometries." *Applied Rheology* 13.3 (2003): 118-24. Print.
- 16) Sui, Changping, Michael J. Farrar, William H. Tuminello, and Thomas F. Turner. "New Technique for Measuring Low-Temperature Properties of Asphalt Binders with Small Amounts of Material." *Transportation Research Record* 2179 (2010): 23-28. Print.
- 17) ASTM Standard D6373-08, *Standard Specification for Performance Graded Asphalt Binder*, ASTM, West Conshohocken, PA.

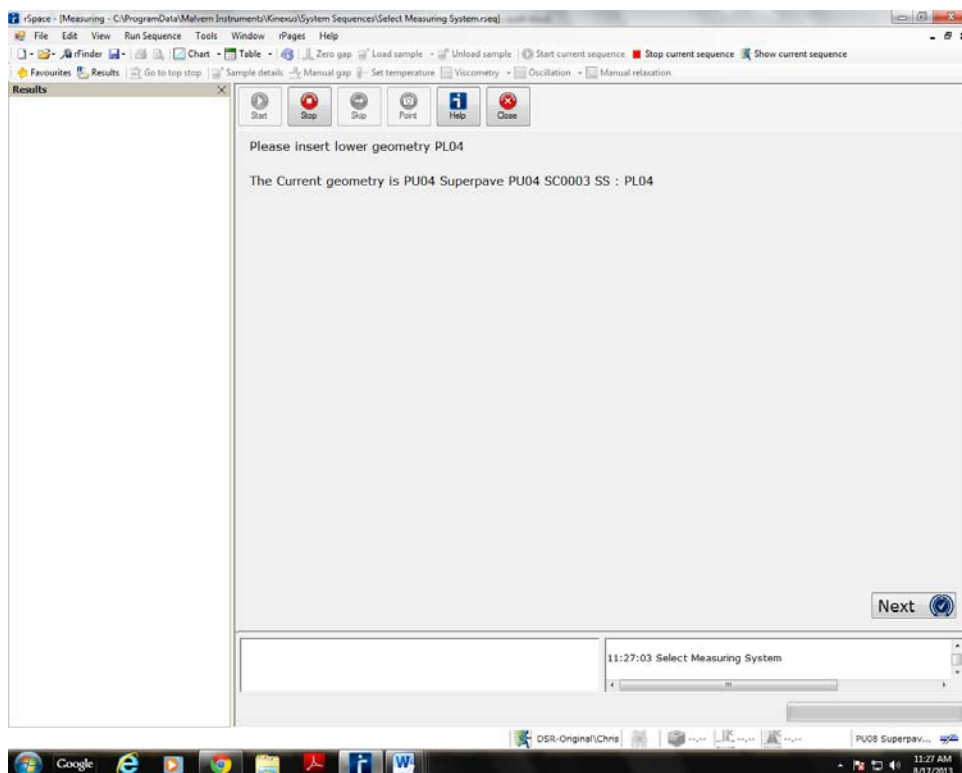
## Appendix A: 4 mm Master Curve Sequence User Manual

WRI Test Sequence with LVER Determination by Strain Sweep with Temperature

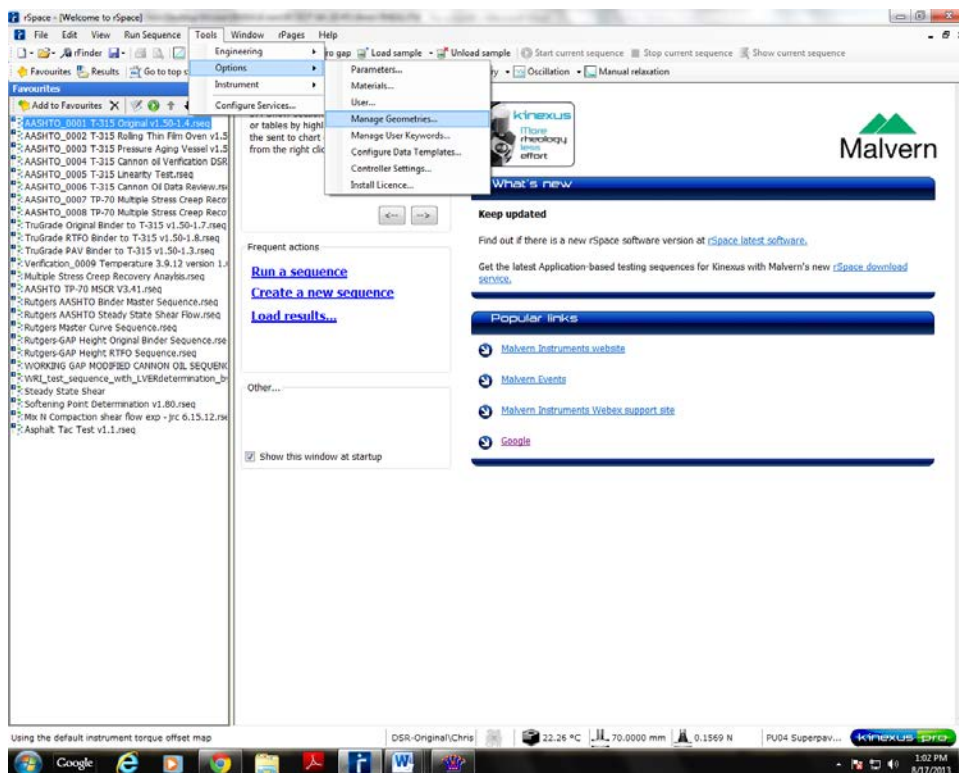
Choices (4 mm master curve testing sequence)

This user manual was created to help Rutgers Laboratory technicians run 4 mm Master Curve Sequences and input the data into RHEA for analysis. Prior to running any tests with this sequence, the technician should familiarize themselves with the equipment necessary to successfully run this test. The first necessary step is ensuring that the proper plates are loaded. The 4 mm parallel plates are required for this test.

Insert 4mm upper and lower geometries

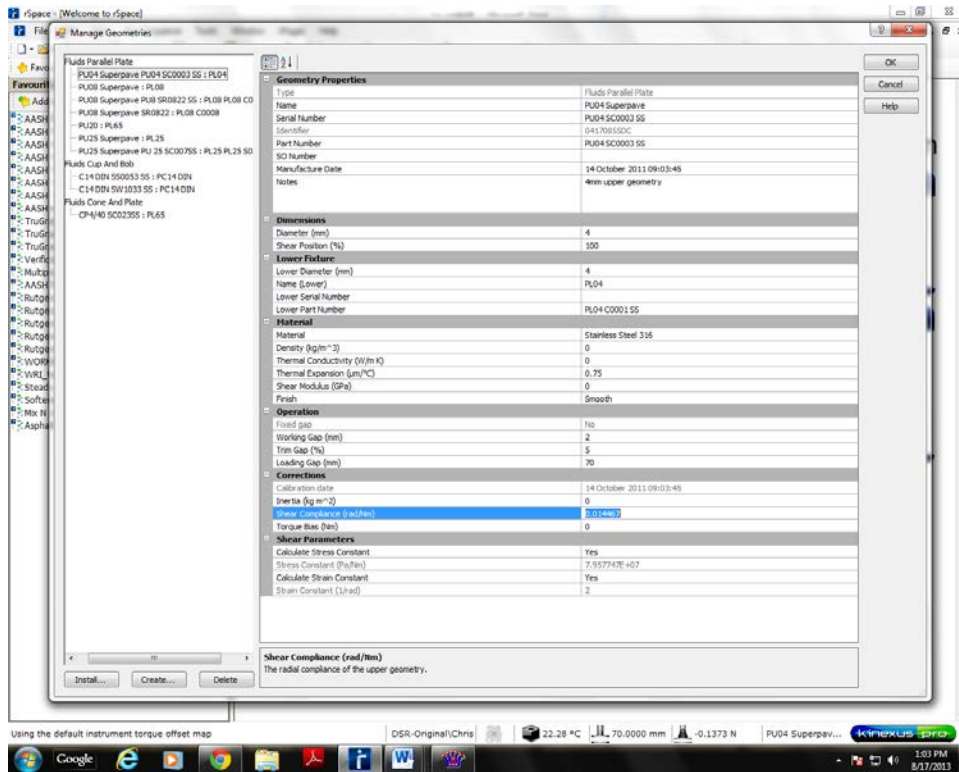


After the 4 mm plates have been inserted and the gap has been zeroed, the technician should check to ensure that the compliance for the geometry is correct. This can be altered by updates to the machine, a new machine or by accident. Go into Tools >> Options >> Manage Geometries

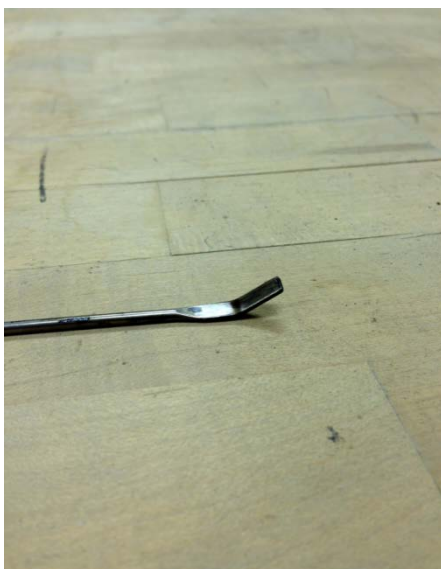


Based on prior testing, the correct Shear Compliance is 0.014467 rad/nm. This will ensure that at low or high temperatures, the DSR will maintain the proper gap. Without this compliance factor, the sample or plates may thermally expand or contract stretching or compacting the sample and skewing the results.





Once the software is in order the technician may move on to the hardware. Due to the size and shape of the 4 mm geometry, an alternative trimming tool had to be machined from a traditional laboratory spatula. The pictures below depict the modified trimming tool as well as a comparison between that and the traditional trimming tool.



Using this trimming tool, the technician should conduct a series of “trim trials”, in the following procedure is followed:

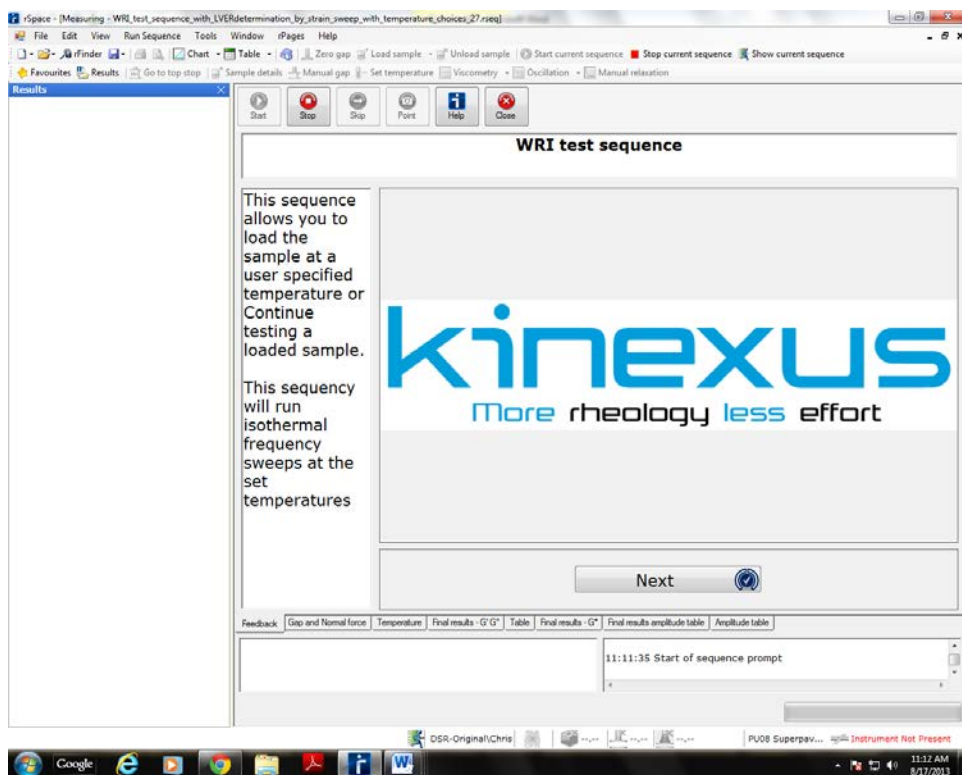
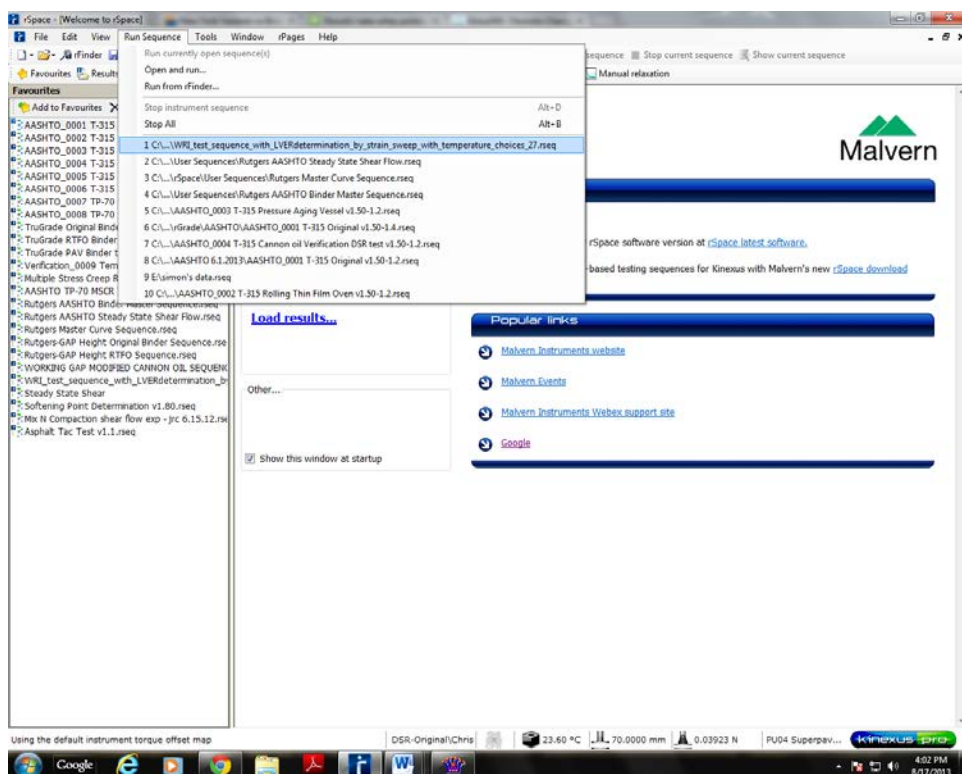
1. Select a stiff RTFO binder or a PAV binder in order to simulate worse case scenario.
2. Set to temp 25C
3. Zero gap at 25C (for this test this is your running temp)
4. Set temp to 45C (this is the loading temperature)
5. Load sample (use 8mm molds)
6. Conduct a rough trim at a gap of 2.5mm
7. Allow the sample to equalize in temperature for 5 min
8. Set gap to 2.1 mm, trim again
9. Inspect sample from all angles, if there is any evidence of gouging, abort the sequence and start over
10. Set gap to 2.0 mm (working gap height for this sequence)
11. Run a frequency sweep with crossover at 25C  
(0.1 - 10 rad/s, 1% strain rate, 3 samples/ decade)

The above sequence should be 3 times per sampling. The results should be recorded and compared with the other samples. This should be repeated until the technician feels comfortable trimming the samples and the error in a sample set is less than 7%, which is the acceptable error for traditional DSR testing. Prior to running any tests with the 4 mm plates the Canon Standard should be run in order to verify that the torque and temperature are correct.

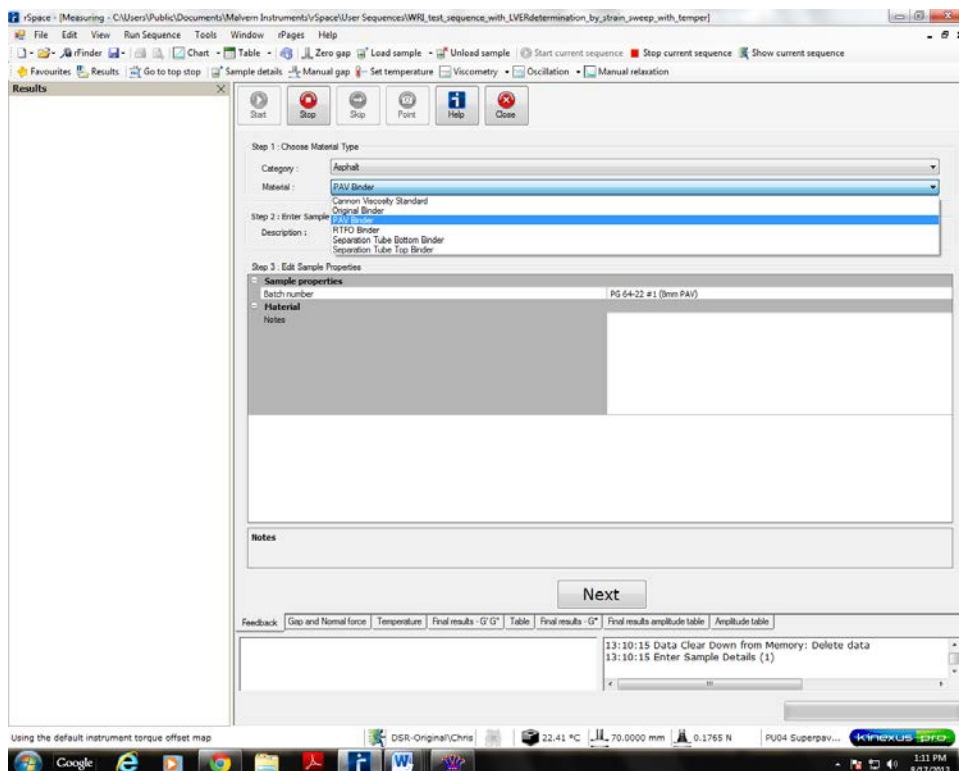
In order to reach the temperatures required for cooling, the DSR must be hooked up to an external chiller since the heat exchanger provided with the machine does not allow the operator to reach temperatures below zero. The chiller created for the initial setup of this test for the Rutgers Binder Lab consists of a 40-quart ice chest and coiled copper tubing, which has nipples and clamps which allow it to be connected directly to the DSR heat exchanger outlets via polyurethane tubing. This chest should be filled with ice and water prior to the start of the test and additional ice should be added as necessary. This system is depicted below.



The technician is now ready to begin the 4 mm master curve testing sequence. Below is the sequence being selected from the recently run sequence list, however it is also the fifth sequence from the bottom in the favorites list on the left.

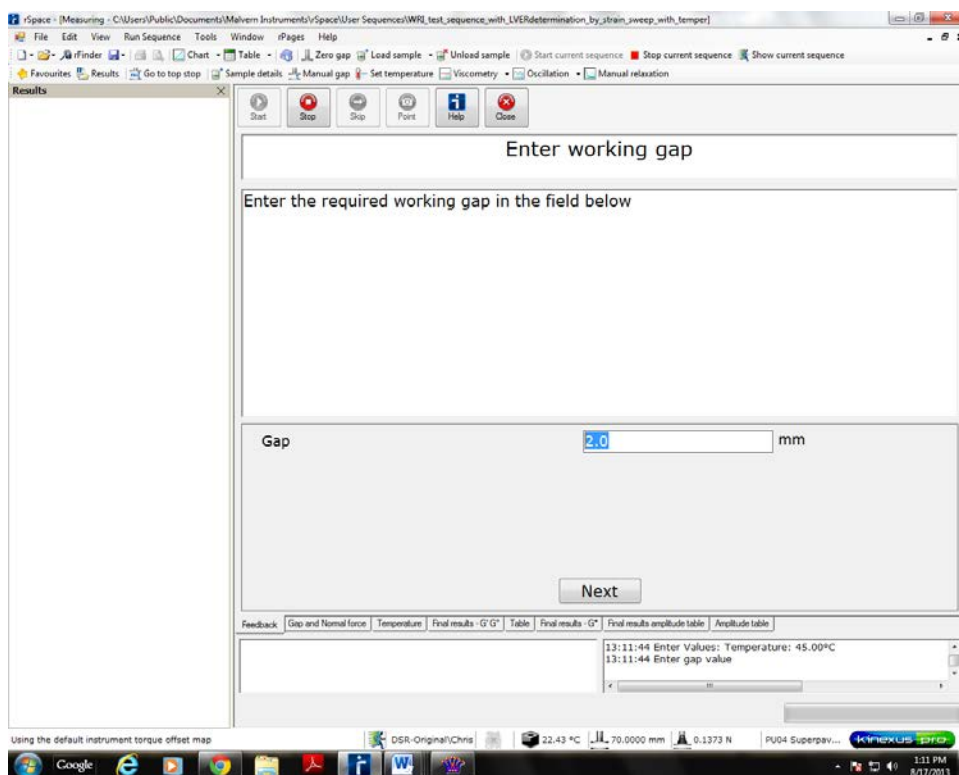


Fill in the information on the binder in question, specifying the type of material to be tested (Original, RTFO, PAV, Cannon Standard & Separation tubes are the current options, but additional choices may be added, such as crack seal, emulsion, etc). Specify the sample name, batch details and any other pertinent or notable information.

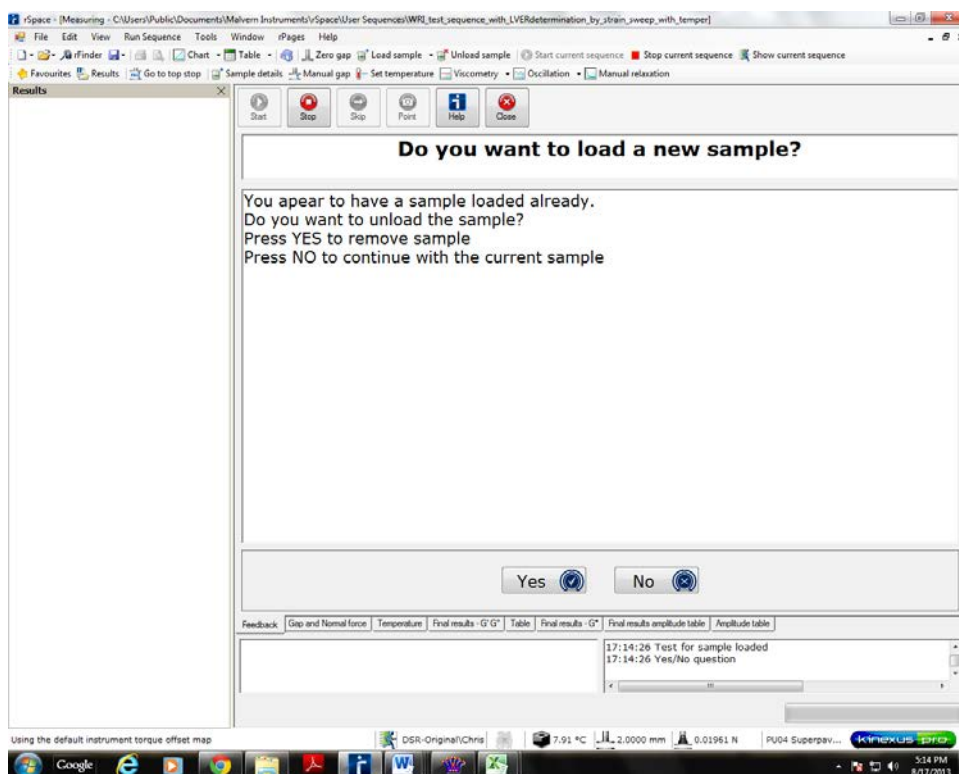


Set the loading temperature. A temperature of 45°C was chosen for the preliminary tests due to the fact that the binder does not experience substantial expansion at this temperature, trimming is possible and it is the same temperature utilized for PAV DSR testing to determine grading with  $G^*(\sin\delta)$ . Additionally if testing crack seal or emulsions this temperature is recommended by literature.

A working gap of 2.0 mm was selected based on prior experiments where gaps between 1.5 and 2.0 mm were used. This working gap is the same as the 8 mm DSR tests.



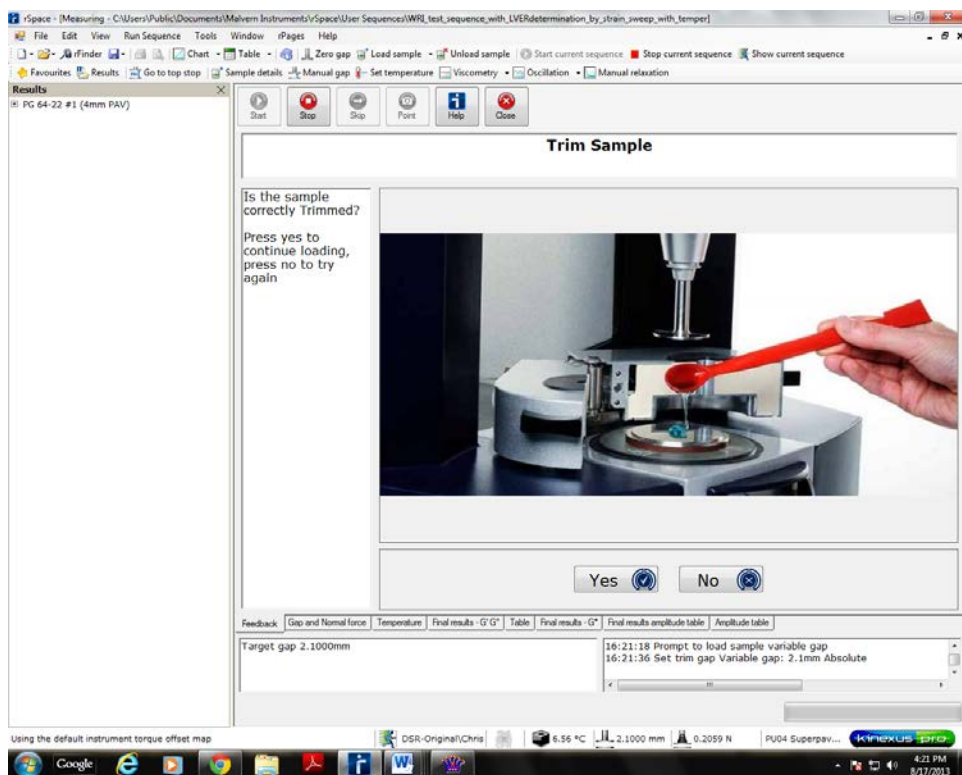
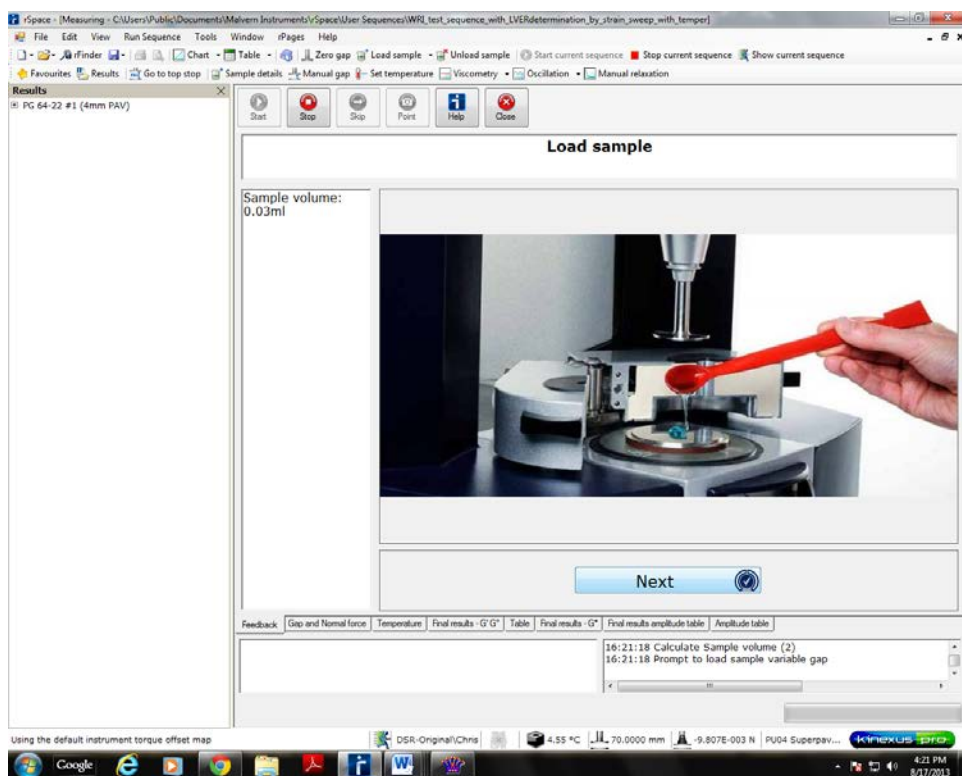
Depending on the stiffness of the material used and the level of confidence the technician has in their trimming abilities, the sample may be loaded during the sequence or it may be preloaded. If preloading is chosen, zero the gap at 0°C, set the temperature to 45°C, load the sample at 2.5 mm, allow it to equilibrate to the ambient chamber temperature, trim it, set the gap to 2.1, allow it to equilibrate and trim it again before the final working gap of 2.0 mm is set. This gives the same 5% bulge that is used in all other DSR testing. If the sample is preloaded, the following option will come up. Select No and continue with the current sample.



If the technician opts to load the sample during the sequence, the gap will zero at 0°C and then increase to 45°C for loading. The sample will load and the gap will go to 2.1 mm.

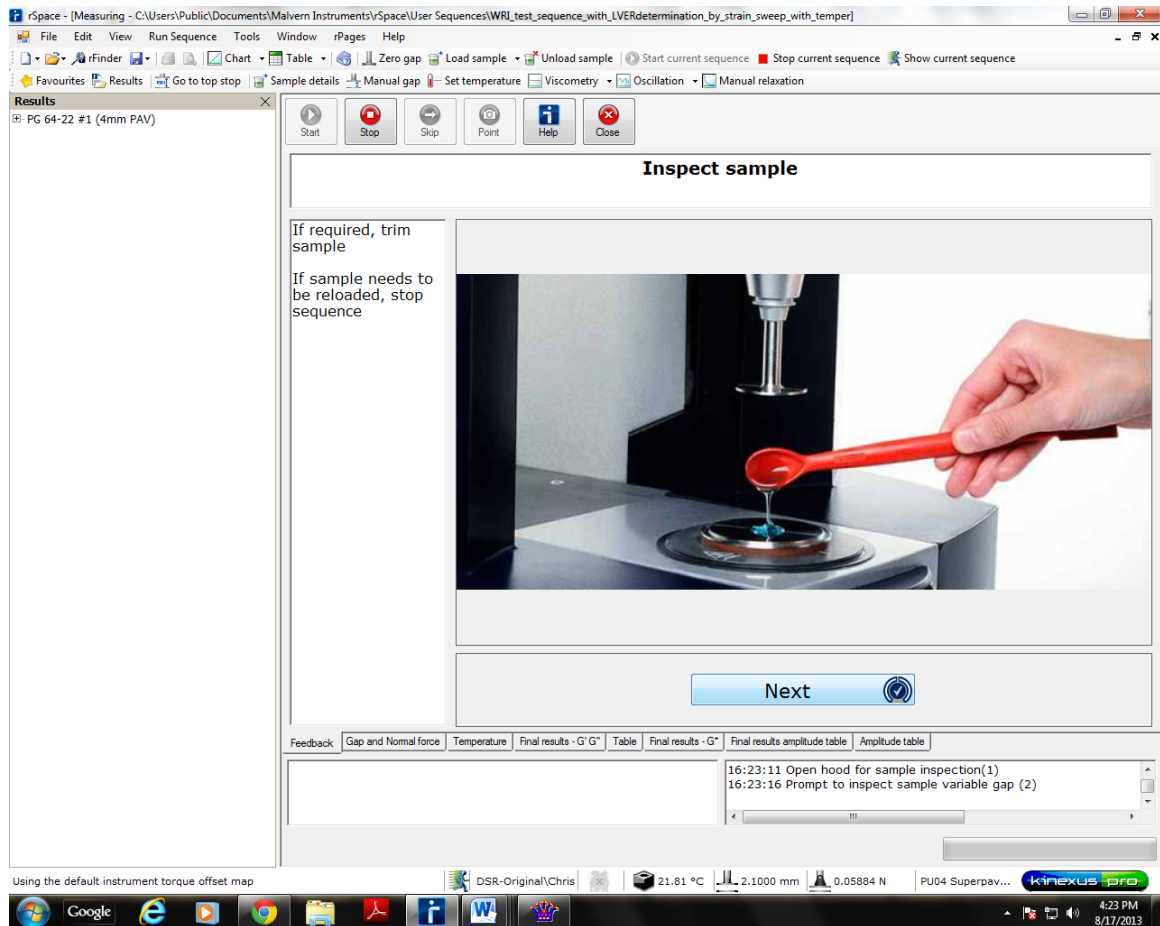
Allow the sample to equilibrate prior to trimming in order to make the process easier and more accurate. Since the molds used are the 8 mm mold, there is excess material and the trimming process should be done in at least two phases.





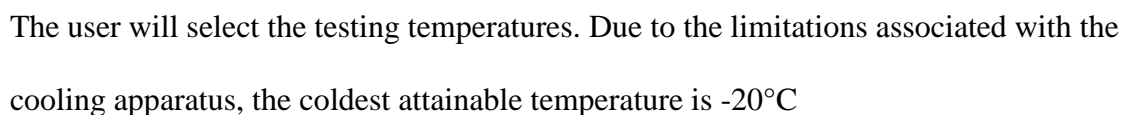


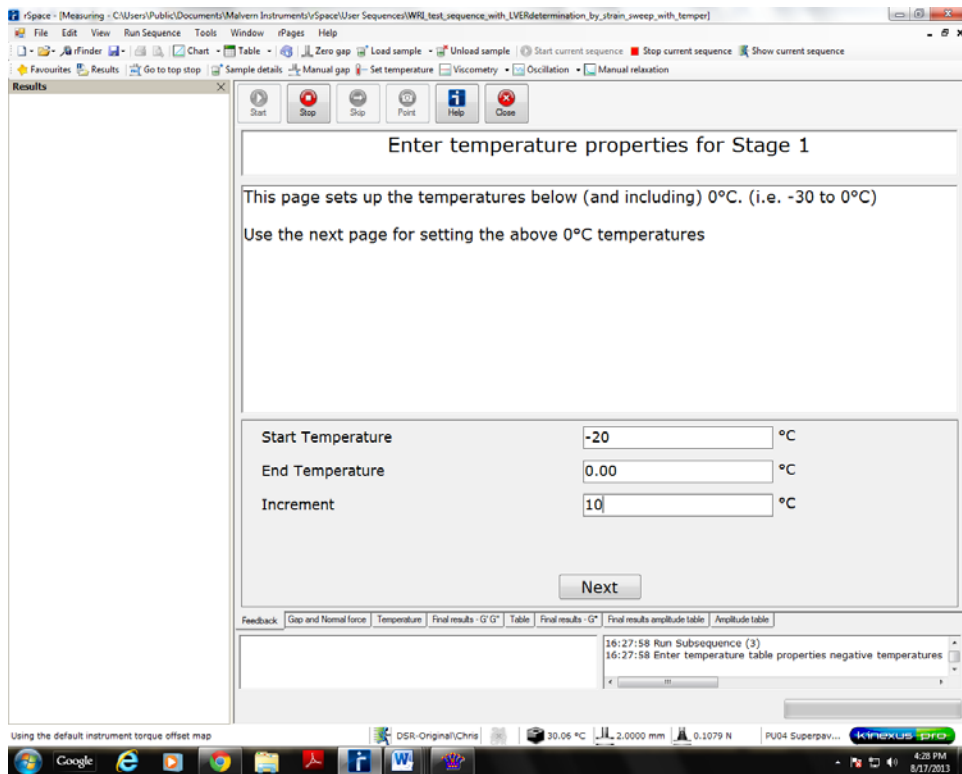
Following trim sample, the temperature drops to 30°C and the samples goes to equilibrium



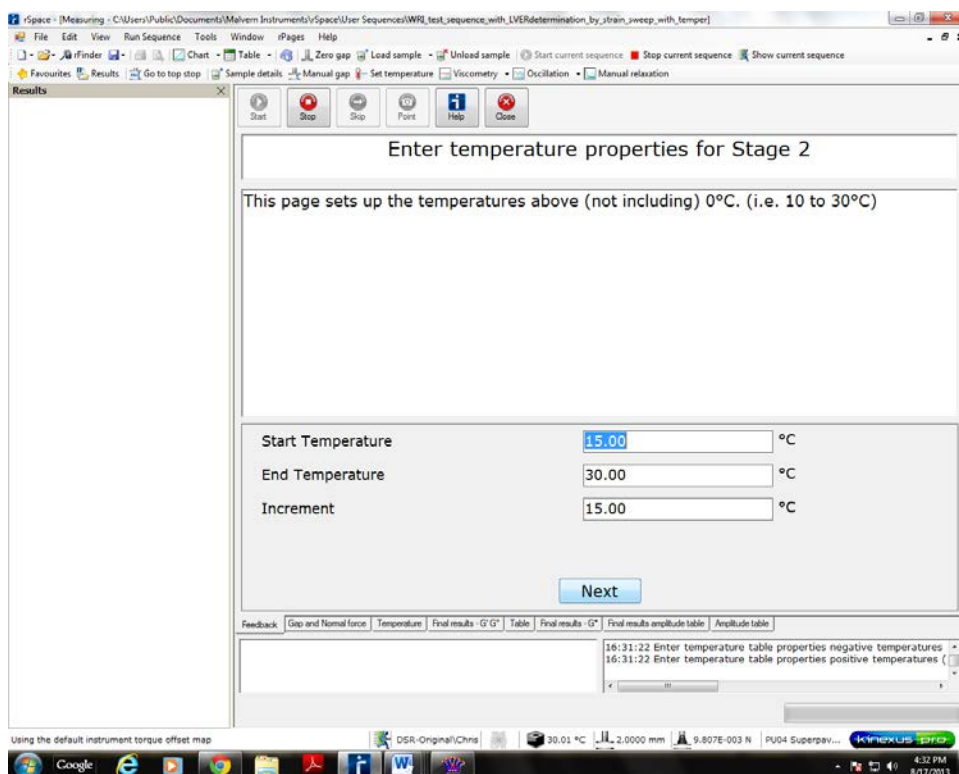
The user is prompted to inspect the sample and see if any additional trimming is required or if the sample has been gouged. In the event it has been noticeably gouged, the test should be aborted at this stage and restarted.

The user will then be prompted to enter the material data once again

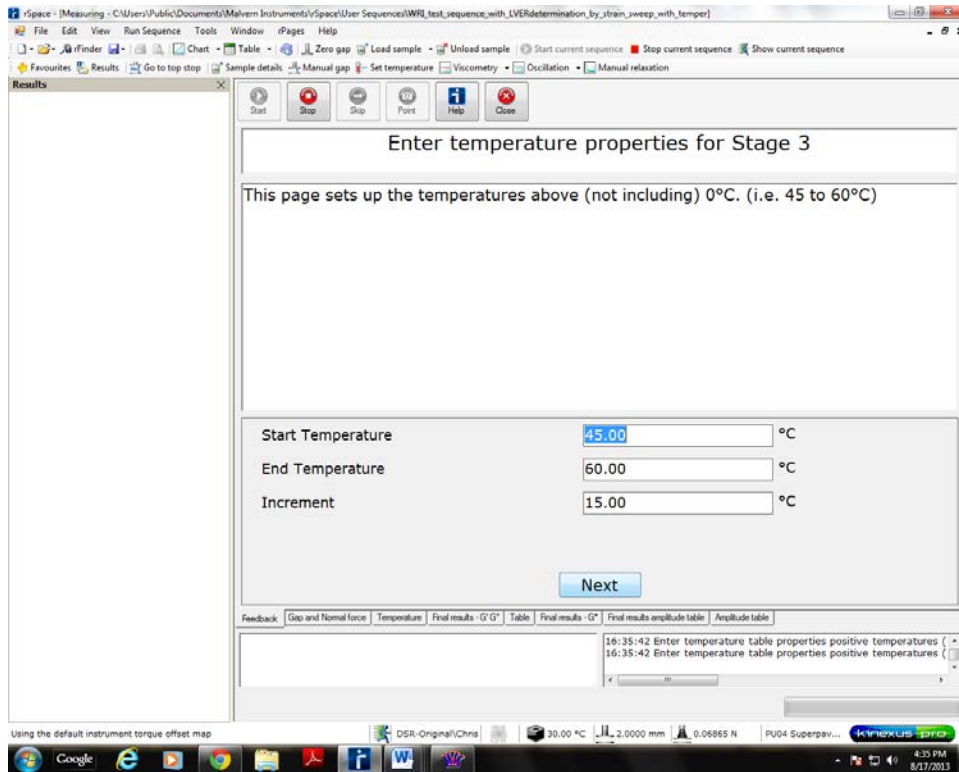




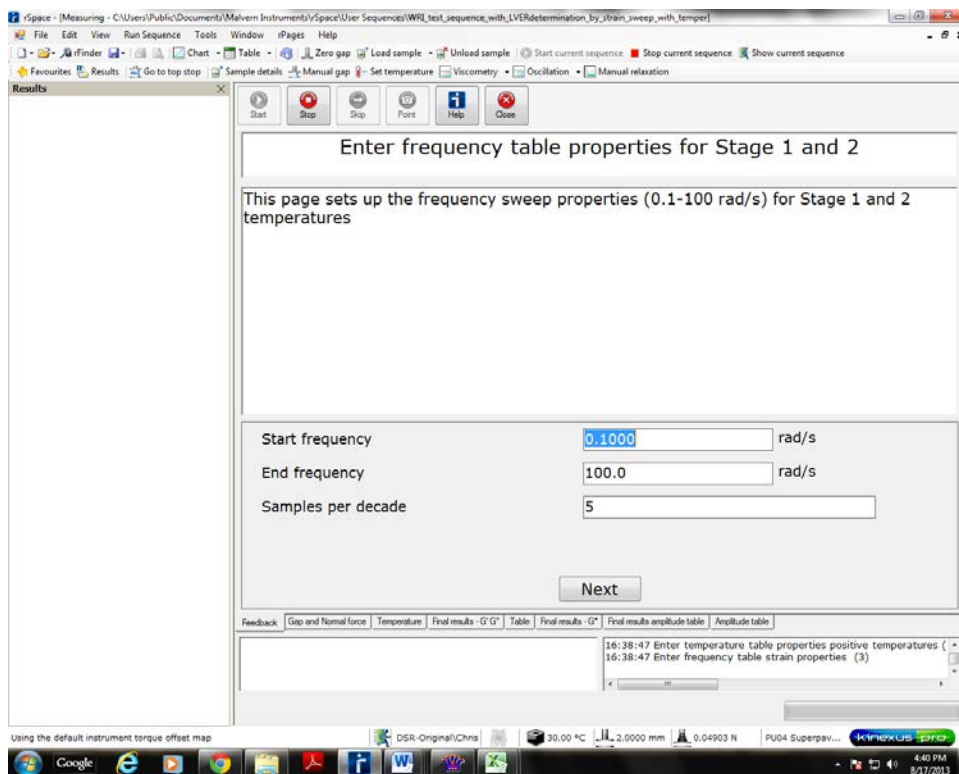
The user will select the intermediate temperatures for the test. These can, but do not have to correlate with numbers used in a traditional master curve. Do not type 0°C in this box or that temperature will be repeated.



Stage 3 is the high temperature range. Depending on the binder, the user will select their high temperature range. At temperatures above 60°C with such a small sample and larger gap, the binder begins to flow, so higher temperatures should be reserved for very stiff binders. Again, do not repeat any temperatures from prior stages or those will be repeated in the results.



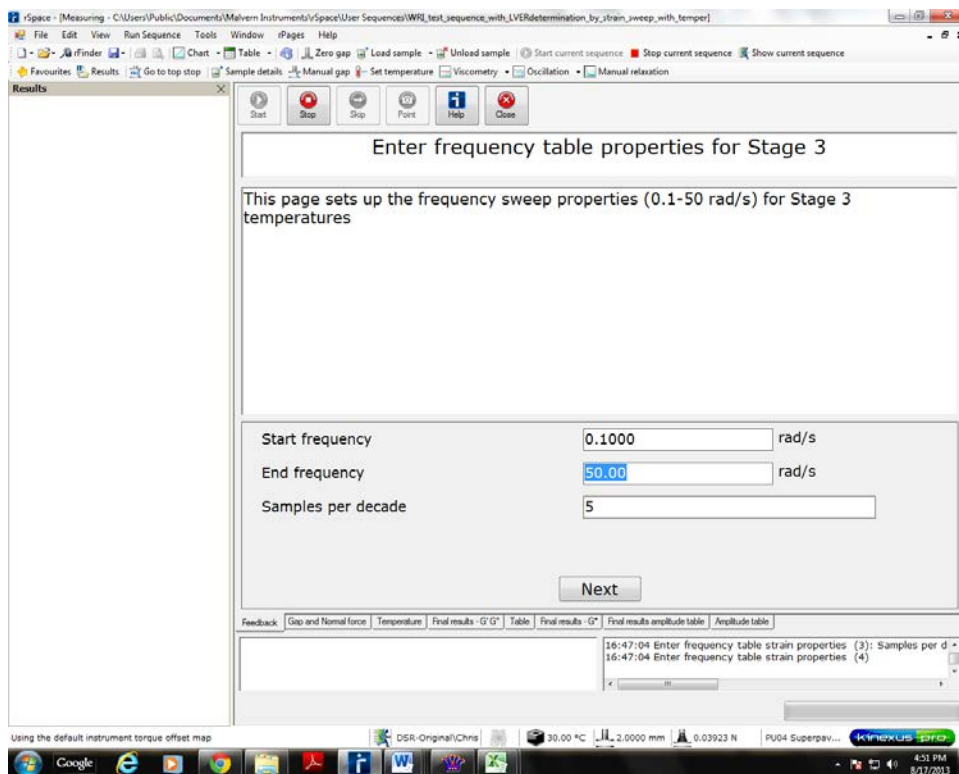
The user will set the frequency range and sampling rate for stages 1 and 2. The input below is acceptable for most binders, however a particularly stiff binder may crack and become unfused from the plates at low temperatures and higher frequencies. If additional data points per decade are required, these values can be manipulated. However for the purpose of making a master curve these inputs were adequate.



The user will select the frequency range and sampling rate for the high temperature range. Unlike the prior stages, this one defaults to 50 rad/s for the upper threshold. When tested at higher frequencies, the samples tend to have very high values of harmonic distortion as well as producing the following error:

K019 : Raw phase angle is too large, inertial effects dominating

This also occurs at very low frequencies for high temperatures. This error creates a point in RHEA that needs to be removed, so this can be avoided all together by selecting a lower upper threshold. However, for stiff materials, high frequencies may be required.



The sample will then begin to run once next is hit. The DSR will drop in temperature after approaching steady state of the shear stress.

The data may be extracted as the test is running and put into excel or extracted at the end as with a traditional master curve. The sequence has long waiting periods associated with the equilibrating, if the sequence is running without supervision, the entire test duration may be on the order of 6-8 hours. However if a technician is present during the test, once the machine has attained and held a temperature for 5-10 minutes, the sequence can be skipped and it will begin to run the test. This will reduce the test duration by one third and potentially allow multiple samples to be tested in one day using this process.

DE 76-22 #1 (8mm RHEA).xlsx - Microsoft Excel

Home Insert Page Layout Formulas Data Review View Acrobat Enterprise Connect

Normal Page Layout Views Custom Full Screen Workbook Views Show/Hide

Zoom 100% Zoom to Selection Zoom New Window Arrange All Freeze Panes Split Hide View Side by Side Synchronous Scrolling Reset Window Position Save Workspace Windows Switch Windows Macros

Security Warning Data connections have been disabled Options...

D80 =AVERAGE(B80:C80)\*10^3

	A	B	C	D	E	F	G	H	I	J	K	L
67	60.07	157	459.4	58.04	2.656							
68	60.06	100	315.3	62.39	2.217							
69	60.06	62.8	231.1	61.88	2.618							
70	60.06	31.4	145.6	61.38	3.241							
71	60.06	10	69.52	61.84	3.266							
72	60.05	6.28	51.66	62.23	4.352							
73	60.05	3.14	33.32	63.33	5.344							
74	60.04	1	16.05	65.12	7.852							
75	60.03	0.628	11.84	65.34	9.211							
76	60.02	0.1	4.384	67.75	17.21							
77	60.01	0.0628	3.834	71.96	66.53							
78												
79	time (s)	S(t)	neg22C BBR data	S(t) AVG	rad/s	G*						
80	8	367	370500	0.125	123500							
81	15	306	314	310000	0.066666667	103333.3						
82	30	247	253	250000	0.033333333	83333.33						
83	60	197	201	199000	0.016666667	66333.33						
84	120	154	156	155000	0.008333333	51666.67						
85	240	118	119	118500	0.004166667	39500						
86												
87	time (s)	S(t)	neg28C BBR data	S(t) AVG	rad/s	G*						
88	8	611	611	611000	0.125	203666.7						
89	15	533	533	533000	0.066666667	177666.7						
90	30	446	446	446000	0.033333333	148666.7						
91	60	371	371	371000	0.016666667	123666.7						
92	120	304	304	304000	0.008333333	101333.3						
93	240	244	244	244000	0.004166667	81333.33						
94												
95												
96												
97												
98												
99												
100												
101												

Ready DE 76-22 #1 (8mm RHEA) Black Space Conversions 10C 20C 30C 40C 50C 60C RHEA Output 100%



The  $S(t)$  values for the BBR data should be averaged and then divided by 3 in order to approximate it to  $G^*$  data. The inverse of the time will give the frequency. Once this has been converted, the user can begin to create their RHEA input file.

The input file must follow the following format. Any deviations will result in an error and the data will not be output.

Line 1: Description, any text, one line

Line 2: 16 items, space separators (14, 15, 16 optional, not used)

1. N for natural data, L for  $\text{Log}_{10}$  data
2.  $n_i$  = number of isotherms
3.  $T_{\text{ref}}$  = reference temperature in degrees Celsius (select a value within the data set)
4. Glassy Modulus Temperature (use  $-30^\circ\text{C}$ )
5. Density correction (use 1)
6. Expansion coefficients (use 1)
7. Expansion coefficient below glassy temp (use 0.00017)
8. Expansion coefficient above glassy temp (use 0.00017)
9. Density at  $25^\circ\text{C}$  (use 1.02)
10. 0 = binder, 1 = mix (use 0)
11. H for Hz, R for rad/sec if frequency, S if time (use R)
12. G = shear, E = tension or bending, D = compliance, S = stiffness (use G)
13. Units (kPa)

Line 3: Isotherm commences; three items

1. Temperature of isotherm, ascending (varies, -20, -10, 0, 10, etc)

2.  $n_t$  = number of times / frequencies

3. 0 = rejected, 1 = selected (use 10

Line 4 to  $(3 + n_t)$   $n_t$  lines of data points

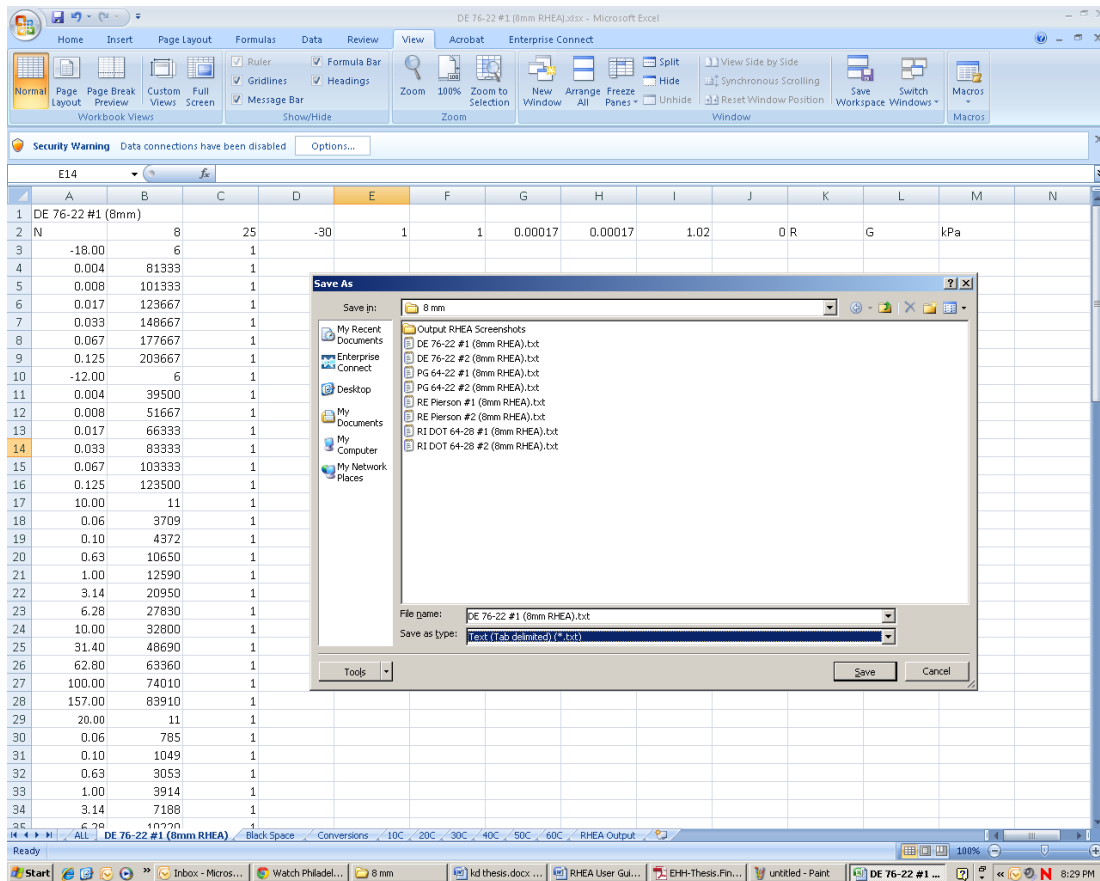
1. Time or frequency ascending

2. Modulus of compliance if time, storage modulus if frequency (use  $G^*$ )

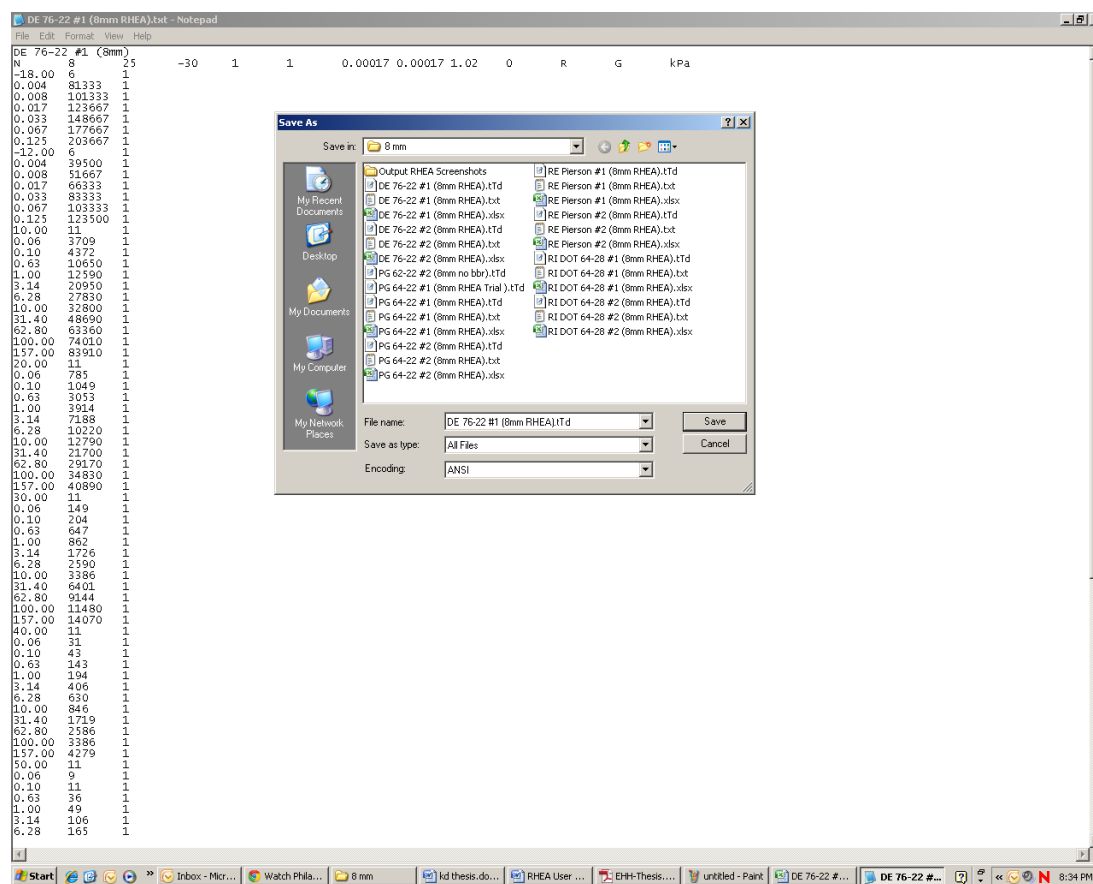
3. Transient Loss Modulus (use 1)

Repeat as from line 3 for each isotherm.

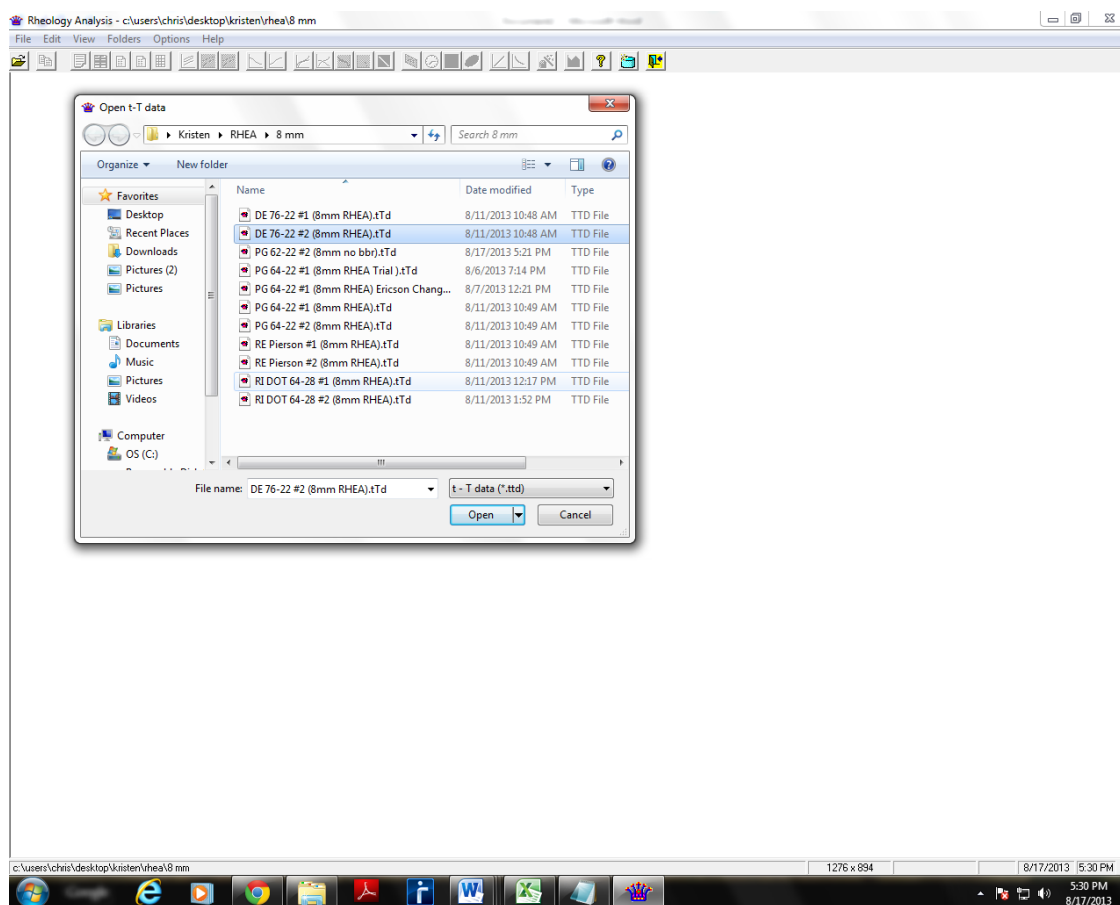
Once this data has been compiled into excel, it is necessary to save it as a tab delimited text file, as that is the only format readable by RHEA.



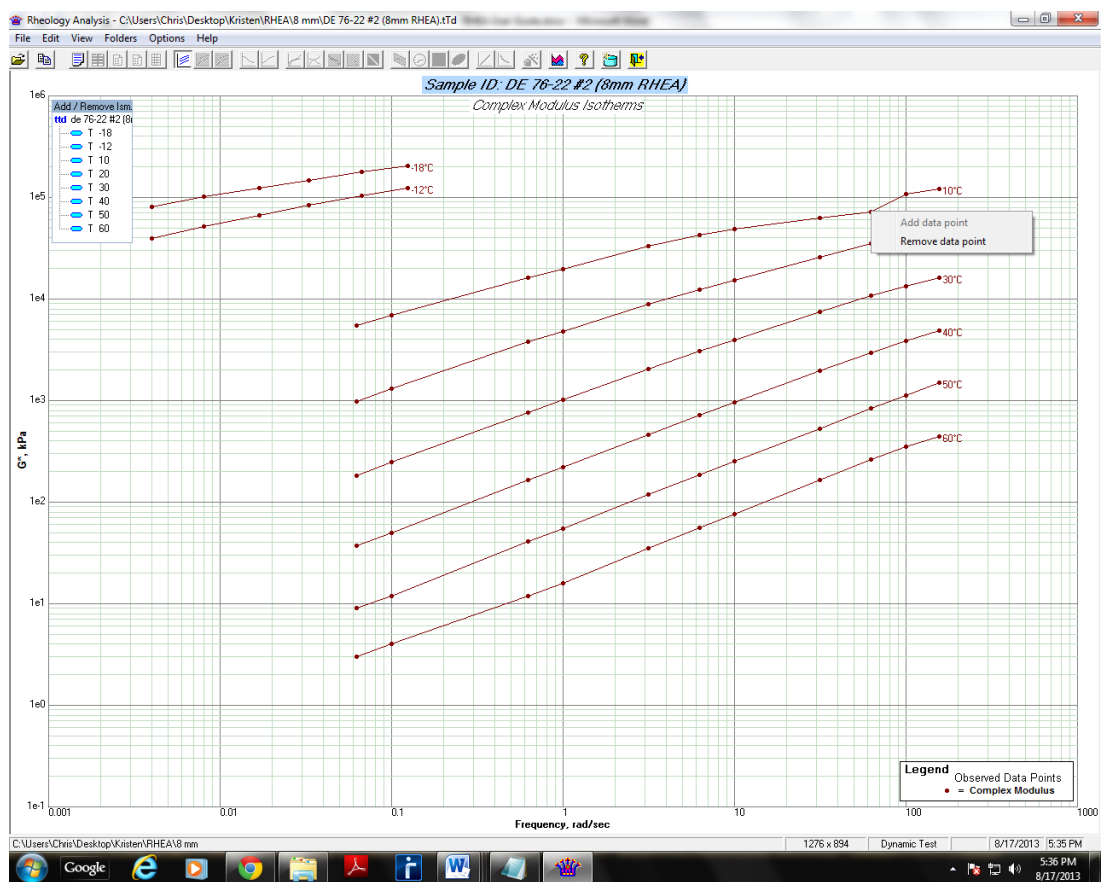
Once a text file has been created, this should then be opened and checked for any errors or issues (formatting errors arise if going from Mac to PC in some instances). This file should then be saved as a .tTd file. This is the file extension RHEA can read, make sure that all file is selected and not text documents.



Once the .tTd file has been created, it can be opened up in RHEA by clicking the folder icon and selecting the appropriate file.

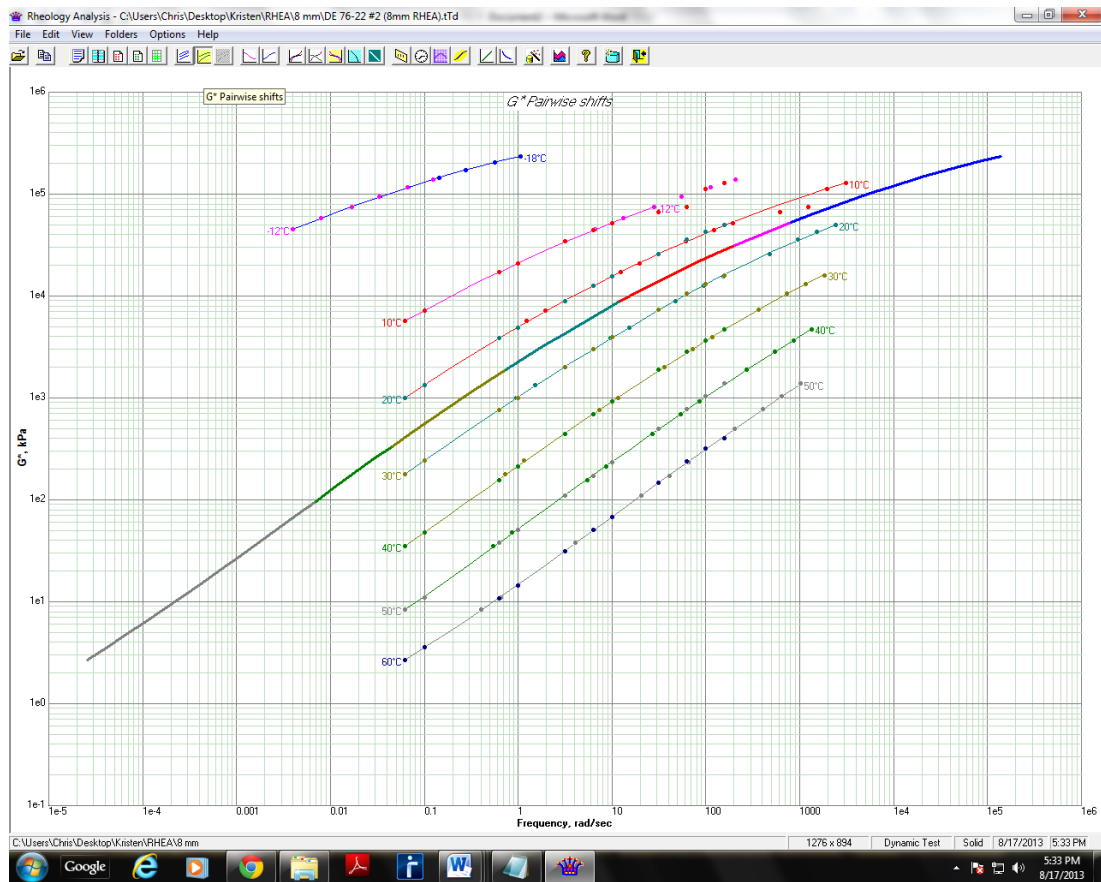


Regardless of the quality of the data, RHEA will always create isotherms as long as the input file is correct. However, in many instances, the other functions may be blacked out because the data points given may not create a master curve. In this instance, data points may be removed in order to allow the master curve and other graphs to become active.

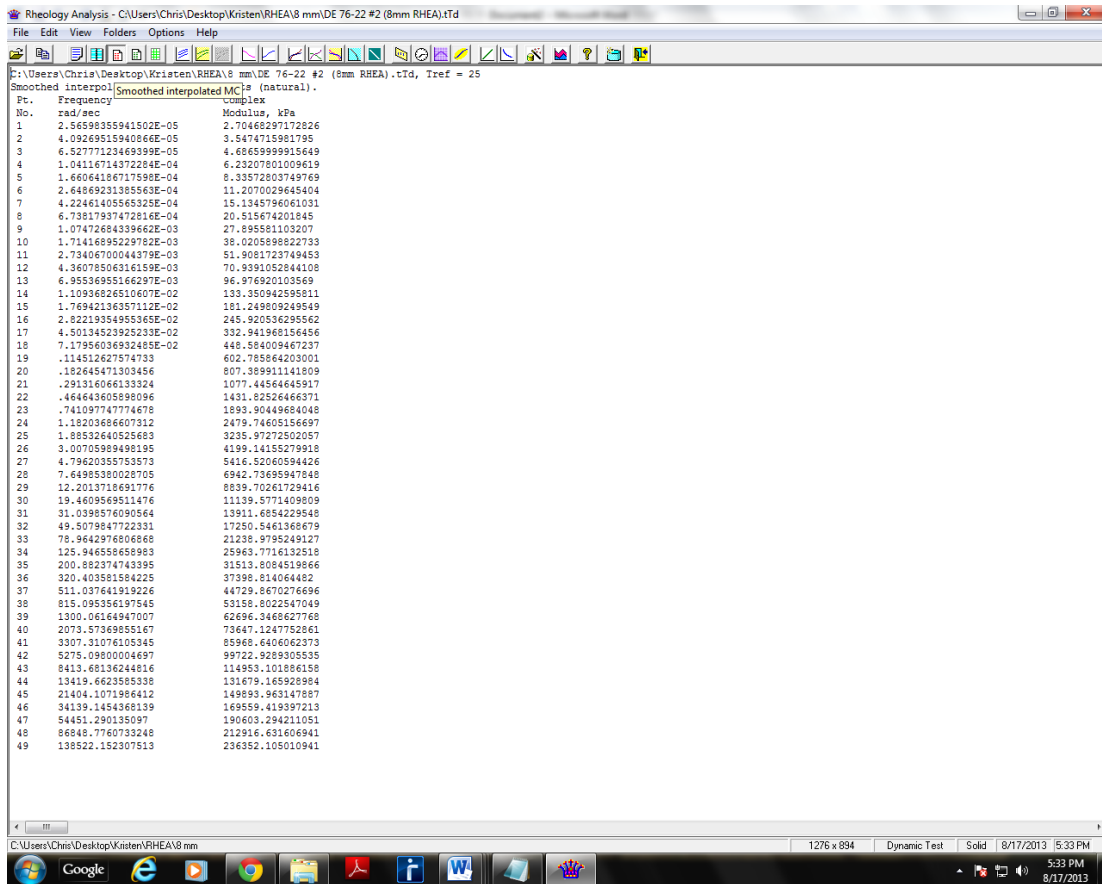


Each of the other functions can be used for separate analysis and to validate the given data, however for the purpose of this user manual not all of the functions will be touched upon.

The pairwise shifts or master curve is the shifted data. Additional points can be added or removed depending on how this graph appears.



The data from the pairwise shifts can be extracted and put into excel, so that it may be compared with other samples or otherwise manipulated. This is done by selecting the Smoother Interpolated MC button. This has all the smoothed and shifted points, with extraneous data that was manually removed excluded.



Since the results range from the viscoelastic to viscous range, the MEPPDG function is not always active. This function can only be used in the viscoelastic realm. As a result, temperatures in that range must be specified to ensure that this function becomes active.

## Appendix C: Continuous Grading Data for Binders Used

Project:	4 mm Master Curve	Date:	1/30/2012
Sample:	RI DOT 64-28	Supplier:	
Technician:	Kristen	Continuous Performance Grade (PG):	66.8-28.3 (20.6)

### Original Binder

Rotational Viscosity (T 316):

Max 3 Pa•s @ 135°C  Pa•s

Dynamic Shear (T 315):

$G^*/\sin\delta$ , Min 1.00kPa  kPa @ Temp =  at 10 rad/s

$G^*/\sin\delta$ , Min 1.00kPa  kPa @ Temp =  at 10 rad/s

### Rolling Thin Film Oven (RTFO) Residue

Percent Change, (1.00% Max Loss):  %

Dynamic Shear (T 315):

$G^*/\sin\delta$ , Min 2.20kPa  kPa @ Temp =  at 10 rad/s

$G^*/\sin\delta$ , Min 2.20kPa  kPa @ Temp =  at 10 rad/s

### Pressure Aging Vessel (PAV) Residue

R 28, 20 hours @ 2.07 MPa

Dynamic Shear (T 315):

$G^*\sin\delta$ , Max 5000kPa  kPa @ Temp =  at 10 rad/s

$G^*\sin\delta$ , Max 5000kPa  kPa @ Temp =  at 10 rad/s

Creep Stiffness (T 313):

S, Max 300 Mpa  MPa

m-value (Min 0.300)

Test Temp @ 60 s, °C  °C

S, Max 300 Mpa  MPa

m-value (Min 0.300)

Test Temp @ 60 s, °C  °C



Project:	4 mm Master Curve	Date:	12/17/2011
Sample:	PG 64-22	Supplier:	
Technician:	Kristen	Continuous Performance Grade (PG):	65.6-27.1 (18.1)

**Original Binder**

Rotational Viscosity (T 316):

Max 3 Pa•s @ 135°C	2.125	Pa•s
--------------------	-------	------

Dynamic Shear (T 315):

G*/sinδ, Min 1.00kPa	1.446	kPa @ Temp =	64	at 10 rad/s
----------------------	-------	--------------	----	-------------

G*/sinδ, Min 1.00kPa	0.689	kPa @ Temp =	70	at 10 rad/s
----------------------	-------	--------------	----	-------------

**Rolling Thin Film Oven (RTFO) Residue**

Percent Change, (1.00% Max Loss):	-0.05240133	%
-----------------------------------	-------------	---

Dynamic Shear (T 315):

G*/sinδ, Min 2.20kPa	2.7165	kPa @ Temp =	64	at 10 rad/s
----------------------	--------	--------------	----	-------------

G*/sinδ, Min 2.20kPa	1.2565	kPa @ Temp =	70	at 10 rad/s
----------------------	--------	--------------	----	-------------

**Pressure Aging Vessel (PAV)****Residue**

R 28, 20 hours @ 2.07 MPa

Dynamic Shear (T 315):

G*/sinδ, Max 5000kPa	4477	kPa @ Temp =	19	at 10 rad/s
----------------------	------	--------------	----	-------------

G*/sinδ, Max 5000kPa	3039.5	kPa @ Temp =	22	at 10 rad/s
----------------------	--------	--------------	----	-------------

Creep Stiffness (T 313):

S, Max 300 Mpa	342	MPa
----------------	-----	-----

m-value (Min 0.300)	0.314
---------------------	-------

Test Temp @ 60 s, °C	-18	°C
----------------------	-----	----

S, Max 300 Mpa	141.5	MPa
----------------	-------	-----

m-value (Min 0.300)	0.3845
---------------------	--------

Test Temp @ 60 s, °C	-12	°C
----------------------	-----	----

Project:	4 mm Master Curve	Date:	5/11/2012
Sample:	RE Pierson Extracted	Supplier:	
Technician:	Chris, Don, Maher	Continuous Performance Grade (PG):	86.5-18.4 (30.5)

**Original Binder**

Rotational Viscosity (T 316):

Max 3 Pa•s @ 135°C  Pa•s

Dynamic Shear (T 315):

G\*/sinδ, Min 1.00kPa  1.6475 kPa @ Temp =  82 at 10 rad/sG\*/sinδ, Min 1.00kPa  .848 kPa @ Temp =  88 at 10 rad/s**Rolling Thin Film Oven (RTFO) Residue**Percent Change, (1.00% Max Loss):  N/A %

Dynamic Shear (T 315):

G\*/sinδ, Min 2.20kPa  3.8545 kPa @ Temp =  82 at 10 rad/sG\*/sinδ, Min 2.20kPa  1.882 kPa @ Temp =  88 at 10 rad/s**Pressure Aging Vessel (PAV)****Residue**

R 28, 20 hours @ 2.07 MPa

Dynamic Shear (T 315):

G\*/sinδ, Max 5000kPa  6477.5 kPa @ Temp =  28 at 10 rad/sG\*/sinδ, Max 5000kPa  4738.5 kPa @ Temp =  31 at 10 rad/s

Creep Stiffness (T 313):

S, Max 300 Mpa  300.5 MPam-value (Min 0.300)  0.2785Test Temp @ 60 s, °C  -12 °CS, Max 300 Mpa  150.5 MPam-value (Min 0.300)  0.314Test Temp @ 60 s, °C  -6 °C

Project:	4 mm Master Curve	Date:	11/14/2011
Sample:	PG 76-22	Supplier:	Diamond Materials
Technician:	Kristen	Continuous Performance Grade (PG):	84.9-25.7 (24.4)

**Original Binder**

Rotational Viscosity (T 316):

Max 3 Pa•s @ 135°C  Pa•s

Dynamic Shear (T 315):

G\*/sinδ, Min 1.00kPa  kPa @ Temp =  at 10 rad/sG\*/sinδ, Min 1.00kPa  kPa @ Temp =  at 10 rad/s**Rolling Thin Film Oven (RTFO) Residue**Percent Change, (1.00% Max Loss):  %

Dynamic Shear (T 315):

G\*/sinδ, Min 2.20kPa  kPa @ Temp =  at 10 rad/sG\*/sinδ, Min 2.20kPa  kPa @ Temp =  at 10 rad/s**Pressure Aging Vessel (PAV)****Residue**

R 28, 20 hours @ 2.07 MPa

Dynamic Shear (T 315):

G\*/sinδ, Max 5000kPa  kPa @ Temp =  at 10 rad/sG\*/sinδ, Max 5000kPa  kPa @ Temp =  at 10 rad/s

Creep Stiffness (T 313):

S, Max 300 Mpa  MPam-value (Min 0.300) Test Temp @ 60 s, °C  °CS, Max 300 Mpa  MPam-value (Min 0.300) Test Temp @ 60 s, °C  °C